

Evaluating the effect of biostimulants on *Hyaloperonospora arabidopsidis*- infected *Arabidopsis thaliana* plants

Hendrik Thiels

Promotor & Copromotor: Sam Crauwels

Supervisor: Johan Yssel

Masterproef ingediend tot het behalen van de
graad van Master of Science in de industriële
wetenschappen: *Biochemie, Biomedical
engineering*

Academiejaar 2022-2023

© Copyright KU Leuven

Deze masterproef is een examendocument dat niet werd gecorrigeerd voor eventuele vastgestelde fouten.

Zonder voorafgaande schriftelijke toestemming van zowel de promotor(en) als de auteur(s) is overnemen, kopiëren, gebruiken of realiseren van deze uitgave of gedeelten ervan verboden. Voor aanvragen i.v.m. het overnemen en/of gebruik en/of realisatie van gedeelten uit deze publicatie, kan u zich richten tot KU Leuven Campus Groep T Leuven, Andreas Vesaliusstraat 13, B-3000 Leuven, +32 16 30 10 30 of via e-mail iiw.groept@kuleuven.be.

Voorafgaande schriftelijke toestemming van de promotor(en) is eveneens vereist voor het aanwenden van de in deze masterproef beschreven (originele) methoden, producten, schakelingen en programma's voor industrieel of commercieel nut, om te refereren naar dit werk in publicaties en voor de inzending van deze publicatie ter deelname aan wetenschappelijke prijzen of wedstrijden.

Preface

“Knowing is not enough; we must apply. Willing is not enough; we must do” - Johann Wolfgang von Goethe.

My journey at the Laboratory for Process Microbial Ecology and Bioinspirational Management (PME&BIM) began in November 2021 to conduct my bachelor’s paper. During this project I was assisted by colleagues Thomas, Laurent and Dorien and was supervised by Johan Yssel. While working on this project I felt really comfortable in the lab and liked working with Johan because he was always friendly, approachable, and proactive in offering help. Therefore, I asked Johan if there was a thesis subject available and immediately put this subject on the first place of my wish list and was genuinely excited to hear that I got to complete my Master in Industrial Engineering Sciences at my lab of choice on a subject of my choice. Consequently, this thesis can be seen as the ultimate culmination point of my 4 years of studying at KU Leuven, which could only be completed with the assistance and support of many great people.

First of all, I would like to thank Johan for his excellent support and guidance, even when this came in the form of Zoom calls from the other side of the world when he was in South Africa. He gave me the opportunity and knowledge to bring this research to a successful end while leaving room for me to be flexible and conduct experiments that I wanted to conduct myself, which was really important for me. All of this while keeping a critical eye to lift the project to a higher level.

Further, I would like to thank Sam Crauwels for providing me with valuable remarks and suggestions on my thesis and experimental work based on his extensive experience, next to always being enthusiastic and full of humour. Without him, the quality of the thesis would be drastically lower than it is now.

Another important and above all, great guy that I could not have imagined not being present to help me is Tin Kocijan. He was always present to help me with interpreting results and explain how certain machinery works, with a bright smile on his face. Another person that was always present in the lab to help me with all sorts of issues was Christel Verreth, she was always ready to help and would drop her own experiments if there was an issue or a question.

I also want to thank my colleague master thesis students Thomas, Toon, and Arne for the great atmosphere in the lab and always being able to have a good laugh and for giving me distraction when performing repetitive tasks.

In addition, I would like to thank Alexa de Knijf to give me permission to conduct several experiments at the Centre of Microbial and Plant Genetics (CPMG) of Prof. Cammue and help me if there was an issue when I was working there.

My thesis itself would also not be of the same quality without the scientific background I got during courses and lab sessions of Veerle Bloemen, Bart Lievens, Hans Rediers, Inge Holsbeeks, Sabine Vercruysse, Arn Mignon, Laura Gobbens, Barbara Colsoul, Leni Borremans and Fien Vanhoegaerden.

To end, I would like to thank my parents and grandparents to believe in me and support my work and studies. Finally, I would like to thank all my friends for all the great memories we made in Leuven, which we will carry for the rest of our lives.

Samenvatting

Om gewassen te beschermen tegen ziekteverwekkers worden deze in de moderne landbouw vaak bespoten met verschillende pesticiden. Dit zijn vaak giftige, niet biologisch afbreekbare bestanddelen die, wanneer zij via neerslag en wind in het milieu terecht komen, biodiversiteit verminderen. Pesticideresiduen vormen ook een gezondheidsrisico wanneer zij in hoge concentraties in voedsel aanwezig zijn. Om afhankelijkheid te verminderen kunnen biostimulanten een vervanger vormen, dit zijn biologische stoffen die een versterkend effect kunnen hebben op de behandelde plant, waardoor de weerstand tegen pathogenen mogelijk wordt verhoogt. Deze stoffen zijn biologisch afbreekbaar en onschadelijk voor het milieu, wat in overeenstemming is met de "Farm to Fork" EU-strategie om voedselsystemen eerlijk, gezond en milieuvriendelijk te maken.

In dit artikel werden de modelplant *Arabidopsis thaliana* en de biotrofe plantpathogeen *Hyaloperonospora arabidopsidis* gebruikt om meeldauwinfecties te simuleren. Zes biostimulanten werden beoordeeld op hun effect op de proliferatie van het pathogeen, namelijk humuszuur (HA1), fulvinezuur (HA2), soja-extract (PH1), moutextract (PH2) en *Ecklonia maxima* zeewierextract van twee leveranciers (SW1) en (SW2). De doeltreffendheid van deze biostimulanten werd geëvalueerd in vier verschillende experimenten en werd vergeleken met een waterbehandeling als negatieve controle en met een difenoconazol houdend fungicide als positieve controle.

Het effect van de biostimulanten op geïnfecteerde *A. thaliana* na behandeling werd gekwantificeerd door het tellen van *H. arabidopsidis*-sporen via microscopie en het kwantificeren van de relatieve pathogene biomassa via quantitative polymerase chain reaction (qPCR). Verder werd een pigmentextractie uitgevoerd op geïnfecteerde planten om chlorofyl- en carotenoïdengehalten te bepalen via spectrometrie. Zo werd het absolute chlorofylgehalte gebruikt als maat voor de groei en biomassa van de plant, het relatieve chlorofylgehalte als maat voor fotosynthesecapaciteit, en het relatieve carotenoïdengehalte als maat voor immuunrespons. Een laatste experiment werd uitgevoerd met de twee best presterende biostimulanten uit voorgaande experimenten, waarbij groeicurven en kinetische parameters van zowel sporulatie als relatieve pathogene biomassa werden opgesteld.

Uit deze experimenten bleek dat moutextract (PH2) en *Ecklonia maxima* zeewierextract van Kelpak® (SW2) de beste prestaties leverden. Beide behandelingen lieten consistent een significante vermindering zien van *H. arabidopsidis*-sporen en biomassa, vergelijkbaar met het fungicide. Beide behandelingen lieten ook verbeteringen zien in de groei en fotosynthesecapaciteit van de planten, vergelijkbaar met die van niet-geïnfecteerde planten, en een verhoogde immuunrespons vergeleken met de waterbehandeling. Bovendien veroorzaakte PH2, net als het fungicide, een vertraagde en verminderde sporulatiepiek en een vervroegde verminderde *H. arabidopsidis* biomassapieak.

Hoewel deze biostimulanten veelbelovende resultaten opleverden, is er nog ruimte om concentraties en toedieningsmethoden te optimaliseren om de doeltreffendheid te verhogen. Ook dienen er veldproeven worden uitgevoerd om een indicatie te krijgen van de doeltreffendheid op productieschaal. Indien deze biostimulanten met succes worden geïntegreerd, kunnen zij leiden tot een wereldwijde verschuiving naar duurzamere landbouwpraktijken, met positieve gevolgen voor het milieu, biodiversiteit en voedselkwaliteit.

Abstract

In modern agriculture, crops are frequently sprayed with pesticides to protect them from pathogens. These are often toxic non-biodegradable components that, when released into the environment via precipitation and wind, reduce biodiversity. Pesticide residues also pose a health risk to all life when present in high concentrations in food. A possible method to reduce pesticide dependence is using biostimulants, which are biological substances that can have an enhancing effect on the treated plant, potentially giving it increased pathogen resistance. These compounds are compostable and harmless to the environment, which is in line with the EU's "farm to fork" strategy to make food systems fair, healthy and environmentally-friendly.

In this paper, the model plant *Arabidopsis thaliana* and biotrophic plant pathogen *Hyaloperonospora arabidopsidis* were used to simulate mildew infections of economically relevant plants (e.g. grapevines and tomato plants). Six biostimulant treatments were evaluated for their effects on controlling pathogen proliferation, being humic acid (HA1), fulvic acid (HA2), commercial soybean extract (PH1), malt extract (PH2), and commercial *Ecklonia maxima* seaweed extracts from two suppliers (SW1) and (SW2). The efficacy of these biostimulants was evaluated in four different experiments and was compared against a water treatment as a negative control and with a difenoconazole-containing fungicide as a positive control.

The effect of the biostimulants on pathogen-infected *A. thaliana* was quantified through *H. arabidopsidis* spore counts via microscopy and relative pathogenic biomass quantification via quantitative polymerase chain reaction (qPCR) post-treatment, with the infection occurring in two separate experiments. Additionally, a pigment extraction was performed on infected plants to determine chlorophyll and carotenoid contents via spectrometry. Thus, absolute chlorophyll content was used as a measure of plant growth and biomass, relative chlorophyll content as a measure of productivity and photosynthetic capacity, and relative carotenoid content as a measure of plant immune response. A final experiment was conducted with the two best-performing biostimulants from the previous experiments and involved tracing growth curves and kinetic parameters of both sporulation and relative pathogenic biomass of *H. arabidopsidis* infected plants.

These experiments showed that malt extract (PH2) and commercial *Ecklonia maxima* seaweed extract from Kelpak® (SW2) performed the best. Here, both treatments consistently showed a significant reduction in *H. arabidopsidis* spores and biomass comparable to the difenoconazole fungicide, also both showed plant improvements in growth and photosynthetic capacity comparable to non-infected plants and an increased immune response compared to the water treatment. In addition, PH2, like the fungicide, caused a delayed and reduced sporulation peak and an early reduced *H. arabidopsidis* biomass peak.

While these biostimulants showed promising results, there is still room to optimise the biostimulant concentration and method of administration to improve efficacy. Field trials should be conducted to provide an indication of efficacy at production scale. If successfully integrated, these biostimulants could lead to a global shift towards more sustainable agricultural practices, with positive impacts on the environment, biodiversity, and food quality.

Keywords: biostimulants, pathogen resistance, *Arabidopsis thaliana*, *Hyaloperonospora arabidopsidis*, difenoconazole.

List of Figures

Figure 1: Lifecycle of <i>A. thaliana</i> (Adapted from eLife, 2015).....	3
Figure 2: <i>Hyaloperonospora arabidopsidis</i> infected <i>A. thaliana</i>	4
Figure 3: Infection stages of <i>H. arabidopsidis</i>	5
Figure 4: Overview of the working principle of humic substances (HA).....	12
Figure 5: Overview of the working principle of protein hydrolysates (PH).....	13
Figure 6: Overview of the working principle of seaweed extracts (SW).....	14
Figure 7: Working principle of SYBR®-green and TaqMan probes.	17
Figure 8: Working principle of calibration curve construction.	18
Figure 9: Infection growth curve.	20
Figure 10: Overview of sample generation.	22
Figure 11: Overview of experiments that are executed.	22
Figure 12: Two trays of <i>A. thaliana</i> plants after one week of growing.	23
Figure 13: Treatment scheme for spore count and qPCR experiments.....	24
Figure 14: Overview of <i>H. arabidopsidis</i> cycling.	25
Figure 15: Overview of Spore counting process.	27
Figure 16: Treatment scheme pigment extraction experiment.	29
Figure 17: Treatment scheme Infection growth kinetics experiment.....	31
Figure 18: Box and whisker plot of initial spore count (1) and confirmation spore count (2), 7 days post-infection.	35
Figure 19: Agarose gel electrophoresis primer specificity test results.	38
Figure 20: Visual representation of correction.	42
Figure 21: Box and whisker plot of the initial absolute pathogen biomass quantification experiment (1) and confirmation experiment (2), 7 days post-infection.	44
Figure 22: Box and whisker plot of the total absolute chlorophyll content indicating plant growth and biomass, 10 days post-infection.....	47
Figure 23: Box and whisker plot of the total relative chlorophyll content indicating plant health and photosynthetic capacity, 10 days post-infection.	49
Figure 24: Box and whisker plot of the total relative carotenoid content indicating plant immune reaction, 10 days post-infection.	51
Figure 25: <i>H. arabidopsidis</i> sporulation growth curves.....	52
Figure 26: <i>H. arabidopsidis</i> biomass growth curves.....	54
Figure 27: Flow diagram of all individual tasks over time.	64

Figure 28: Calibration curve <i>A. thaliana</i> actin primers of DNA extracted using the DNeasy Powersoil Pro Kit (Qiagen, n.d.).	65
Figure 29: Calibration curve <i>H. arabidopsis</i> actin primers of DNA extracted using the DNeasy Powersoil Pro Kit (Qiagen, n.d.).	66
Figure 30: Calibration curve <i>A. thaliana</i> actin primers of DNA extracted using phenol/chloroform extraction.	67
Figure 31: Calibration curve <i>H. arabidopsis</i> actin primers of DNA extracted using phenol/chloroform extraction.	68

List of Tables

Table 1: Overview table containing information about all used treatments.	24
Table 2: Overview of the temperature/time profile of the qPCR reaction used	28
Table 3: Overview of primer specifications.	28
Table 4: Sampling scheme for the infection growth kinetics experiment.	30
Table 5: Post hoc test (Dunnett's T3) p-values of the initial spore count experiment (1) and confirmation experiment (2), 7 days post-infection.	36
Table 6: Relative amplification data for the <i>A. thaliana</i> and <i>H. arabidopsis</i> actin genes in uninfected and infected plant samples, 7 days post-infection. Primer concentration was 100µM.	39
Table 7: Relative amplification data for the <i>A. thaliana</i> and <i>H. arabidopsis</i> actin genes in uninfected and infected plant samples, 7 days post-infection. Arab. actin primer was 100µM, <i>H. arabidopsis</i> actin primer concentration was 20 µM (5-fold dilution).	39
Table 8: Relative amplification data for the <i>A. thaliana</i> actin and <i>H. arabidopsis</i> RLXR29 gene in uninfected and infected plant samples, 7 days post-infection. <i>H. arabidopsis</i> RLXR29 primer concentration was 20µM.	40
Table 9: qPCR results correction factor construction.	42
Table 10: Post hoc test (Tukey HSD) p-values of the initial absolute pathogen biomass quantification experiment (1) and confirmation experiment (2), 7 days post-infection.	45
Table 11: Post hoc test (Dunnett's T3) p-values of the absolute chlorophyll content experiment 10 days post-infection.	47
Table 12: Post hoc test (Dunnett's T3) p-values of the total relative chlorophyll content experiment 10 days post-infection.	49
Table 13: Post hoc test (Tukey HSD) p-values of the relative carotenoid content experiment 10 days post-infection.	51
Table 14: Effect of treatment on <i>H. arabidopsis</i> sporulation kinetic parameters.	53
Table 15: Type III analysis p-values of the biomass kinetic curves.	55
Table 16: Effect of treatment on <i>H. arabidopsis</i> biomass growth parameters.	55

Table 17: Overview of all experimental outcomes.....	57
Table 18: Calibration curve values <i>A. thaliana</i> actin primers of DNA extracted using the DNeasy Powersoil Pro Kit (Qiagen, n.d.).	65
Table 19: Calibration curve values <i>H. arabidopsidis</i> actin primers of DNA extracted using the DNeasy Powersoil Pro Kit (Qiagen, n.d.).	66
Table 20: Calibration curve values <i>A. thaliana</i> actin primers of DNA extracted using phenol/chloroform extraction.	67
Table 21: Calibration curve values <i>H. arabidopsidis</i> actin primers of DNA extracted using phenol/chloroform extraction.	68

List of Equations

Equation 1: $2^{-\Delta\Delta C_T}$ -method	18
Equation 2: Equation used to calculate amplification efficiency.	19
Equation 3: Trendline equation of the exponential growth phase.....	21
Equation 4: Equation on how to calculate doubling time (Td).	21
Equation 5: Formula to convert DNA mass to the number of DNA copies.	28
Equation 6: Arnon equation for relative chlorophyll-A concentration.	29
Equation 7: Arnon equation for relative chlorophyll-B concentration.	30
Equation 8: Arnon equation for total relative carotenoid concentration.	30

Nomenclature

AA	Amino acids
AT	<i>Arabidopsis thaliana</i>
BIT	1,2-benzisothiazolin-3-one
dNTPs	Deoxynucleotide triphosphates
HA	Humic substances
HA1	Humic acid
HA2	Fulvic acid
HAMPs	Host-associated molecular patterns
Hpa	<i>Hyaloperonospora arabidopsidis</i>
IAR	Induced acquired resistance
PAMPs	Pathogen-associated molecular patterns
PCR	Polymerase chain reaction
PH	Protein hydrolysates
PH1	Commercial soy
PH2	Malt extract
SAR	Systemic acquired resistance
SDHI	Succinate dehydrogenase inhibitor
SW	Seaweed extract
SW1	<i>Ecklonia maxima</i> seaweed extract (Afrikelp®)
SW2	<i>Ecklonia maxima</i> seaweed extract (Kelpak®)
TOML	Time of max load
qPCR	Quantitative polymerase chain reaction

CONTENTS

Preface	iv
Samenvatting	v
Abstract	vi
List of Figures	vii
List of Tables	viii
Nomenclature	x
1 Introduction	1
1.1 Background information	1
1.2 Research scope and objectives.....	1
1.3 Thesis outline.....	2
2 Literature review	3
2.1 <i>Arabidopsis thaliana</i> as a model plant	3
2.2 <i>Hyaloperonospora arabidopsidis</i> as a model pathogen for infection analysis 4	
2.2.1 The infection mechanism of <i>H. arabidopsidis</i>	5
2.2.2 The economic relevance of downy mildew pathogen infections	6
2.3 Measures to control infectious diseases in agriculture.....	7
2.3.1 Cultural practices	7
2.3.2 Chemical control measures.....	7
2.3.3 Biological control measures	9
2.4 Pathogen resistance mechanisms in plants.....	10
2.4.1 Innate plant immune system	10
2.4.2 Acquired plant immune system	10
2.5 Biostimulant treatments.....	11
2.5.1 Humic acids as biostimulants	11
2.5.2 Protein hydrolysates as biostimulants	13
2.5.3 Seaweed extracts as biostimulants	14
2.6 Quantifying disease resistance in model plants.....	15
2.6.1 Pathogenic effect quantification: infection scoring	15
2.6.2 Pathogenic spread quantification: spore count.....	15
2.6.3 Pathogenic biomass quantification: quantitative polymerase chain reaction (qPCR).....	16

2.6.4	Assessing <i>A. thaliana</i> growth, productivity, and immune response to <i>H. arabidopsidis</i> by quantifying chlorophyll and carotenoid content	19
2.6.5	Defining the growth kinetics of an <i>H. arabidopsidis</i> infection	20
3	Materials and methods	22
3.1	Experimental setup	22
3.2	<i>Growth and maintenance A. thaliana</i>	23
3.3	Treatments of <i>A. thaliana</i> using foliar feeding	24
3.4	<i>H. arabidopsidis</i> maintenance and infection	25
3.5	DNA extraction methods used	26
3.6	<i>H. arabidopsidis</i> sporulation quantification: spore count	27
3.7	<i>H. arabidopsidis</i> biomass quantification: qPCR	28
3.8	Assessing <i>A. thaliana</i> growth, productivity, and immune response when infected with <i>H. arabidopsidis</i> by chlorophyll and carotenoid quantification	29
3.9	<i>H. arabidopsidis</i> infection growth kinetics	30
3.10	Statistical analysis	32
4	Results & discussion	33
4.1	<i>Hyaloperonospora arabidopsidis</i> sporulation quantification by spore count	33
4.2	<i>H. arabidopsidis</i> biomass quantification by qPCR	37
4.2.1	Optimization of qPCR	37
4.2.2	Absolute quantification of <i>H. arabidopsidis</i> biomass	41
4.3	Assessing <i>A. thaliana</i> growth, productivity, and immune response to <i>H. arabidopsidis</i> by quantifying chlorophyll and carotenoid content	46
4.3.1	Plant growth: absolute chlorophyll content	46
4.3.2	Plant productivity: relative chlorophyll content	48
4.3.3	Plant immune reaction: relative carotenoid content	50
4.4	<i>H. arabidopsidis</i> infection growth kinetics	52
4.4.1	<i>H. arabidopsidis</i> sporulation kinetics	52
4.4.2	<i>H. arabidopsidis</i> biomass growth kinetics	54
5	Conclusion	56
6	Limitations	58
	References	59
	Appendix	64

1 INTRODUCTION

1.1 Background information

Currently, fungal plant diseases have become less problematic in the agricultural sector than in the past, owing to the numerous breakthroughs in developing various types of fungicides and pesticides, such as the development of succinate dehydrogenase inhibitor (SDHI) fungicides. However, these compounds are generally synthetic, persistent in nature, and toxic towards humans and wildlife. They not only impact the target plants but are also dispersed by, for instance, wind or rain, leading to harm in the surrounding environment, such as poisoning water and reducing local biodiversity (Repetta et al., 1996). Moreover, they pose health risks not only to farmers who have frequent exposure to them but also to consumers who may develop various diseases, including cancer, after prolonged exposure to pesticide residues (Rouabhi, 2010).

Ideally, these compounds should be substituted with biological substances that are safe for the environment and human health. Biostimulants are a case in point. They are natural aggregates that can be sprayed onto plants, resulting in increased plant growth, improved stress tolerance, and augmented disease resistance (Du Jardin, 2015). The latter characteristic is particularly intriguing and could offer a solution to the pesticide predicament by fortifying the plant instead of exterminating the disease (Sible et al., 2021).

1.2 Research scope and objectives

The objective of this study is to assess the effectiveness of six commercially available biostimulants in reducing infection caused by the common oomycete plant pathogen *Hyaloperonospora arabidopsidis* using *Arabidopsis thaliana* as a model plant. To evaluate the resistance to infection, various parameters such as the relative spore content reduction, pathogen biomass reduction, alterations in pathogenic and plant growth rates, plant photosynthetic productivity, and plant immune response will be examined. The study will culminate in identifying one or more biostimulants that demonstrate encouraging outcomes for further field trials. If the results from these trials prove positive, a recommendation for the use of a specific biostimulant can be made to the agricultural sector.

1.3 Thesis outline

In section two an overview of relevant literature is given, including background information on the use of *A. thaliana* as a model plant, *H. arabidopsidis* as a model pathogen, infection control in agriculture, general pathogen resistance mechanisms in plants, biostimulants, difenoconazole fungicides, and finally quantification methods for disease resistance.

In section three, the materials and methods used for all experiments are given. This section includes the maintenance of *A. thaliana*, the treatments that are used, and *H. arabidopsidis* maintenance and infection. These are then followed by the experiments themselves, being the spore count, the DNA extraction methods, pathogen biomass quantification, pigment extraction and finally pathogen growth kinetics.

In section four results are presented and discussed accordingly, including results of all previously cited experiments. In section five, the concluding information is given. Finally, in section six, limitations are given that need to be considered when reviewing the results and continuing further experiments such as field trials.

2 LITERATURE REVIEW

2.1 *Arabidopsis thaliana* as a model plant

Arabidopsis thaliana is a commonly used model plant in scientific research due to its fast and easy growth, short lifecycle, and close relationship to other plant species, allowing for extrapolation of results (Meinke et al., 1998). It is a member of the Brassicaceae family being the first plant to be completely sequenced, which contributes to its prominence in scientific literature (Arabidopsis Genome Initiative, 2000) and resulted in the description of a relatively short genome of 135 megabases. The study of *A. thaliana* has provided valuable insights into plant hormone signalling, as well as genetic and molecular mechanisms of plant growth and development (Bhalerao & Fischer, 2017).

Under favourable conditions, *A. thaliana* can reach maturity within just two weeks, forming a small-leaved rosette attached to a main stem with inflorescence. The formation of seedpods occurs approximately two to three weeks after flowering, with factors such as temperature, light, and humidity influencing the process (Koornneef & Meinke, 2010).

Moreover, *A. thaliana* is frequently used as a host plant for studying the interactions between plants and various microbes, including bacteria, fungi, and viruses (Jones and Dangl, 2006). Such studies have provided insights into the mechanisms of plant defence against pathogens, as well as the strategies used by microbes to overcome plant defences. For instance, the ability of *Salmonella Typhimurium* to hijack the mitogen-activated protein kinase (MAPK) signaling pathway to promote bacterial growth by overcoming the innate immune response has been studied using *A. thaliana* (Schikora et al., 2008; García-Angulo, 2017).

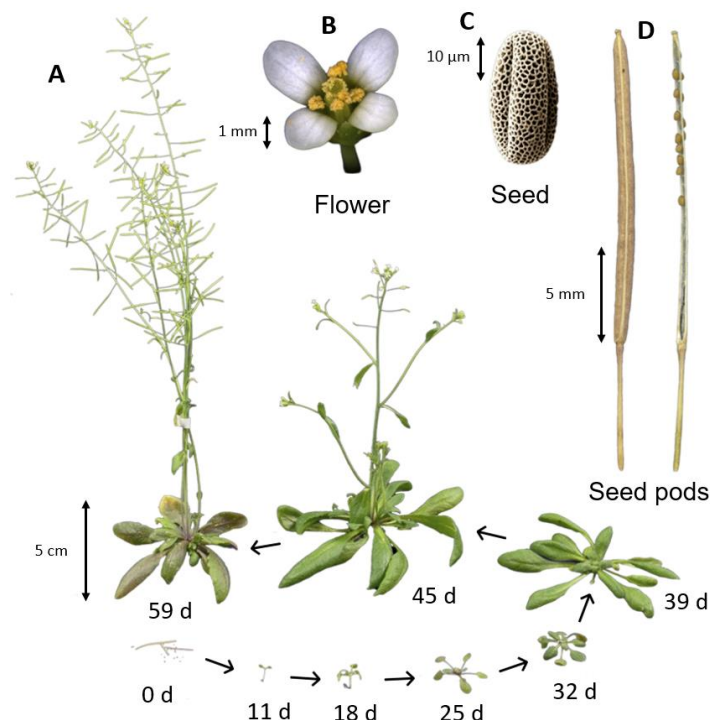


Figure 1: Lifecycle of *A. thaliana* (Adapted from eLife, 2015). (A) a matured AT plant in the seedpod phase, (B) AT flower, (C) microscopic image of AT seed, (D) AT seedpod, (bottom) Lifecycle of AT plant in 50 days.

2.2 *Hyaloperonospora arabidopsis* as a model pathogen for infection analysis

Currently, there are thousands of known plant pathogens, with new species yet to be discovered. These organisms, including bacteria, fungi, and viruses, affect different parts of the host plant in various ways, and their consequences can range from small losses in yield and quality in the agricultural sector to significant shifts in ecosystem biodiversity (Wang et al., 2022). One such pathogen is the Peronospora genus, commonly known as downy mildew, which affects a wide range of crops such as grapes, lettuce, cucumber, onions, and Brassicaceae (e.g., broccoli and cauliflower; Thakur & Mathur, 2002). The Peronospora species that infects AT is called *Hyaloperonospora arabidopsis* (Hpa) leads to different symptoms in its host plants, such as yellowing and later wilting of the leaves, delayed growth, and reduced seed production. The pathogen is an obligate biotroph, which implies that it depends entirely on its host plant for survival and reproduction without causing the host plant to undergo senescence (Coates & Beynon, 2010).

H. arabidopsis is an oomycete, a fungus-like microorganism that is commonly found in soil, plant tissues, and aquatic environments (Thines, 2018). However, these are more closely related to brown algae and diatoms than to fungi (Tomé et al., 2014). Oomycetes are characterized by their filamentous structure, consisting of branching hyphae, and their capacity to reproduce sexually as well as asexually (Koch & Slusarenko, 1990), thus producing motile zoospores or sporangiophores equipped with a flagellum (Desjardins et al., 1969). Unlike fungal microorganisms, oomycetes possess a cellulose cell wall instead of a chitin cell wall (Thines, 2018). Notably, oomycetes are frequently plant pathogens, and *Phytophthora infestans*, causing the Irish potato famine (1845 – 1852; Schoina & Govers, 2015), is perhaps the most well-known among them, leading to the death of approximately one million Irish citizens (Fones et al., 2020).



Figure 2: *Hyaloperonospora arabidopsis* infected *A. thaliana*. The wilting of the leaves is visible as white dust-like particles on the surface of plant tissue after 7 days.

2.2.1 The infection mechanism of *H. arabidopsis*

The contact between a zoospore and plant material is commonly referred to as the start of the Hyaloperonospora infection and is made possible by spore dispersal through environmental factors such as wind and rainfall (McDowell et al., 2011). Spores contain specific molecules known as pathogen-associated molecular patterns (PAMPs) that can be detected by the host plant's pattern recognition receptors (PRRs), initiating an immune response by the adaptive (acquired) immune system (Fantozzi, 2016). Consequently, the spores will also detect chemical signals in the form of host-associated molecular patterns (HAMPs) from the presence of plant material (Bailey et al., 2011), resulting in spore germination and formation of a so-called germ tube (Telli et al., 2020). This tube then forms appressoria, specialized structures that use a combination of mechanical pressure and cell wall degrading enzymes such as cellulases to penetrate the host's epidermal cell layer (Grenville-Briggs & Van West, 2005). Once inside the tissue, Hyaloperonospora species typically form "intercellular" haustoria, formed in the intercellular spaces between plant cells (Ried et al., 2019). The haustoria of Hyaloperonospora are conventionally branched, finger-like structures that penetrate the host plant tissues and extract nutrients from the host cells (Whisson et al., 2007). Due to this invasive growth, plant cell functions are disrupted causing cell death and disease symptoms such as "white rust" and yellow leaf spots due to disruption of chloroplasts (Kaur et al., 2011). Eventually, after enough nutrients are collected, the necrotrophic phase is initiated and specialized structures called sporangia are formed extracellularly containing numerous asexual zoospores (Pfeufer & Harrison, 2022). These are then released to trigger new infections, either in the same or on another host plant.

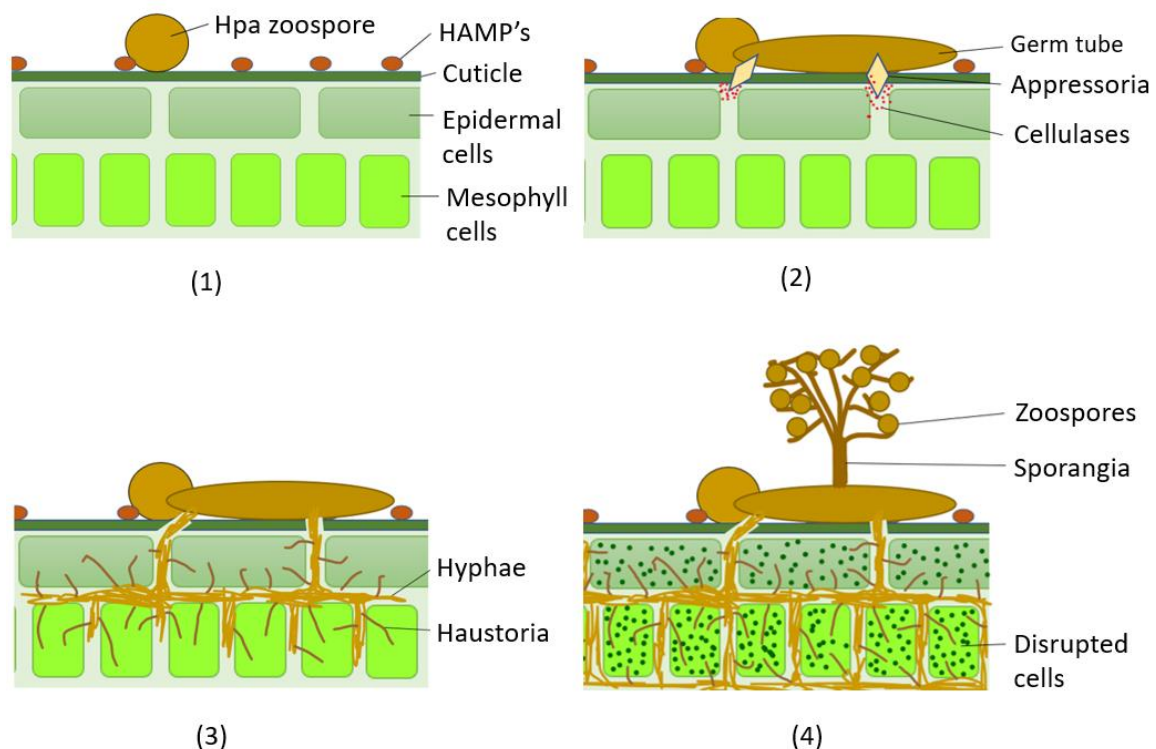


Figure 3: Infection stages of *H. arabidopsis*. (1) *H. arabidopsis* zoospore contacts plant tissue, picking up HAMP signals to start germination. (2) The germ tube has formed, producing appressoria that penetrate the plant's epidermal layer. (3) Intracellular hyphae are formed, creating haustoria that extract nutrients from host cells. (4) When enough nutrients are collected, sporangia are developed containing zoospores (Adapted from Ried et al., 2019).

2.2.2 The economic relevance of downy mildew pathogen infections

Hyaloperonospora arabidopsidis, is a serious threat to agriculture and the global food supply. It affects a wide range of crops, including grapes, lettuce, cucumber, onions, and cruciferous vegetables such as broccoli and cauliflower (Thakur & Mathur, 2002). In 2015, crops that are susceptible to downy mildew plant pathogens were worth at least \$7.5 billion (€ 7 billion) of the United States agriculture economy (USDA, 2015) and will be higher today (2023) (Crandall et al., 2018).

Downy mildew can significantly reduce crop yields and quality, leading to economic losses for the agricultural industry as a whole. The pathogen infects multiple plant parts and causes chlorosis, the loss of green colouration of leaves, as well as necrosis of cells, both leading to a reduction in photosynthetic activity (Mandal et al., 2009). The infected plants also become more susceptible to other diseases and pests, further reducing their economic productivity (Magyarosy et al., 1976).

The severity of downy mildew infections depends on various factors, including the crop species, the stage of growth, the weather conditions, and the virulence of the pathogen (Lebeda & Cohen, 2011). In some cases, the disease can cause complete crop failure, resulting in a total loss of income for farmers. For example, downy mildew in grapes can lead to reduced berry size, delayed ripening, and reduced sugar content, resulting in lower yields and inferior wine quality (Rossi et al., 2008) almost destroying the entire wine industry in France in the 1980s (Gessler et al., 2011). For example, a severe outbreak of downy mildew in a vineyard can result in up to 50% yield losses, which can translate into significant economic losses for grape growers (Travadon et al., 2013)

The economic losses associated with downy mildew infections can be substantial, affecting not only farmers but also consumers and the broader economy. The costs of disease control measures, such as fungicides, labour, and equipment, can be high, increasing the production costs for farmers and reducing their profitability (Lhermie et al., 2020). In some cases, farmers may also experience reduced demand or lower prices for their products due to the reduced quality and yields caused by the disease (Pimentel et al., 1992).

The economic impact of downy mildew can be particularly severe in developing countries such as Nepal (Atreya et al. 2012), where small-scale farmers may have limited resources and access to disease control measures. In these regions, downy mildew can lead to food insecurity, poverty, and social instability, exacerbating the already challenging economic conditions. For example: In the mid-1970s, the loss of corn to downy mildew in the Philippines was estimated at \$23 million (€ 21,6 million; USDA, 2013)

2.3 Measures to control infectious diseases in agriculture

Controlling the spread as well as the number of infections due to downy mildew is critical to minimizing the economic impact on agriculture and ensuring food safety. Measures that farmers can take to manage disease include cultural practices, chemical control, and biological control (Alabouvette et al., 2006).

2.3.1 Cultural practices

Cultural practices are conventional methods that are not pathogen-specific and are commonly employed to produce healthy plants. These methods entail crop rotation, pruning, and removal of infected plant debris, among others, to curtail the spread of diseases to healthy plants. Long-term crop rotation, when complemented with resistant cultivars, such as maize, can forestall the development of a primary inoculum for most soil-borne diseases (Guillemaut, 2003). Proper application of cultural practices reduces the need for chemical and biological control to combat disease (Alabouvette et al., 2006).

2.3.2 Chemical control measures

The most effective and commonly used method for controlling downy mildew is chemical control through the use of fungicides. For instance, in 1996, fungicides used for downy mildew control represented 16.7% of the global fungicide market sales amounting to 7.2 billion SFr (€ 7.2 billion) (Gisi, 2002). These fungicides can prevent or eliminate pathogen infection in plants. However, their effectiveness is countered by their negative impact on the environment, human health, and food safety (Chambers et al., 2014). The use of fungicides causes low specificity and low accuracy. Low specificity results in biodiversity loss since not only pests but also beneficial or rare organisms are killed, such as rare butterfly species (Beketov et al., 2013), leading to a decline in diversity or a shift in species population. Low accuracy causes fungicides to be disposed of in areas other than their intended targets due to wind or precipitation, with 85-90% of chemicals not reaching their intended targets (Repetto et al., 1996).

Exposure to fungicides can result in a range of health issues, such as acute toxicity, chronic toxicity due to long-term exposure (e.g., farmers and factory workers), and allergic reactions that cause rashes and respiratory problems (Saunders & Watkins, 2001). While fungicides mostly improve food safety by preventing the production of toxic mycotoxins by certain species, such as *Aspergillus flavus*, which produces carcinogenic aflatoxins (Arrus et al., 2005), they can also have negative effects on food safety by leaving residues that can be transferred to food products (González-Rodríguez et al., 2008). To address this issue, the European Food Safety Authority (EFSA) sets strict maximum residue limits (MRLs) for agricultural food products. Moreover, improper use of fungicides can lead to the development of fungicide-resistant fungal strains, which can reduce the effectiveness of fungicides in controlling fungal diseases (Van Den Bosch et al., 2011).

2.3.2.1 Commercial fungicide: Duaxo spray (COMPO)

COMPO Duaxo spray is a commercially available fungicide spray that is specifically made for ornamental plants such as roses but can also be used for other plants such as *A. thaliana*. It contains 2 main compounds: active ingredient difenoconazole and preservative 1,2-benzisothiazolin-3-one (COMPO, n.d.). Due to its commercial availability and active ingredients that are commonly used in

Difenoconazole

Difenoconazole is a broad-spectrum fungicide used to control a wide range of fungal diseases in various crops, including cereals, fruits, vegetables, and ornamental plants (Hua et al. 2020). It is often used preventatively, before the onset of disease symptoms, to protect crops from fungal infections (Mondino et al., 2015).

It belongs to the class of triazole fungicides and works by cutting off the biosynthesis of ergosterol, which is an important compound for maintaining the structure and integrity of the fungal cell membrane. Without it, the cell membrane becomes more permeable and less able to function properly (Worthington, 2012).

By inhibiting the activity of the C14-demethylase enzyme, difenoconazole prevents the formation of ergosterol, which leads to the accumulation of other sterols that are less effective at maintaining the structure of the fungal cell membrane. As a result, difenoconazole disrupts the cell membrane of the fungus, causing it to leak essential nutrients and leading it to apoptosis (Worthington, 2012; Lamberth et al., 2021).

It is considered relatively safe for humans and the environment when used according to the manufacturer's instructions. However, it is important to follow proper safety precautions when handling and applying difenoconazole to avoid any potential health risks. Difenoconazole, like most pesticides, can pose health risks to humans if it is not used properly (Bozdogan, 2014). The level of risk depends on the amount and duration of exposure, as well as the way of contact: inhalation of difenoconazole can cause irritation of the respiratory system, such as coughing and wheezing, and may lead to more serious respiratory problems with prolonged exposure (Voiculescu et al., 2022). Skin contact with difenoconazole may cause skin irritation or rash, and eye contact can cause irritation or redness (Alshammari et al., 2021). Ingestion of difenoconazole can cause gastrointestinal symptoms such as nausea, vomiting, and diarrhea, and may be toxic to the liver by inducing oxidative stress in liver cells (Song et al., 2020).

Long-term exposure to difenoconazole may cause adverse health effects, including reproductive and developmental effects, cancer, and damage to the liver and kidneys due to carcinogenic stereoisomers of the compound (Voiculescu et al., 2022). Therefore, it is important to follow proper safety precautions when handling and applying difenoconazole, such as wearing protective clothing, using appropriate equipment, and avoiding unnecessary exposure (Bozdogan, 2014).

It is also important to note that difenoconazole can be toxic to non-target organisms (Bozdogan, 2014). They have been proven to be growth-inhibiting and cardiotoxic for fish, mice, and aquatic invertebrates (Mu et al., 2013; Lin et al., 2021), and can cause harm to the environment if not used responsibly (Hua et al. 2020).

1,2-benzisothiazolin-3-one (BIT)

1,2-benzisothiazolin-3-one, synonymously referred to as BIT, is a synthetic biocide that is commonly used as a preservative in various industrial and consumer products. It is effective against a wide range of microorganisms, including bacteria, fungi, and algae (Cheng et al., 2020). Specifically inhibiting the activity of certain enzymes that are essential for the growth and survival of these microorganisms such as sulfhydryl and metalloenzymes by penetrating the cell membrane (Wang et al. 2019; Kim et al., 2014). These enzymes engage in critical metabolic processes such as respiration, energy production, and protein synthesis, and their inhibition can lead to apoptosis. An example of this is the inhibition of active transport and oxidation of glucose (Fuller et al., 1985).

BIT can pose some health risks to humans if it is not used properly or if there is exposure to high concentrations. The level of risk depends on the amount and duration of exposure, as well as the method of application. Skin contact with BIT can cause skin irritation, allergic reactions, and dermatitis, particularly when used in high concentrations or when applied directly to the skin (Gruvberger et al., 2018). Inhalation of BIT can cause respiratory irritation, including coughing and wheezing, and can exacerbate pre-existing respiratory conditions (Chew & Maibach, 1997). Ingestion of BIT can cause gastrointestinal symptoms such as nausea, vomiting, and diarrhea (Pel, n.d.). As such, it is important to follow proper safety precautions when handling and using products containing BIT, including wearing protective gloves and ensuring proper ventilation.

In addition, BIT can be toxic to aquatic organisms and should be disposed of properly to avoid environmental contamination. It is important to note that overuse or misuse of BIT can contribute to the development of antimicrobial resistance (Furumuma et al. 2014). Therefore, it is important to follow proper handling procedures when using products containing BIT and avoid unnecessary use.

2.3.3 Biological control measures

Biological control involves several biological processes to combat pathogenic growth, such as (i) using microbial antagonists, or natural enemies of the pathogen, (ii) beneficial microbes, (iii) genetic manipulation, and (iv) biological compounds like biostimulants to reduce disease severity (Alabouvette et al., 2006).

- (i) Microbial antagonism includes the addition of parasitic organisms of the plant pathogen such as fungi like *Trichoderma* to eliminate *Rhizoctonia solani* (Chet & Baker, 1981). Alternatively, antibiosis is a possible option, in this process, a secondary metabolite is produced by the antagonist that is toxic to the target microorganism (Weller & Thomashow, 1993). Another way of implementing microbial antagonism is the use of microorganisms that share the same ecological niche as the pathogen by competing for physiological requirements such as nutrients (Alabouvette et al. 2006).
- (ii) Beneficial microbes are microorganisms that are used in agriculture, providing crops with various benefits (e.g., improved crop yield). These are either naturally occurring in soil or added as part of a microbial inoculant (Santos et al., 2019). An example would be symbiotic arbuscular mycorrhizal fungi, increasing phosphorus uptake in return for plant carbohydrates (Benami et al., 2020).

- (iii) Further, genetic manipulation can be used to increase disease resistance. These mostly cause overexpression of pathogen resistance-related genes such as chitinase (Bliffeld et al. 1999) breaking down chitin, the main component of fungal cell walls, leading to lysis and eventually death of the fungal cells (Vega & Kalkum, 2012). However, the European Union (EU) has strict regulations in place regarding genetically modified organisms (GMOs). These regulations are intended to protect the environment and human health, as well as the safety of the food supply, but also making the use of GMOs particularly hard (GMO legislation, n.d.).
- (iv) Lastly, biostimulants are biological substances or microorganisms that are applied to plants to improve their growth, health, and productivity. These can be any biological component as long as they have a desired effect such as enhancing nutrition efficiency, abiotic stress tolerance, pathogen resistance, and crop quality traits (Du Jardin, 2015).

2.4 Pathogen resistance mechanisms in plants

Plants possess a diverse array of defence mechanisms to combat pathogenic organisms and environmental stressors, including both abiotic and biotic stresses (Rausher, 2001). Similar to humans, plants possess both innate and adaptive immune systems, where the former provides general defences against all harmful stimuli, while the latter is specific to the type of stress and is only activated upon infection or stimulation (Kyralli et al., 2007). Due to their inability to move away from harmful stimuli, plants are reliant on their innate and acquired immune responses to protect themselves.

2.4.1 Innate plant immune system

Pathogenic organisms are initially faced with physical barriers when attempting to invade plants, such as the cuticle, trichomes, and thick cell walls, which can prevent attachment to the plant's exterior or the penetration of the outer layer (Miedes et al., 2014). Additionally, spores can be trapped, preventing their movement (Gupt et al., 2021). Furthermore, plants synthesize a variety of chemical compounds, often secondary metabolites, which are present on their outer and intercellular surfaces, delaying pathogenic growth and even exhibiting toxic effects (Piubelli et al., 2004). One well-known group of these compounds is alkaloids, which are nitrogen-containing organic molecules that exhibit a broad range of effects on invasive organisms, often with fungicidal and antibacterial properties. Another type of compound metabolized by *A. thaliana* is terpenoids, which are hormonal compounds with antimicrobial, antifungal, and anticancer properties that could serve as natural pesticides or pharmaceuticals (Kamran et al. 2022; Zacchiono et al. 2017).

2.4.2 Acquired plant immune system

The acquired immune system of plants consists of a wide variety of different signalling pathways contributing to a targeted reaction aimed at a specific infection. A plant's acquired immune system can be split up into two subcategories, its systemic acquired resistance (SAR) and its induced acquired resistance (IAR) (Kamle et al., 2020). Both are initiated upon infection or contact with elicitors such as salicylic acid, which is a plant hormone that is produced in

response to infection or stress (Ali et al., 2018). The only difference between them is their intended way of defence. SAR is identified by its direct effect on the invading organism, triggering the production of components such as phytoalexins, having antimicrobial activity and inhibiting the growth of pathogens (Hammerschmidt, 2009), as well as reactive oxygen species (ROS), damaging the pathogen's cell walls and membranes, making them more susceptible to other defence mechanisms (Gadjev, 2006). IAR on the other hand does not depend on direct elimination or inhibition of the invading pathogen but rather on increasing the physical or chemical barrier of the host plant (Kamle et al., 2020). An example of this would be the formation of lignin barriers, a structural polymer, around infected cells to prevent the spread of for example fungal cells. Another example is callose deposition, a polysaccharide that can trap pathogenic spores (Lee et al., 2019).

2.5 Biostimulant treatments

Biostimulants are biological substances or microorganisms that are applied to plants to improve their growth, health, and productivity. These can be any biological component as long as they have a desired effect such as enhancing nutrition efficiency, abiotic stress tolerance, pathogen resistance, and crop quality traits (Du Jardin, 2015). Biostimulants do not primarily contain any plant nutrients such as nitrogen, phosphorus, or potassium, but rather contain substances that enhance plant growth and development (Sible et al., 2021). The main categories are humic acids, seaweed extracts, and protein extracts containing functional amino acids and peptides (Du Jardin, 2015).

In terms of pathogen resistance increasing effects, there are a couple of differences between biostimulants, and conventional pesticides are. The first difference in between biostimulants and pesticides is their mode of action: conventional pesticides target microorganisms such as pathogens by inhibiting their growth (Stoytcheva, 2011) while biostimulants enhance intracellular processes to stimulate pathogen resistance (Du Jardin, 2015). Biostimulants have thus a positive effect on their target while pesticides have a negative effect. Another difference is composition: traditional pesticides are typically composed of synthetic and/or chemical compounds (Alghamdi et al., 2020), often having low biodegradation efficiency (Lapertot et al., 2006) and toxic effects concerning the immediate environment (Mahmood et al., 2016). Due to this discrepancy, another key difference arises, namely the disparity in regulation: while pesticides are heavily regulated and are obliged to undergo heavy testing, biostimulants are currently unregulated in most countries (Mrid et al., 2021).

2.5.1 Humic acids as biostimulants

Humic acids (HA), also including fulvic acids, are aromatic organic compounds that are formed during composting processes through the breakdown of plant and animal material by microorganisms in the soil (Steelink, 1963). During the composting process, organic compounds undergo rapid degradation until biological stability is reached. Afterward, a curing phase is initiated in which recalcitrant organic compounds, compounds that have a high resistance to biodegradation (Knapp & Bromley-Challoner, 2003), are further transformed into humic substances, being humic and fulvic acids (Palumbo et al., 2018). These two types of humic substances can be characterized by solubility: while humic acids are only soluble in water with low acidity (high pH), fulvic acids are soluble in water of all different pH values

(Canellas et al., 2015). Also, fulvic acid generally contains less aromatic carbon as well as fewer free radicals leading to an overall lower reactivity compared to humic acids (Bernoux & Cerri, 2005).

The functional benefits of humic substances regarding plants can be reduced to their high ion exchange capacity (IEC). This is a measure of a compound's ability to exchange ions with its environment, absorbing the respective molecule. In the case of humic substances, the capacity can vary depending on the specific functional groups present in the molecule (Meléndrez, 2020), either being able to bind positively charged cations (e.g. Fe^{2+}) or negatively charged anions (e.g. phosphate) (Pandey et al., 2000).

For example, humic substances may contain carboxylic acid ($-\text{COOH}$) functional groups, which are electronegative due to the presence of the oxygen atom, making these molecules more acidic and reactive to other compounds in the environment (De Melo et al., 2016). Similarly, humic substances may contain amino ($-\text{NH}_2$) or amide ($-\text{CONH}_2$) functional groups, which are generally less electronegative compared to carboxylic acid groups (Prilutskaya et al., 2019). These functional groups can form hydrogen bonds with water making the components soluble and can also be a chelation site for metal ions (Bocanegra et al., 2006), being an important source of metal ions such as magnesium (Mg^{2+}), necessary for fundamental physiological and biochemical processes such as chlorophyll synthesis (Wang et al., 2017) as well as iron ions (Fe^{2+}) (Bocanegra et al., 2006). In the roots of a plant, positive ions such as hydrogen are pumped away giving the root a slight negative charge, increasing the uptake of positive cationic nutrients attached to humic substances, leading to a more positive root and an increased uptake of anionic nutrients (Meléndrez, 2020).

The compounds can also be taken up via leaves in a process called foliar feeding. This process overarches multiple mechanisms such as cuticular penetration or diffusion, in which humic substances penetrate the waxy cuticle layer of plant leaves and enter the leaf tissue (Smilkova et al., 2019). Humic substances can thus be seen as some kind of water-soluble balls of plant nutrients that can easily be taken up via roots or leaves, enhancing several plant characteristics such as increased growth (Canellas et al., 2015).

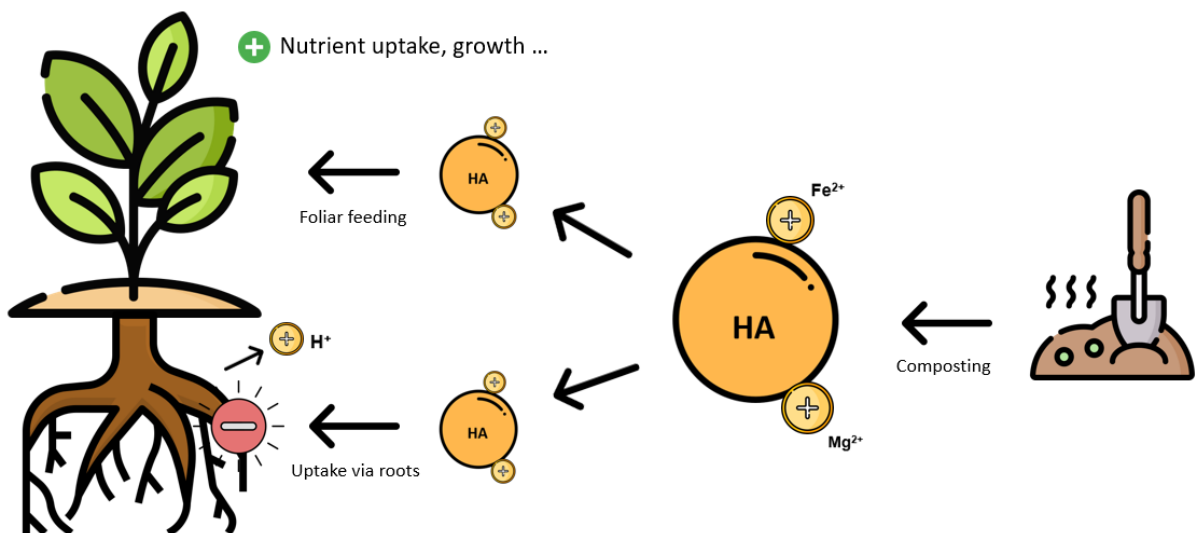


Figure 4: Overview of the working principle of humic substances (HA). Humic acids are extracted from compost, containing metal ions, and can be taken up by plants via foliar feeding or root uptake. These positive ions will neutralize the negative load in the roots, increasing absorption of negatively charged nutrients and resulting in increased growth (Adapted from Meléndrez, 2020).

2.5.2 Protein hydrolysates as biostimulants

Protein hydrolysates (PH) are non-microbial organic compounds that are mainly consisting of a mixture of peptides and amino acids. These compounds are the result of several enzymatic hydrolysis steps during the degradation of plant- or animal-derived materials such as soy or malt extract (Colla et al., 2015). After uptake via plant roots or leaves, protein hydrolysates have been shown to increase iron and nitrogen metabolism, water uptake, nutrient uptake as well as nutrient usage efficiency (Cerdán et al., 2009). Also, changes in root architecture were observed, leading to an increase in the number of lateral roots as well as an increase in nutrient uptake (Ertani et al., 2009).

Effects of these compounds can be divided into 2 groups: direct and indirect effects. Direct effects can for instance be the increase in metabolic capabilities and processes due to extensive root formation (Colla et al. 2015, Ertani et al., 2017). Other examples of a direct effect can be enhanced photosynthesis due to increased chlorophyll production as well as increased protein production due to the uptake of amino acids and peptides from the protein hydrolysates (Rouphael et al., 2017). Indirect effects can also be present and are more difficult to track. An example of an indirect effect is the ability of protein hydrolysates to stimulate the growth and activity of beneficial soil microorganisms that participate in nutrient cycling, leading to increased plant health and growth (Kauer et al. 2021). The protein hydrolysates can also contain certain peptides that can serve as signalling molecules, triggering cascades that can result in plant responses such as increased growth, stress tolerance as well as disease resistance (Colla et al. 2015). These can even trigger the activation of certain genes that engage in stress responses, leading to improves performance under suboptimal conditions (Ertani et al., 2017).

The two types of protein hydrolysates that are examined in this paper are commercial soy as well as malt extract. The last one being a concentrated solution of malted grains, obtained from malt grains that have been allowed to germinate by being soaked in water and then dried and grinded into a powder. Protein hydrolysates can be added to the leaves to be taken up by cuticular penetration or to the soil to be taken up by the root epidermal cells (Paul et al., 2019).

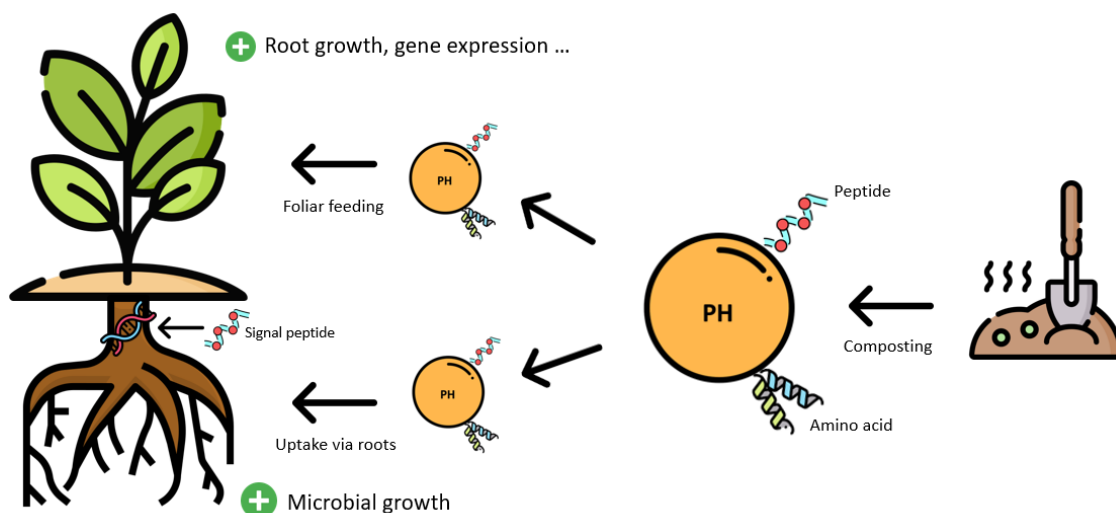


Figure 5: Overview of the working principle of protein hydrolysates (PH). These compounds are extracted from plant- or animal-derived material by composting and contain certain peptides and amino acids. These can be taken up by plants via foliar feeding or root uptake and can trigger cellular cascades resulting in increased root growth and increased resistance gene expression (Adapted from Colla et al., 2015).

2.5.3 Seaweed extracts as biostimulants

A third and last kind of biostimulant that will be assessed are the Seaweed extracts (SW). These are non-microbial compounds extracted from various kinds of algae and contain a mix of bioactive compounds such as polysaccharides, proteins, vitamins, minerals, and plant growth regulators like cytokinins (Chojnacka et al., 2012). These seaweed extracts are mostly coming from red, brown, and green macroalgae, of which the brown macroalgae such as Laminariales (kelp) are mostly used in agriculture and horticulture (Wiencke et al., 2014).

Next to providing plants with essential nutrients such as amino acids and vitamins, the main objective of most seaweed extracts is to provide the plant with growth hormones such as cytokinins and auxins (Stirk & Van Staden, 1996).

Cytokinins are important growth hormones that are produced naturally in distinct parts of the plant but can also be produced synthetically (Mok, 2019; Oshchepkov et al., 2020). These stimulate several processes such as cell division and differentiation of cells in plant meristematic tissue (Ioio et al., 2007), development of organelles such as chloroplast and delaying the senescence of plant tissue, leading to higher stress tolerance (Walters & McRoberts, 2006). Auxins are also plant hormones but are mostly produced in young plant tissues such as the shoot apex and developing leaves (Shimizu-Sato et al., 2009). They are also involved in the process of plants' phototropic bending by developmental plasticity to photoreceptor signals toward light to have higher photosynthesis efficiency (Küpers et al., 2020). Auxins play a vital role in regulating cell elongation in the stem and roots of plants, this is a process that is used for the enlargement of cells and is initiated after cell differentiation, which is regulated by cytokinin (Evans & Cleland, 1985). Seaweed extracts can thus be seen as compounds coming from algae containing nutrients as well as hormones such as cytokinin and auxin that induce a cascade of events such as increased plant growth, higher stress tolerance and a delay in senescence.

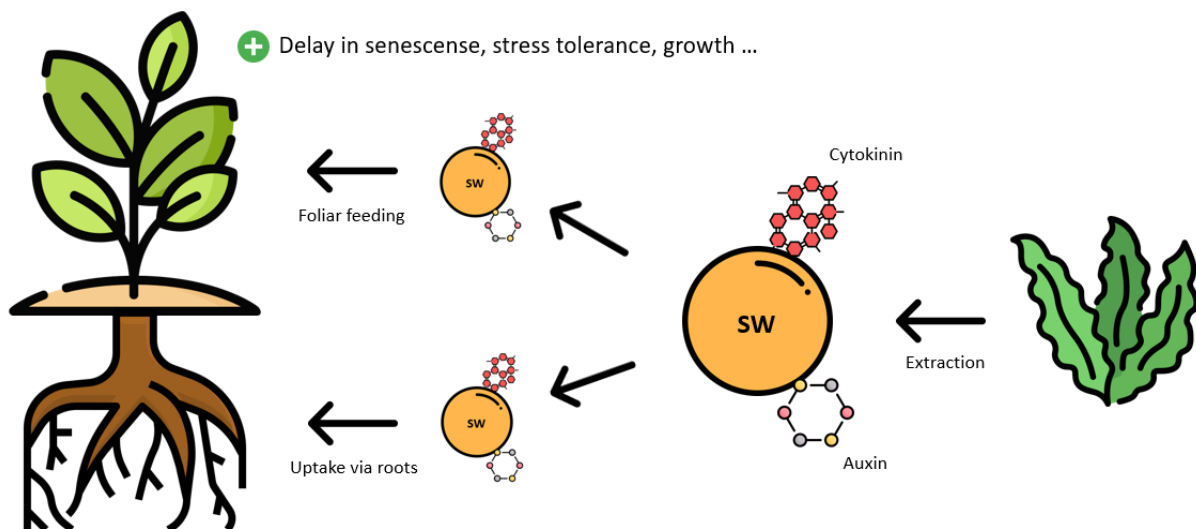


Figure 6: Overview of the working principle of seaweed extracts (SW). These compounds are extracted from seaweed (*Ecklonia maxima*) and contain important plant hormones such as cytokinins and auxins that can be taken up via the plant's roots or via foliar feeding, resulting in effects like delayed senescence and higher stress tolerance (Adapted from Chojnacka et al., 2012).

2.6 Quantifying disease resistance in model plants

Several methods can be used to quantify disease resistance, three of them are discussed below. These are all used to monitor the progression of infection by measuring the amount of pathogen over time to examine the effectiveness of certain treatments, in this case, the addition of biostimulants (Brouwer et al., 2003).

2.6.1 Pathogenic effect quantification: infection scoring

The first method of disease quantification is a straightforward one: numerical values are assigned to various disease symptoms, such as leaf spots, necrosis, and chlorosis. These values can then be used to calculate an overall disease severity score, providing information on the increase or decrease in disease resistance of a certain treatment (Fetch et al., 1999). One example of a plant disease scoring system is the Horsfall-Barratt scale, which was developed in the 1940s and is still used today. The Horsfall-Barratt scale assigns numerical values to disease symptoms based on their severity, ranging from 0 (no symptoms) to 9 (complete plant death) (Horsfall & Barratt, 1945).

However, several studies have shown that there is not always a direct correlation between disease symptoms and actual infection progression (Bent et al., 1992; Hoffman et al., 1999). Another concern is that different observers might assign varying scores for the same result due to different training, experience, or perception (Graham & Madden, 2014). Also, the scoring of an infection may not accurately reflect the actual impact of the plant's growth or yield, being a poor indicator of straightforward the effect of certain treatments (Savary et al., 2012). These reasons being why infection scoring will not be conducted in this thesis.

2.6.2 Pathogenic spread quantification: spore count

Hyaloperonospora arabidopsidis produces motile zoospores or sporangiophores that are equipped with a flagellum (Desjardins et al., 1969). Counting these spores is a widely used method to determine and quantify the severity of plant diseases, being a good indicator of pathogen growth and especially sporulation (Tomé et al., 2014). The number of sporangiophores being inversely proportional to the disease resistance of the plant and thus also a good way to examine the reduction in disease severity due to the addition of different bio stimulants. The quantification method involves sampling tissue such as leaves from an infected plant, placing it into a water solution, vortexing it to allow the spores to be released, and then counting the spores using a hemacytometer (Tomé et al., 2014). In this way, a concentration of a number of spores per millilitre is created that can be used to determine the level of disease severity (Madden et al., 2007; Bock et al., 2017).

One of the main advantages of spore count disease quantification is that it provides a cheap, easy, straightforward, and accurate measure of disease severity. However, counting the cells is a time-consuming and demanding job. Also, spore count disease quantification may not provide a complete picture of the severity or extent of the disease. While spore counts can indicate the presence of a disease, they may not provide information on the extent of the damage or the impact on plant health (Niemeier et al., 2006). Lastly, it is only applicable to spore-producing pathogens with its accuracy depending on the correlation between the number of sporangiophores and the infection itself (Roberts, 1995).

2.6.3 Pathogenic biomass quantification: quantitative polymerase chain reaction (qPCR)

Quantitative polymerase chain reaction (qPCR) is a powerful molecular biology technique that can be used to quantify the amount of a specific DNA sequence in a sample. In plant pathology, qPCR has emerged as a valuable tool for detecting and quantifying plant pathogens (Venbrux et al., 2023), as well as for monitoring disease progression and assessing the effectiveness of disease management strategies (Leboldus & Isabel, 2018). One of the key advantages of qPCR is its high sensitivity and specificity, which allows for the accurate detection and quantification of low levels of pathogen DNA in plant tissues (Sчена et al., 2013). qPCR is based on polymerase chain reaction (PCR) that makes use of a Taq-polymerase, Deoxynucleotide triphosphates (dNTPs), primers, a buffer solution, template DNA and a thermocycler.

2.6.3.1 Primer design

Primer design is an essential step in qPCR since effective primer design can determine the success of an experiment (Dieffenbach & Dveksler, 2009). Therefore, primers need to meet some conditions: first of all, to avoid non-specific amplification, the primers should be specific to the target sequence and not bind to any other non-target. This can be achieved by making use of long primers as well as using BLAST (Basic Local Alignment Tool) to check possible matches (Ye et al., 2012).

Further, length is important since longer primers provide higher specificity but have a lower amplification efficiency. Therefore, a good length for primers is generally around 18 to 30 bases (Behind the Bench Staff, 2019). Additionally, the melting temperature (T_m) of the primers should be around the same temperature. If the primers have different T_m values, one primer may anneal preferentially over the other, leading to unequal amplification of the target sequence resulting in a reduction of amplification efficiency (Bustin, 2010).

Another condition is that the primers cannot be complimentary since this will lead to the formation of primer dimers, lowering amplification efficiency (Rychlik, 2007). For an optimal reaction, the primers should have a GC content between 40 and 60% since primers with a low GC content may not bind strongly enough to the target sequence, while primers with a high GC content may form stable secondary structures, which can interfere with binding and amplification (Tsuchiya et al., 2015). Also, it is recommended to choose a primer with a 3' end ending with a G or a C, known as a GC-clamp, to increase the stability of the complementary bond with the target DNA and prevent loose ends (Behind the Bench Staff, 2019).

2.6.3.2 The use of fluorescent dyes in qPCR

Fluorescent dyes are widely used in quantitative polymerase chain reactions (qPCR) to enable real-time monitoring of the amplification process. These dyes emit a fluorescent light signal that is proportional to the amount of amplified DNA and can be detected, allowing for precise quantification of target sequences (Bustin et al. 2009). The two most frequently used methods of quantification are (i) SYBR®-green and (ii) TaqMan assays (Cao & Shockey, 2012).

- (i) SYBR®-green is a double-stranded DNA binding dye that intercalates between the base pairs of the amplified double-stranded DNA (dsDNA) during PCR amplification due to its planar structure (Fig. 7). When intercalated, the dye will emit a fluorescent light that can be detected and is proportional to the amount of DNA at a given moment during the PCR as products are generated (Chen et al., 2019). Advantages of SYBR®-green are that it can be easily used in any qPCR reaction since it does not require a specific sequence to hybridize to. Also, it is relatively cheap compared to probe-based assays (Tjadini et al. 2014). A major drawback of the SYBR®-green assay is that the dye is nonspecific and can thus generate false positive signals due to nonspecific products like primer dimers.
- (ii) TaqMan probes are single-stranded oligonucleotides that are designed to specifically bind to a complementary target single-stranded DNA (ssDNA) sequence during PCR amplification. The probe contains a fluorophore and a quencher molecule that prevents fluorescence until the quencher molecule is cleaved off during amplification by the 5'–3' exonuclease activity of Taq polymerase (Cao & Shockey, 2012). The main advantage of using a probe-based assay like TaqMan is that unlike with SYBR®-green assays, only target DNA will give a fluorescent signal due to the specific binding of the probe onto target DNA, leading to an increased specificity (Arikawa et al., 2008). However, this increase in specificity also leads to an increase in price per PCR reaction, as well as more preparation since a sequence needs to be chosen on the PCR product for the probe to hybridize to. Also, the probes need to be ordered from an external company, which takes a couple of days (Tjadini et al. 2014; Arikawa et al., 2008).

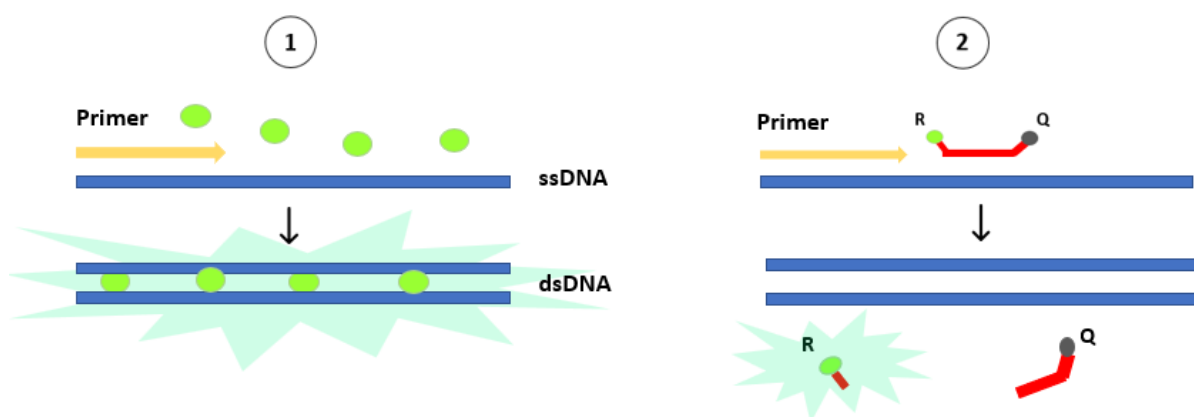


Figure 7: Working principle of SYBR®-green and TaqMan probes. SYBR® Green (1) is an intercalating dye that inserts into dsDNA and will emit a fluorescent signal. The TaqMan probe (2) binds to a complementary ssDNA amplicon after which the primer elongation will result in the cleavage of the reporter and initiate a fluorescent signal (Adapted from Mészáros, 2022.)

2.6.3.3 Data analysis of qPCR results

The fluorescent signal produced by the samples is converted into a cycle threshold (Ct) value, which is defined as the cycle number at which the fluorescence signal generated by the amplification of the target nucleic acid crosses a threshold level that is set above the background fluorescence (Bustin et al., 2009). In this way, we get a relative value that is inversely proportional to the initial amount of target DNA which can be examined in 2 different ways, using either relative or absolute quantification.

Relative quantification

Relative quantification can be done using the $2^{-\Delta\Delta C_T}$ -method (Livak & Schmittgen, 2001) which gives a number that represents the fold change in the presence of pathogen DNA. This method is mostly used in gene expression assays but can also be used for disease quantification. Concretely, a $2^{-\Delta\Delta C_T}$ value of 1 indicates an equal amount of amplicon regions between the control and treatment samples. A value of 2 would indicate a two-fold increase in amplicon regions in the treatment sample compared to the control, while a value of 0.5 would indicate a two-fold decrease in gene expression in the treatment sample compared to the control. The formula for calculating $2^{-\Delta\Delta C_T}$ is as follows:

Equation 1: $2^{-\Delta\Delta C_T}$ -method

$$2^{-\Delta\Delta C_T} = 2^{-(CT, \text{target} - CT, \text{reference}) \text{ sample2} - (CT, \text{target} - CT, \text{reference}) \text{ sample1}}$$

Absolute quantification

To get an absolute DNA concentration, a calibration curve needs to be constructed. This is done by taking one of the DNA samples and making a dilution series. The DNA content of each sample is then measured via a mySPEC microvolume spectrophotometer (VWR, n.d.), and all dilution series samples are treated in the same way as normal samples following the same preparation steps for qPCR as well as the qPCR itself (Bustin et al., 2009). The Ct values obtained from qPCR for each dilution are then plotted against the corresponding DNA concentration values, resulting in a calibration curve. This curve can then be used to determine the concentration of the target nucleic acid in unknown samples by filling the Ct values of the unknown samples in the equation of the calibration curve (Burns et al., 2005).

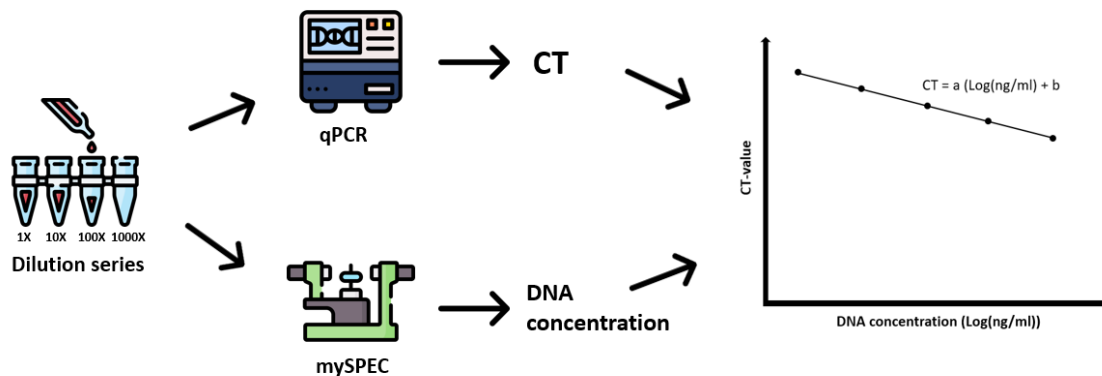


Figure 8: Working principle of calibration curve construction. Firstly, a dilution series is prepared that is then analysed via qPCR and mySPEC spectrometry, respectively resulting in Ct-values and DNA concentrations that can be plotted to form a calibration curve (Adapted from Burns et al. 2005).

Further, the quality of a PCR reaction can be determined by calculating the reaction efficiency, using equation 2, where "slope" is the gradient of the amplification curve in a qPCR assay (Ruijter et al., 2013). An efficient PCR reaction will have an E-value around 1, indicating that the target DNA sequence is doubling with each PCR cycle. A less efficient PCR reaction will have an E-value less than 1, indicating that the amplification of the target DNA sequence is slower or incomplete (Bustin et al., 2009). This could be due to the presence of contaminating or inhibiting components such as nucleases or salts coming from the DNA extraction (Farrar et al., 2015). An E-value of more than 1 is also possible, meaning that there was aspecific amplification of non-target DNA leading to an efficiency of over 100%. In general, an E value of 0,9 (90%) to 1,1 (110%) is considered to be a good range for PCR efficiency (Bustin et al., 2009; Ruijter et al., 2013).

Equation 2: Equation used to calculate amplification efficiency.

$$E = 10^{\left(-\frac{1}{\text{slope}}\right)} - 1$$

2.6.4 Assessing *A. thaliana* growth, productivity, and immune response to *H. arabidopsidis* by quantifying chlorophyll and carotenoid content

Chlorophyll is primarily found in plant leaves, supporting photosynthesis and thus energy production. Therefore, it is closely related to current plant biomass, leaf area, as well as nutrient uptake and biomass production. For that reason, absolute chlorophyll content can be used as a marker for plant growth (Al-Huqail et al., 2020). Plant growth can also easily be examined by dry weight after the infection period. However, dry weight might not be a reliable factor since it also includes the weight of debris, litter, and the pathogen biomass itself. Therefore, absolute chlorophyll content is a more appropriate indicator.

The relative chlorophyll content is the amount of chlorophyll that is present in a sample divided by the mass of the plant material in that sample. Higher relative chlorophyll content is associated with better photosynthetic performance and higher plant productivity. Reduced relative chlorophyll content may suggest a decline in plant health and productivity due to adverse conditions (Zhang et al., 2011). *H. arabidopsidis* invades the host plant's tissues, including the leaf mesophyll, and disrupts chloroplasts, leading to a decline in relative chlorophyll content and subsequently reduced photosynthetic activity (Tremblay et al., 2016). Therefore, it would be a requirement of a potential commercial biostimulant treatment that it allows the plant to have high photosynthetic performance while experiencing infection (Palta, 1990).

Another pigment that is found in plants are carotenoids, these play a crucial role in photosynthesis by absorbing light energy from regions of the spectrum that chlorophyll cannot absorb efficiently (Demmig-Adams et al. 1996). An interesting property of carotenoids is that they are not constitutively present in plants but are rather synthesised or upregulated in response to abiotic stress, including pathogen attacks (Wang et al. 2013). This inducible synthesis makes carotenoids reliable markers for plant defence mechanisms, as their presence or increased levels can indicate that the plant is actively responding to stress and defending itself against pathogens (Pintó-Marijuan & Munné-Bosch, 2014). Their induced production during stress is due to numerous resistance processes being initiated. An example of this is the production of phytoalexins, toxic compounds that are produced by the plant's

acquired immune system upon infection, that uses carotenoids as a precursor (Nishi & Kurosaki, 2012). Another example is the fact that carotenoids can serve as carriers for antipathogenic proteins as well as serve as antioxidants to neutralize reactive oxygen species (ROS), protecting plant cells from oxidative stress and accumulating at the infection site (Fiedor & Burda, 2014).

2.6.5 Defining the growth kinetics of an *H. arabidopsidis* infection

Infection growth kinetics in plants refer to the rate at which a pathogen spreads within a plant host over time. The kinetics of infection growth are influenced by various factors, including the characteristics of the pathogen, environmental conditions, and disease resistance, in which we are interested (Ghorbanpour et al., 2019). This is done by infecting plants with a pathogen and then taking samples at different time points. These samples will undergo a spore count and a qPCR to quantify disease severity and to set up a growth curve (Fig. 9) (Peleg & Corradini, 2011).

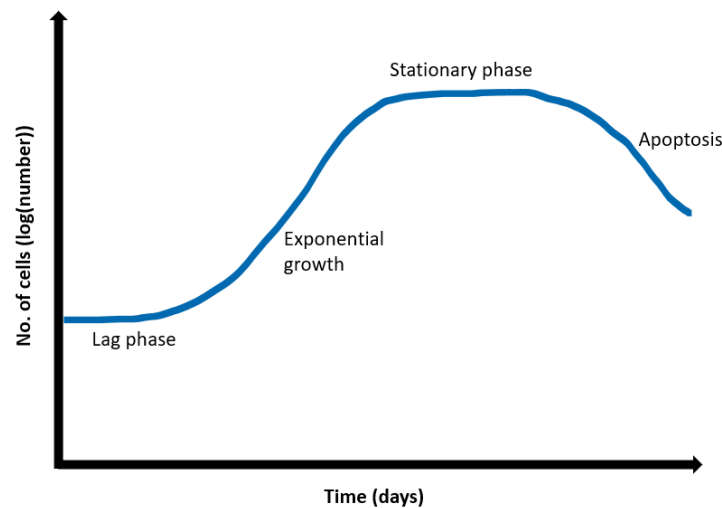


Figure 9: Infection growth curve. This growth curve contains four different phases: a lag phase in which the pathogen is acclimatizing (Ayala et al., 2021), an exponential growth phase in which the pathogen cells replicate, and the population size will undergo a constant increase (Quan et al., 2021), a stationary phase in which further population growth is limited due to shrinking nutrients as well as host deterioration (Varela et al., 2021) and finally the death phase in which the population declines due to the absence of nutrients and the accumulation of toxic components (Lu et al., 2021).

2.6.5.1 Defining the kinetic growth parameters

This growth curve will give useful information concerning pathogenic growth such as doubling time, growth rate, start of death phase, apoptosis rate and maximal pathogen load. These can be used to determine an increase or decrease in pathogen resistance of plants due to biostimulant treatments. Growth rate refers to the rate at which the number of oomycete cells in a population increases per unit of time. Doubling time refers to the amount of time it takes for a bacterial population to double in size. Both are inversely proportional to a plant's disease resistance (Kudela, 2009). Apoptosis rate on the other hand refers to the population decrease over time and is proportional to disease resistance (Lu et al., 2021).

To calculate the kinetic parameters, the exponential growth phase needs to be identified. This was done by setting up a logarithmic growth curve with time in days on the x-axis and the logarithmic load on the y-axis. The exponential phase would be the linear portion of the curve, having a trendline equation as described below (eq. 3).

Equation 3: Trendline equation of the exponential growth phase.

$$\mathbf{Load = Ae^{B*Time}}$$

Firstly, growth rate can be calculated by dividing the difference in load at the start and end of the exponential phase by the number of days between those data points. Specific growth rate (μ) equals the B term (eq. 3) and is generally seen as more significant since it takes into account the initial infection load, which is not the case with the ordinary growth rate. Doubling time (Td) is the time that the oomycete population needs to double and is calculated as described below (eq. 4).

Equation 4: Equation on how to calculate doubling time (Td).

$$\mathbf{Doubling\ time\ (Td) = \frac{Ln(2)}{specific\ growth\ rate\ (\mu)}}$$

Other kinetic parameters such as max load and time of max load (TOML) can be easily deduced from the growth curve itself.

3 MATERIALS AND METHODS

3.1 Experimental setup

This project aims to examine the effect of six different biostimulants on the disease resistance to *Hyaloperonospora arabidopsidis* of *Arabidopsis thaliana*, being a model plant for agricultural crops such as grapevine. This was done by conducting four experiments on infected plant material (Fig. 10) being a spore count, a biomass quantification via qPCR, a pigment extraction, and an infection kinetics analysis to give preliminary information about which compounds show increased disease resistance and which compounds do not. For the spore count and biomass quantification experiments, independent repeats were performed to achieve higher reliability of results. This preliminary information could be the basis for further field tests that could eventually lead to a recommendation for the use of a certain biostimulant in the agricultural industry.

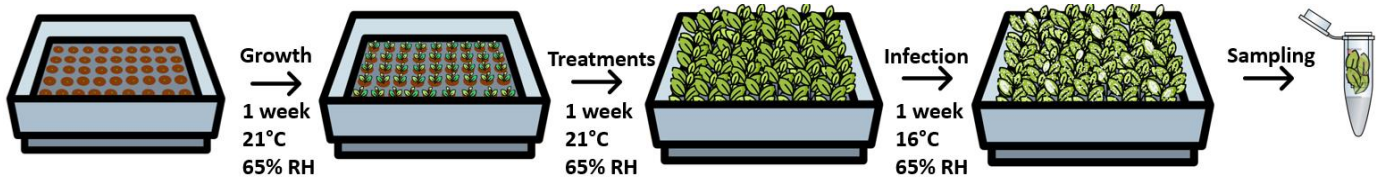


Figure 10: Overview of sample generation. After sowing, the plants were grown for one week before treatment. After treatment, another week was provided for the treatments to have their anticipated effect. The plants were then infected with *H. arabidopsidis* and left for a week for pathogen development. Finally, the plants could be sampled for experimental usage.

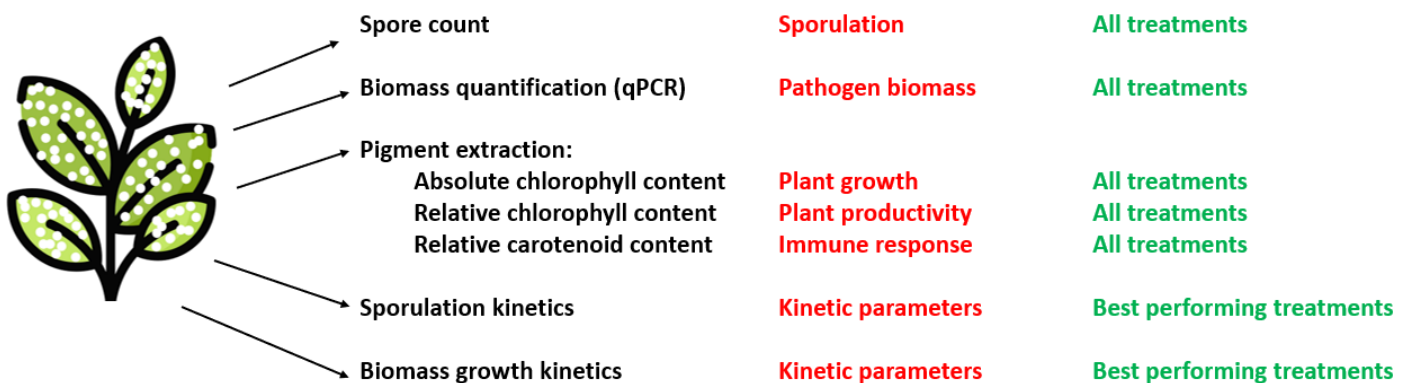


Figure 11: Overview of experiments that are executed. Experiments are depicted in black, investigated entities in red and the included treatments in green.

3.2 Growth and maintenance *A. thaliana*

The *A. thaliana* plants were grown in plastic trays containing 28-wells each. These wells were filled with a mix of potting soil and perlite, to supply the plants with nutrients as well as provide an aerated matrix to form a root network. All the wells were slightly wetted with tap water and received around ten *A. thaliana* seeds (surface sterilized) via a pipette. Briefly, seed surface sterilization involved a five-minute ethanol rinse, followed by a short water rinse. This was repeated three times. These plant trays were placed in a larger tray that contains water and were grown for a week in a plant growth cabinet at 22.5 °C and 65% RH (relative humidity) with a 16 h day and 8 h night cycle and a light intensity of 150 $\mu\text{mol}\cdot\text{m}^{-2}\cdot\text{s}^{-1}$ before being treated with biostimulants and controls. When there were wells that showed significantly more than the 10 anticipated plants, these were trimmed down.



Figure 12: Two trays of *A. thaliana* plants after one week of growing. The seeds were placed with around ten at a time in a well of a 28-well tray that was placed into a water-containing plastic tray. This construction was placed into a growth chamber (22.5 °C, 65% RH) for further growth.

3.3 Treatments of *A. thaliana* using foliar feeding

Plants were treated with 80µl of the corresponding solution (Fig. 13; Table 1). It is important to divide the total volume evenly over all the leaves by pipetting droplets. Each treatment was applied to seven different wells. After the treatment, the plants were grown for one more week in a micro clima modular climate chamber (Snijders Labs, 2021) according to the conditions mentioned above to give them time to take up the applied treatment solution so they can have their intended effect.

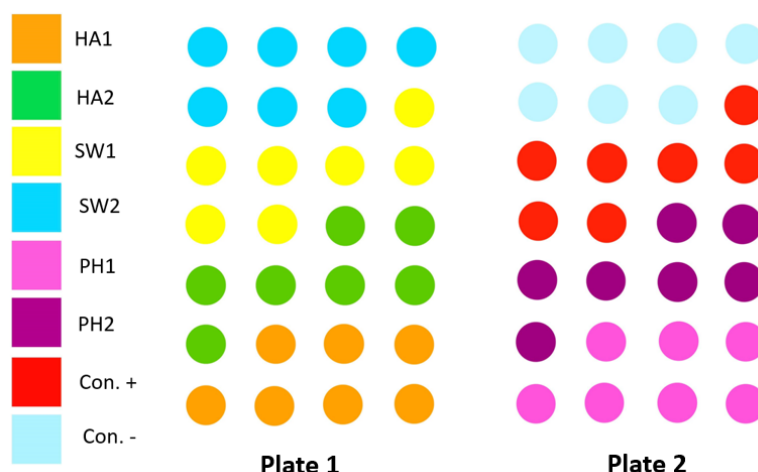


Figure 13: Treatment scheme for spore count and qPCR experiments. The scheme is made up of two 28-well trays. All wells were treated according to the legend, depicting a treatment connected to a colour that represents the wells undergoing the respective treatment (n=7).

Table 1: Overview table containing information about all used treatments.

Category	Name	Abbrev.	Concentration	Dilution	Company
Humic acids	Humic acid	HA1	39 %	500	Bioquant
	Fulvic acid	HA2	29 %	500	Bioquant
Protein hydrolysates	Commercial soy	PH1	5 % N, 10% AA	500	COMPO
	Malt extract	PH2	3 g/l	/	OXOID
Seaweed extracts	<i>Ecklonia maxima</i>	SW1	/	500	Afrikelp®
	<i>Ecklonia maxima</i>	SW2	/	500	Kelpak®
Controls	Water	CON. -	/	/	/
	Duaxo spray	CON. +	167 mg/l	10	COMPO

After preparation, all solutions were sterilised by autoclaving (20 min, 121 °C). All used biostimulants and controls were non-microbial compounds that could not be killed off by a heating program. Also, sterilisation should not influence the working principle or efficiency of the biostimulants (García-Sánchez et al., 2018).

3.4 *H. arabidopsis* maintenance and infection

After the treatment of 1 week, the plants were infected with plant pathogen *H. arabidopsis*. The pathogen itself does not grow on any agar-like growth medium and was thus kept on live *A. thaliana* plants in a growth chamber (Panasonic, 2012; 16 °C, 65% RH) to have an active source of pathogens by a process called cycling.

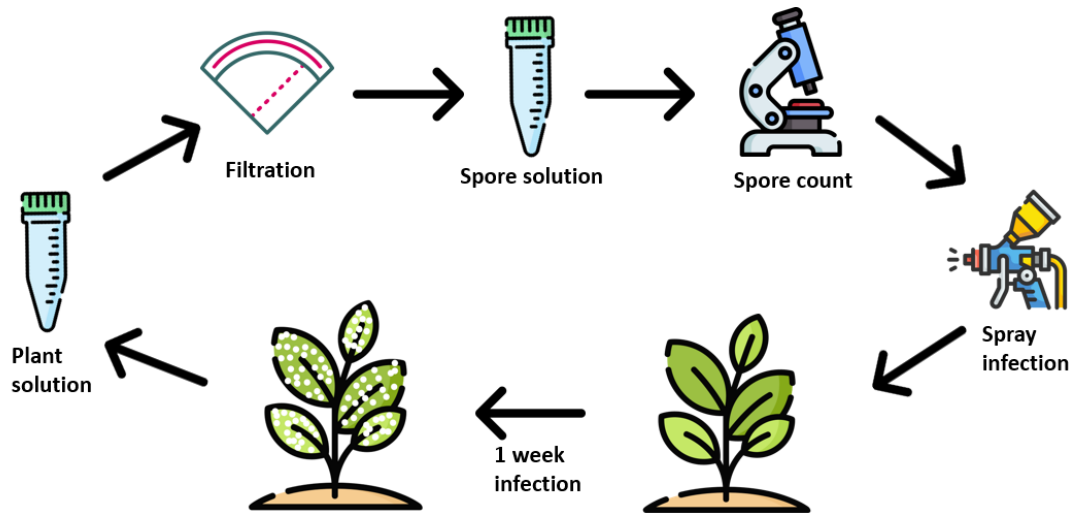


Figure 14: Overview of *H. arabidopsis* cycling. Various seedlings in a single well were infected by spraying a spore solution onto them using air pressure. These were then put into an infection box in a growth cabinet (16°C, 65% RH) for a week for pathogen development and spore formation. After the week of oomycete growth, the plants were taken out of the cabinet and were transferred into a falcon tube with 20ml of sterilised demi-water using a pincer. The tube was vortexed for the sporangiophores to detach from the plant surface and dissolve into the water. After this, the solution was transferred to another falcon tube while passing through a Miracloth filtration paper (EMD Milipore corp., 2009) to remove debris. A Neubauer hemacytometer and a light microscope were then used to reach a concentration of 50.000 spores/ml by diluting the solution accordingly.

The infection of the plants used for experimental purposes occurred in the same way as the cycling. This was done by spraying the spore solution coming from the cycling procedure onto the plants using an air pressure spray gun in one smooth movement to ensure an evenly spread solution (Tomé et al., 2014). After the spray infection, to prevent the pathogen from contaminating any other plant trays that are in the growth cabinet, the plants were put into a completely taped-off infection box. The infection boxes stayed in the growth cabinet for one week at 16 °C and 65% RH with a 12 h day and 12 h night cycle and a light intensity of 150 $\mu\text{mol}\cdot\text{m}^{-2}\cdot\text{s}^{-1}$ to give the pathogen time to fully develop.

3.5 DNA extraction methods used

To extract the sample DNA, both (i) DNeasy Powersoil Pro Kit (Qiagen, n.d.) and (ii) phenol-chloroform DNA extraction methods were used.

- (i) Firstly, the DNeasy Powersoil Pro Kit was used conformed to the manufacturer's guidelines. In brief, up to 250 mg of plant material was added to a Powerbead Pro tube with Lysis buffer (CD1). After homogenization to cause cell lysis (2 times for 30 seconds, 15.000 rpm) the tubes were centrifuged (Eppendorf 5425, n.d.), and the supernatant was transferred into a new tube to remove heavy soil particles. A new buffer (CD2) was added into the new tube containing the supernatant from the last step to remove inhibitors from the DNA extracts. After centrifugation the supernatant was transferred into a new tube and a high salt concentration buffer (CD3) was added, resulting in the binding of the DNA to the silica filter membrane in the spin column while other components will pass through the filter during the centrifugation process. The flow-through was then discarded and an ethanol-containing buffer (EA) was added to the spin column to remove residual proteins and non-aqueous contaminants during a centrifugation step. This step was repeated and then another ethanol-based buffer was added (CD5) to remove other possible residual components. A second centrifugation step was then conducted to remove residual CD5 buffer. Finally, the elution buffer (CD6) was added to the spin column, the low salt concentration causing the silica-bound DNA to release and flow to the elution tube.
- (ii) For the phenol-chloroform DNA extraction the protocol was followed as described by Lievens et al. (2005). In which up to 250 mg of plant material was added to sterilized microtube, with around 50 mg of sterilized lysis sand and around 12 two-millimetre polystyrene beads (Supleco, n.d.) together with 300µl lysis buffer (2.5M LiCl, 50mM Tris HCl pH8, 4% Triton X-100 and 62,5 mM Na₂EDTA pH4). Then 300 µl of the lower layer of the phenol/chloroform/isoamyl alcohol (25/24/1) was added to the microtubes and homogenized (two times 30 sec, 5.5 m/s) by a FastPrep homogenizer (OMNI, n.d.). After the homogenization and centrifugation (time, g), 150µl of the supernatant watery layer containing the DNA was transferred to a clean tube next to 300µl of 100% ethanol. The samples were incubated overnight at -20 °C and then centrifuged at 10.000 rpm for five minutes. After discarding the supernatant, the remaining pellet was washed two times using 70% ethanol by centrifuging it for five minutes at 10.000 rpm while discarding the supernatant. After airdrying the pellets, the DNA was dissolved in 30 µl of 10 mM Tris pH 8.

3.6 *H. arabidopsidis* sporulation quantification: spore count

A spore count using a Motic Type 101M light microscope (Motic, 2011) and a Neubauer-improved haemocytometer (Marienfeld, 2016) were used to determine the influence of the different treatments on pathogen sporulation. This experiment started from two 24-well trays that were treated as indicated (Fig. 13), containing 8 different treatments with seven wells per treatment. This will lead to the relative spore content respective to each sample, expressed in the number of spores per mg of plant material, by multiplying each spore concentration with the added volume of sterile demi-water and then dividing it by the sample's respective weight. To confirm pathogen sporulation results, an independent repeat experiment was included following an identical setup.

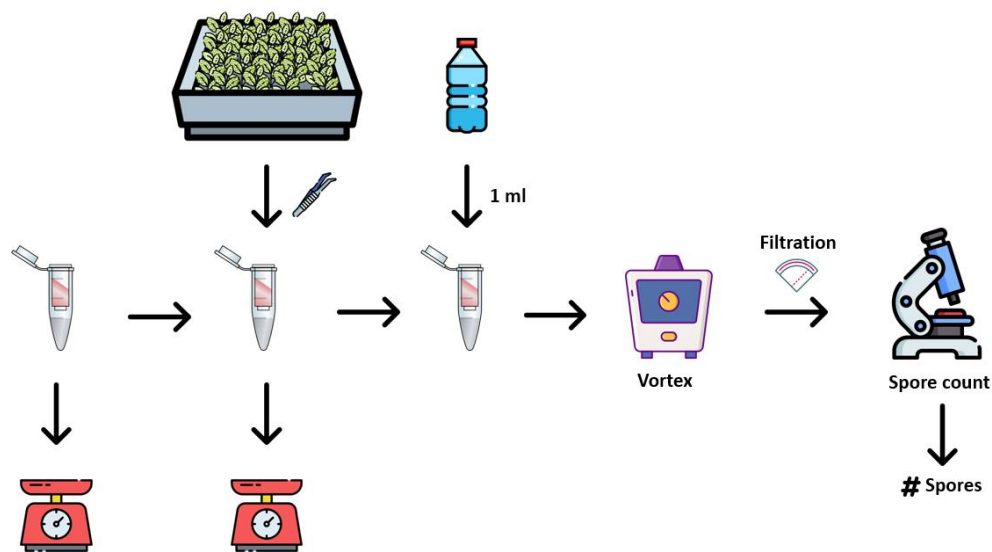


Figure 15: Overview of Spore counting process. Firstly, 54 Eppendorf tubes (1,5 ml) were labelled for each sample and weighed. The tubes were then filled with plant material from their respective well using a pincher and weighed again to get the total weight of the tube and the sample together. The netto weight of plant material weight was later used for relative quantification. Afterward, 1ml of sterile demi water was added to all tubes and they were vortexed at full speed to dissolve the spores into the water phase. Then the solution was decanted into a new Eppendorf while passing through filtration paper to filter out sand and plant debris. The spore solutions could now be counted by transferring ten μl on each side of the counting chamber, covering it with a cover slip, placing it under a light microscope and finally counting all sporangiohores in each section to form an average number of spores per ml.

3.7 *H. arabidopsidis* biomass quantification: qPCR

A qPCR experiment was conducted to quantify pathogenic biomass on all treated *A. thaliana* plants by amplifying the DNA extract samples using a SYBR®-green based qPCR with specific primers (Table 2).

In particular, the iTaq™ Universal SYBR® Green SuperMix (Bio-Rad Laboratories, n.d.) was used. This is a pre-made master mix that contains all necessary components for a qPCR reaction apart from primers, including Taq polymerase, SYBR® Green dye, dNTPs, buffer, and MgCl₂. Each reaction consists of 10 µl of SuperMix, 7 µl of nuclease-free water, 0,5 µl of each primer solution and eventually 2 µl of DNA extract. The qPCR itself was conducted using a StepOnePlus Real-Time PCR System (Applied Biosystems, n.d.).

Table 2: Overview of the temperature/time profile of the qPCR reaction used

Step	Denaturation	Denaturation	Annealing	Elongation
Cycles	1		34	
Temperature	94 °C	94° C	T _{ann}	72 °C
Time	10 min	1 min	1 min	2 min

Primers that were used for the reaction are depicted below (Table 3). Primer pairs 1 and 2 are both targeting the gene responsible for actin production for *A. thaliana* and *H. arabidopsidis* respectively (Huibers et al., 2021; Anderson & McDowell, 2015). Actin can be used as a reference gene for biomass. Another option to use as a primer to amplify *H. arabidopsidis* DNA would be a primer specific for the RXLR29 coding region (3) (Cabral et al., 2011). This region codes for a protein that is part of the so-called RXLR effectors, being expressed during plant infection to suppress its immune system (Pel et al., 2014).

Table 3: Overview of primer specifications.

Target	Nr.	F/R	Sequence (5'-3')	Length	T _{anneal}
Arab. Actin	1	F	AATCACAGCACTTGCACCA	121 bp	56.2 °C
Arab. Actin		R	GAGGGAAGCAAGAATGGAAC		
Hpa Actin	2	F	GTGTCGCACACTGTACCCATTTAT	199 bp	59.6 °C
Hpa Actin		R	ATCTTCATCATGTAGTCGGTCAAGT		
Hpa RXLR29	3	F	CACCATGGAGGTGGTCCTGATC	148 bp	56.0 °C
Hpa RXLR29		R	TTACTTGCCAGGACGCGC		

The actin gene is a single-copy gene; thus, the formula below (eq. 5) can be used in order to calculate the number of detected cells for both the *H. arabidopsidis* actin and *A. thaliana* actin DNA concentrations.

Equation 5: Formula to convert DNA mass to the number of DNA copies.

$$\text{Number of copies} = \frac{\text{Amount (ng)} * 6.022 * 10^{23}}{\text{Length (bp)} * 1 * 10^9 * 660}$$

3.8 Assessing *A. thaliana* growth, productivity, and immune response when infected with *H. arabidopsidis* by chlorophyll and carotenoid quantification

The experiment was initiated by preparing three trays (Fig. 10). After 1 week of growth (22,5 °C, 65% RH), the plants were treated by dividing 30 µl of solution between each plant's leaves accordingly (Fig. 16). After the treatment, the plants were left alone for a week for the biostimulants and controls to have their full effect and then infected with *H. arabidopsidis*. After the infection period of ten days, all replicates were sampled. During the sampling, roots were cut off to minimize carotenoid content in the samples due to root residues.

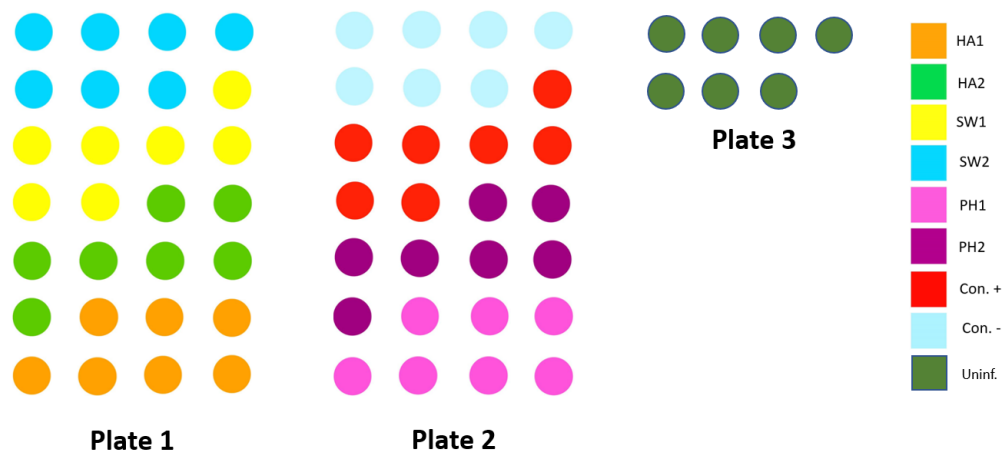


Figure 16: Treatment scheme pigment extraction experiment. All wells were treated according to the legend, depicting a treatment connected to a colour that represents the wells undergoing the respective treatment (n=7).

Chlorophyll content was determined by submerging the plant tissue in 1ml of 80% acetone and homogenizing it using a FastPrep homogenizer (OMNI, n.d.) to extract the chlorophyll (24h, 4 °C). Prolonged exposure to light was avoided at all times to evade chlorophyll degradation. After the incubation period, the extract is centrifuged (3 min, 15 000 rpm) to remove debris and form a supernatant layer that can be transferred to a clean cuvette using a pipette.

A SpextraMax ABS Plus spectrophotometer (Molecular Devices, 2020) was then used to analyse the absorbance at different wavelengths, being 665 nm for chlorophyll-A and 649 nm for chlorophyll-B. Quantification could be done by making use of the Arnor equations for extraction of *A. thaliana* chlorophyll in 80% acetone (eq. 6; 7) (Crowell et al., 2003), which is expressed in microgram chlorophyll per milligram of plant material. Absolute chlorophyll concentration can easily be calculated by leaving out the mass factor in the equations below.

Equation 6: Arnor equation for relative chlorophyll-A concentration.

$$chl_A \left(\frac{\mu g}{mg} \right) = \left((12.21 * OD^{663}) - (2.81 * OD^{646}) \right) * \frac{V}{M}$$

Equation 7: Arnor equation for relative chlorophyll-B concentration.

$$Chl_B \left(\frac{\mu g}{mg} \right) = \left((20.13 * OD^{646}) - (5.03 * OD^{663}) \right) * \frac{V}{M}$$

Relative carotenoid concentration could be found using the same extraction solution as for the chlorophyll extract in a spectrophotometric assay at a wavelength of 470 nm, using the Arnor equation below (eq. 8) (Crowell et al., 2003), which is expressed in microgram carotenoid per milligram of plant material.

Equation 8: Arnor equation for total relative carotenoid concentration.

$$Crt_{TOT} \left(\frac{\mu g}{mg} \right) = \left((1000 * OD^{470}) - (3.27 * Chl_A) - (104 * Chl_B) \right) * \frac{V}{229 * M}$$

3.9 *H. arabidopsidis* infection growth kinetics

The experiment set up to determine the infection growth kinetics of *H. arabidopsidis* followed that of form the spore count and qPCR experimental setup (Fig. 10). However, samples were taken at different moments in time in order to construct a growth curve. The best-performing biostimulant treatments, in terms of disease repellence were examined (malt extract (PH2) and *E. maxima* seaweed extract (Kelpak®; SW2)), compared to the positive (difenoconazole fungicide) and negative control (water).

Replicate plants were infected by dividing 100 µl of *H. arabidopsidis* spore solution with a concentration of 60 000 spores/ml over all the seedling's leaves via a pipette. Five different sampling moments were conducted, being on day 0, day 1, day 4, day 8 and day 10 with the infection day referred to as day 0. Samples at day 0 were taken to identify the initial infection dose. Each sampling moment was conducted on four different wells (experimental replicates) of each of the 4 treatments (Table 4).

Table 4: Sampling scheme for the infection growth kinetics experiment.

Name	Abrev.	D0	D1	D4	D8	D10	<u>Total</u>
<i>Ecklonia maxima</i> (Kelpak®)	SW2	4	4	4	4	4	20
Malt extract	PH2	4	4	4	4	3	20
Difenoconazole fungicide	Con. +	4	4	4	4	4	20
water	Con. -	4	4	4	4	4	20
<u>Total</u>		16	16	16	16	16	80

Around ten plants are grown in each well and treated according to the scheme below (Fig. 17). When sampling, a similar approach was used as in the spore count and qPCR experiments, however, spores were isolated, and DNA was extracted from the same sample. First, the plants of a single were divided into 2 different Eppendorf's, one was used for qPCR and one for the spore count, with the one for the spore count weighed before and after the filling to normalize results according to mass. Spore count samples were filtered and counted immediately using the same method as discussed previously (Section 3.6). Samples that needed to be used for qPCR were stored at -20 °C until all samples were collected so the DNA extraction and the qPCR reaction can occur at the same moment for all samples. Following spore counting and biomass quantification, the kinetic parameters were derived as discussed previously (Section 2.6.5.1).

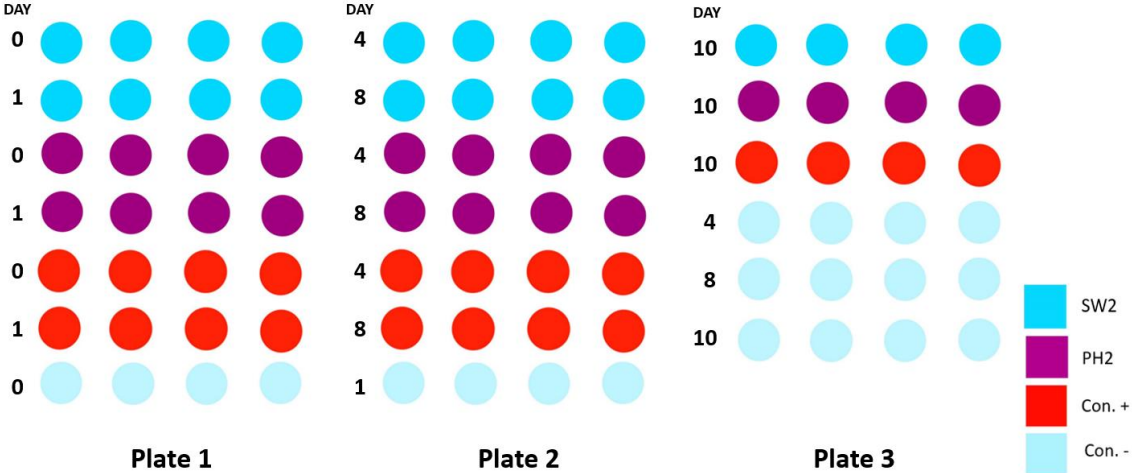


Figure 17: Treatment scheme Infection growth kinetics experiment. All wells are treated according to the legend, depicting a treatment connected to a colour that represents the wells undergoing the respective treatment (n=4).

3.10 Statistical analysis

To check if there are any significant differences between treatments, a parametric ANOVA test was used to compare the means of the independent groups by comparing the variation between and within groups. This test is preceded by a post hoc test (Tukey HSD), which will indicate in between which exact groups there is a significant difference.

Furthermore, the one-way ANOVA and post hoc tests assume a dataset that is normally distributed, therefore a normality test (Shapiro-Wilk) is conducted to determine if a given data set follows a normal distribution or not. Both tests also assume equal variances between samples, thus, an equality of variances test is conducted (Levene's). When these conditions are not met, non-parametric variants of ANOVA and post hoc tests are used (Welch's ANOVA; Dunnett's T3 test). These tests will yield a p-value, which is a probability value that indicates the likelihood of obtaining a test statistic as extreme or more extreme than the one calculated from the data. All statistical tests cited above use a confidence level of 0.95 ($\alpha = 0.05$) and will be conducted using SPSS Statistics Version 7 (IBM Corp., 2020).

To analyse the significance of linear models such as the growth curves (Section 2.6.5), a Type III analysis of variance following the Satterthwaite method was used with the treatment and timepoint as explanatory variables, yielding results similar to ANOVA and post hoc tests in finding a significant difference in between treatments. Also, to analyse if there are significant influences of time points, treatments and the interactions between both on the analyzed variables, a degrees-of-freedom analysis following the Kenward-Roger method is conducted, yielding p-values indicating significant influences. Both analyses use a linear mixed-effect model, assuming that there is a linear relationship between the two variables. However, random effects of group-specific characteristics allow for variations between the groups, these random effects being differences in disease and treatment responses between replicates. Both analyses were conducted in an R statistics environment (R Core Team, 2013) and made use of libraries "lme4", "lmerTest", and "emmeans" (Prince et al., 2022).

4 RESULTS & DISCUSSION

4.1 *Hyaloperonospora arabidopsidis* sporulation quantification by spore count

A spore count experiment was conducted on *H. arabidopsidis* infected *A. thaliana* that was inoculated with all treatments. This to examine which treatments show the highest reduction in pathogenic sporulation. Also, a repetition experiment was executed to confirm the initial results.

When comparing both experiments, there were no notable differences visible (Fig. 18). This was confirmed when conducting an unpaired t-test. When reviewing these results, one can conclude that there are no significant differences found ($\alpha = 0.05$) between any of the treatments of both experiments, indicating high reliability of results.

The Shapiro-Wilk normality test revealed all datasets to be normally distributed. However, the Levene's test indicated non-equal variances (p-value = 0.01; 0.03), therefore non-parametric tests needed to be used. The Welch's ANOVA test for both experiments yielded a p-value lower than 0.001, meaning that there were significant differences between treatments in terms of spore-reducing effects. Based on a post hoc test ($\alpha = 0.05$), a visualising table (Table 5) was set up for both the initial experiment as well as the confirmation experiment, containing p-values and shades of red, purple, and green that resemble different ranges of significance.

Differences between treatments in terms of their spore-reducing effects can be observed (Fig. 18). The malt extract (PH2; 442 ± 145 ; 483 ± 135 spores/mg plant material), humic acid (HA1; 828 ± 165 ; 1015 ± 323 spores/mg plant material), fulvic acid (HA2; 986 ± 391 ; 1075 ± 447 spores/mg plant material) and *Ecklonia maxima* seaweed extract (SW2; Kelpak®; 843 ± 411 ; 952 ± 282 spores/mg plant material) samples showed a noticeable reduction in spore load compared to the negative control (Con.-; 1423 ± 591 ; 1767 ± 566 spores/mg plant material). With PH2 being significantly different in both experiments (p-value = 0.008; 0.001) and SW2 (p-value = 0.318; 0.018) in the repetition experiment. This suggested that applying these treatments will have a positive spore-reducing effect compared to only adding water, showing a lower relative average spore content than the negative control. However, while no relevant literature can be found on the use of malt extract as a biostimulant, plant-derived PH treatments have been shown to reduce *Plasmopara viticola* sporulation, which is a mildew plant pathogen similar to *H. arabidopsidis* (Barrada et al., 2022). According to research done by Gleń-Karolczyk & Boligłowa (2015), *E. maxima* seaweed extract (Kelpak®) treated horseradish plants experienced a *Verticillium dahliae* sporulation reduction of up to 78.63%. However, they also found that it had sporulation-inducing effects on other plant pathogens such as *Botrytis cinerea*. Effects on *H. arabidopsidis*-infected plants were not included.

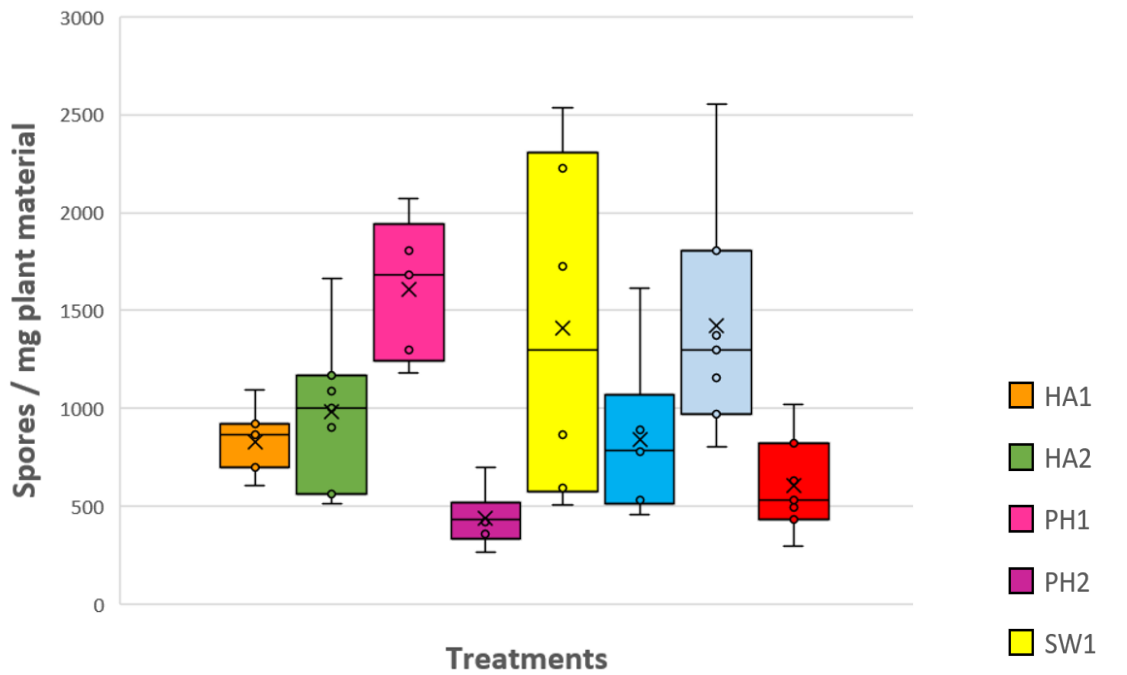
Comparing all other treatments to the positive control (605 ± 246 ; 510 ± 184 spores/mg plant material), no significant difference could be observed between the positive control and the HA1 (p-value = 0.983; 0.571), HA2 (p-value = 0.763; 0.409), PH2 (p-value = 0.998; 1.000) and SW2 (p-value = 0.979; 0.638) biostimulant treatments, meaning that these treatments had similar spore-reducing effects as the difenoconazole/1,2-benzisothiazolin-3-one containing positive control. However, since the HA1 and HA2 treatments were not found to be significantly different from the negative control (HA1; p-value = 0.242; 0.076; HA2; 0.623; 0.081) due to

their large spread, results of the treatments could be seen as inconsistent and unpredictable. Therefore, it could be concluded that the humic acid treatments administer a higher reduction in spore formation compared to water but not yet as high as the fungicide. Similar results are found by El-Ghamry et al. (2009), where HA-treated faba bean plants showed a reduction in disease severity based on *Botrytis fabae* sporulation strongly dependant on HA concentration, probably due to maximizing nutrient uptake efficiency (Stevenson, 1994).

Also, it could be observed that the *Ecklonia maxima* (Afrikelp®; SW1) treated plants showed a high variation in relative spore content (1411 ± 873 ; 1484 ± 611) spores/mg plant material). A possible explanation for this could be that there is a big difference in plant response to this biostimulant relative to its growth stage. Since there are around 10 plants per well, it's possible that these do not germinate at the same moment (Rajala & Peltonen-Sainio, 2001). This high variation in results of the SW1 treated plants was also observed in later experiments and cannot be confirmed, nor refuted by literature since no articles could be found that use Afrikelp® *E. maxima* seaweed extract in combination with plant pathogens. However, research done by Righini et al. (2020) also indicated that their *E. maxima*-derived biostimulant showed a higher sporulation fluctuation without a significant reduction compared to other tested seaweed extract treatments, being *Anabaena minutissima* and *Jania adhaerens*. This experiment was conducted on cucumber plants infected with *Podosphaera xanthii*, which is also a mildew disease with a similar mode of infection to *H. arabidopsidis*, thus likely yielding comparable results.

Finally, in both experiments, none of the treatments were found significantly less performant in terms of spore load compared to the negative control, leading to the conclusion that none of the biostimulant treatments promotes sporulation of *H. arabidopsidis*.

(1)



(2)

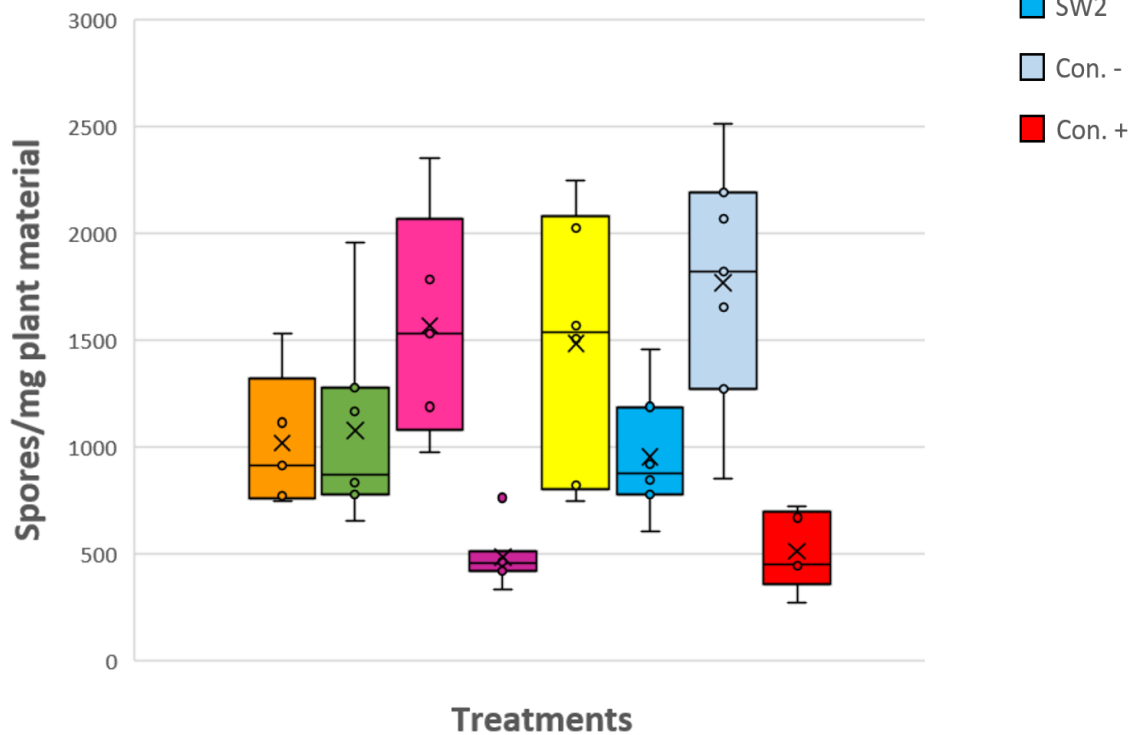


Figure 18: Box and whisker plot of initial spore count (1) and confirmation spore count (2), 7 days post-infection. On the y-axis, the relative spore content is depicted. On the x-axis, all treatments are given in their distinct colours (n=7). Plots are generated using Excel (Microsoft Corp. 2018).

Table 5: Post hoc test (Dunnett's T3) p-values of the initial spore count experiment (1) and confirmation experiment (2), 7 days post-infection. Each section contains a p-value respective to the Tukey test result of the treatments in the same row and column. Significantly different results are indicated in green, results that are not significantly different are indicated in red/purple (n=7).

(1)

	HA1	HA2	PH1	PH2	SW1	SW2	CON -	
	0.983	0.763	0.010	0.998	0.049	0.979	0.031	Con +
		0.998	0.088	0.788	0.311	1.000	0.242	HA1
			0.291	0.397	0.698	0.999	0.623	HA2
				0.003	0.996	0.123	0.996	PH1
					0.013	0.786	0.008	PH2
						0.391	1.000	SW1
							0.319	SW2

p-value:

0.00 - 0.01	Green	Difference
0.01 - 0.03	Light Green	
0.03 - 0.05	Dark Green	No difference
0.05 - 0.10	Light Red	
0.10 - 0.30	Red	
0.30 - 0.50	Dark Red	
0.50 - 0.80	Red	
0.80 - 0.95	Light Purple	
0.95 - 0.99	Dark Purple	
0.99 - 1.00	Very Dark Purple	

(2)

	HA1	HA2	PH1	PH2	SW1	SW2	CON -	
	0.571	0.409	0.009	1.000	0.011	0.638	0.001	Con +
		1.000	0.574	0.410	0.611	1.000	0.076	HA1
			0.633	0.251	0.671	1.000	0.081	HA2
				0.002	1.000	0.313	0.945	PH1
					0.003	0.455	0.001	PH2
						0.347	0.929	SW1
							0.018	SW2

p-value:

0.00 - 0.01	Green	Difference
0.01 - 0.03	Light Green	
0.03 - 0.05	Dark Green	No difference
0.05 - 0.10	Light Red	
0.10 - 0.30	Red	
0.30 - 0.50	Dark Red	
0.50 - 0.80	Red	
0.80 - 0.95	Light Purple	
0.95 - 0.99	Dark Purple	
0.99 - 1.00	Very Dark Purple	

4.2 *H. arabidopsidis* biomass quantification by qPCR

A qPCR reaction was conducted on *Hyaloperonospora arabidopsidis*-infected *Arabidopsis thaliana* that was inoculated with all treatments. This was to examine which treatments showed the highest reduction in pathogenic biomass. Also, a repetition experiment was executed to confirm the initial results. Data from the qPCR experiments came in the form of a range of Ct-values and could be examined using absolute quantification. Firstly, the qPCR reaction conditions had to be optimized. Then to reduce the lack in specificity of the *H. arabidopsidis* actin primer set, a correction factor was determined. Furthermore, the absolute numbers of *H. arabidopsidis* cells detected were expressed relative to the number of *A. thaliana* cells detected in the knowing that when more plant material is sampled, the number of *H. arabidopsidis* cells detected will likely be higher.

4.2.1 Optimization of qPCR

To optimize the qPCR reaction to quantify pathogenic biomass, a couple of experiments were conducted. These consisted of testing two different primer pairs (Hpa actin; Hpa RXLR29) to quantify *H. arabidopsidis* biomass and adjusting primer concentration. This was done to improve the sensitivity and specificity of the qPCR runs and to minimize variability between replicates.

4.2.1.1 *H. arabidopsidis* actin primer pair

In silico primer pair evaluation

To check if the primers are specific for their target sequence, several Basic Local Alignment Search Tool (BLAST) searches were conducted. Matching the *H. arabidopsidis* actin forward primer to the *A. thaliana* genome, revealed several matches with a 100% query coverage and 100% shared identity with a sequence in *A. thaliana* chromosome one. When blasting the reverse primer, another match with 100% query coverage and 94,74% identity appeared compared to chromosome one. Therefore, the *H. arabidopsidis* primer is not specific and could also amplify *A. thaliana* DNA during a qPCR reaction. When checking the specificity of the *A. thaliana* primers compared to the *H. arabidopsidis* genome, no notable matches were found. However, since both primer sets were available in the lab and prominent in literature, it was useful to double-check the specificity in an experimental way using qPCR and agarose gel electrophoresis.

In vitro primer pair evaluation

In a first experiment, the DNA was extracted from three samples of uninfected *A. thaliana* plants and three samples of *H. arabidopsidis*-infected *A. thaliana* plants using the DNeasy Powersoil Pro Kit. Two qPCR reactions were then initiated using the Platinum SYBR® Green qPCR SuperMix, one reaction using the *A. thaliana* actin primers and the other one using the *H. arabidopsidis* actin primers. Contrary to expectations, no amplification was detected in both runs by the machine, indicating a problem during the sample preparation, DNA extraction or PCR reaction itself.

Albeit the StepOnePlus Real-Time PCR system detected no amplification, bands did appear on a 1,5% agarose gel of the qPCR products (Fig. 19). This could indicate that there was an issue with the SYBR® green dye. Possible explanations could be that the SYBR® green dye was expired and lost its functionality, or since the dye is photosensitive (Singer et al., 1999) it might have been exposed to light for an extended period of time, losing its functionality. However, results from the agarose gel electrophoresis run suffice to draw reliable conclusions regarding primer sensitivity.

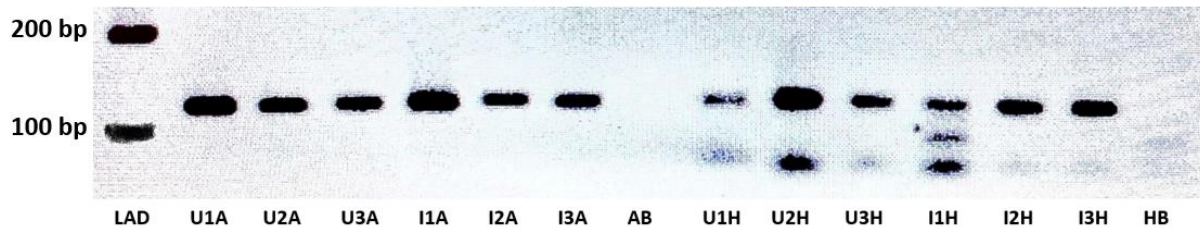


Figure 19: Agarose gel electrophoresis primer specificity test results. On the left lane, a small smart ladder (Eurogenetec, 2021) was used to indicate fragment length. The identity of the other bands can be derived from their name: the first character indicates if the sample is from an uninfected (U) or an infected (I) plant, the second character indicates the sample number and the last character indicates whether the *A. thaliana* actin (A) or the *Hyaloperonospora* actin (H) primer was used in the respective qPCR reaction. The AB and HB lanes are blanks for the *A. thaliana* actin (A) and the *Hyaloperonospora* actin (H) primer reactions respectively.

All products of the *A. thaliana* actin primer qPCR (xxA) showed a single band around the 120-130 bp region on all lanes, being the 121 bp amplicon region in the *A. thaliana* DNA. Since all samples contain plant DNA, the 121 bp band was observed in all samples of the *A. thaliana* actin primer qPCR reaction. The specificity of the *A. thaliana* actin primer pair could be concluded from missing secondary bands on the infected plant lanes (IxA).

All products of the *H. arabidopsidis* actin primer qPCR (xxH), showed a band in the 120-130 bp region, as well as a band made up of fragments smaller than 100 bp. The I1H lane showed an additional third band of around 100 bp, probably due to contamination since this band was not present in the other two infected plant samples (IxH). Since there was product formation in the uninfected plant samples, the primer pair was concluded to be non-specific. Analysing the lanes of the infected plants, no bands were visible at the 200 bp region, indicating that there was no *H. arabidopsidis* DNA amplified. This could be due to three possible reasons, being either that the primers were not both complementary to the *H. arabidopsidis* DNA, that the DNA extraction method did not manage to extract sufficient DNA for PCR amplification or that the elongation stage (30 s, 72 °C) was too short to yield significant results.

However, to confirm that the non-working SYBR® Green SuperMix did not influence primer behaviour, an identical experiment was conducted using the iTaq™ Universal SYBR® Green SuperMix (Bio-Rad Laboratories, n.d.). Additionally, a different thermocycling profile was used, being 1 minute at 95 °C for denaturation, 1 minute at annealing temperature and 2 minutes at 72°C for optimal elongation. To confirm if the reaction was capable to pick up differences in concentration, half fractions of plant material were included in samples A1 and H1. The results of the experiment are summarized below (Table 6).

Table 6: Relative amplification data for the *A. thaliana* and *H. arabidopsidis* actin genes in uninfected and infected plant samples, 7 days post-infection. Primer concentration was 100µM.

		Plant material Frac.	Arab. Actin Average Ct	Hpa Actin Average Ct	$2^{-\Delta\Delta C_T}$	AVG $2^{-\Delta\Delta C_T}$
Uninfected	A1	½	15.490	25.880	0.410	0.940
	A2	1	14.395	23.540	0.972	
	A3	1	15.640	24.705	1.028	
Infected	H1	½	14.575	18.070	24.420	50.407
	H2	1	14.530	18.140	45.098	
	H3	1	15.300	18.565	57.281	
BLANK		/	30.835	32.880	/	/

Analysing the qPCR results, amplification of DNA in the uninfected samples was present using the *H. arabidopsidis* actin primer since the average Ct-values were lower than the average Ct value of the blank sample. However, when looking at the $2^{-\Delta\Delta C_T}$ -values, a clear distinction between the uninfected and infected samples could be observed, having a 50-fold higher presence of amplicon regions compared to the uninfected samples. The primer also seemed to be able to detect differences in added plant material since the $2^{-\Delta\Delta C_T}$ -values of samples A1 and H1 were around half of their respective group average, meaning that the *H. arabidopsidis* actin primer could be used for quantification but would lead to an overestimation due to aspecific amplification. A common practice to increase primer specificity is lowering its' concentration. Therefore, the *H. arabidopsidis* actin primer concentration was diluted 5-fold to a concentration of 20 µM and was subjected to another qPCR reaction (Table 7):

Table 7: Relative amplification data for the *A. thaliana* and *H. arabidopsidis* actin genes in uninfected and infected plant samples, 7 days post-infection. Arab. actin primer was 100µM, *H. arabidopsidis* actin primer concentration was 20 µM (5-fold dilution).

		Arab. Actin Average CT	Hpa Actin Average CT	$2^{-\Delta\Delta C_T}$	AVG $2^{-\Delta\Delta C_T}$
Uninfected	A1	16.915	26.515	1.210	1.009
	A2	16.051	26.053	0.915	
	A3	17.568	27.589	0.903	
Infected	H1	16.188	18.177	236.494	384.798
	H2	17.435	18.290	518.967	
	H3	17.117	18.351	398.446	
BLANK		31.442	30.648	/	/

This qPCR setup showed promising results, having a 385-fold higher amplification compared to the uninfected samples. However, there was still a difference in Ct-values in between the uninfected samples and the blank sample, indicating that the use of a correction factor would be a good option to reduce the effect of non-specific amplification.

4.2.1.2 *H. thaliana* RXLR29 primer pair

In silico primer pair evaluation

Upon blasting the primer pair against the *A. thaliana* genome, no significant matches were observed, except for a 90% query match between the forward primer and chromosome 3, while no notable match was identified with the reverse primer on this chromosome. Therefore, even if the amplification of chromosome 3 were to occur, it would be negligible since it would not be exponential. In contrast, when subjected to blasting against *Hyaloperonospora arabidopsidis*, the forward and reverse primers exhibited promising E-values of 0.004 and 4×10^{-5} respectively, when compared to the RXLR effector gene. Consequently, these primers were deemed suitable for qPCR applications. Furthermore, both primers possess a 3' C end, which enables a robust bond at the 3' end, thus resulting in a lower loss of 3' ends and a higher degree of amplification. Additionally, this primer pair had a similar annealing temperature as the *A. thaliana* actin primer, allowing for the use of both primers in the same thermocycler and reducing the number of qPCR runs as well as waiting time.

In vitro primer pair evaluation

This primer pair was then tested using the same method as the previous two test experiments using the same DNA samples and the same SYBR® Green SuperMix. Furthermore, the same amplification scheme was used except for the annealing temperature (56 °C). The primer concentration was diluted 5-fold in TRIS-buffer (20 µM) to reduce primer dimer formation.

Table 8: Relative amplification data for the *A. thaliana* actin and *H. arabidopsidis* RLXR29 gene in uninfected and infected plant samples, 7 days post-infection. *H. arabidopsidis* RLXR29 primer concentration was 20µM.

		Arab. Actin	Hpa RLXR		AVG
		Average CT	Average CT	$2^{-\Delta\Delta C_T}$	$2^{-\Delta\Delta C_T}$
Uninfected	A1	16.709	15.295	0.728	1.033
	A2	15.828	14.878	1.004	
	A3	17.439	16.935	1.368	
Infected	H1	15.305	15.385	2,049	1,538
	H2	15.256	15.243	1.923	
	H3	17.289	15.695	0.642	
BLANK		31.487	18.372	/	/

Regarding these results (Table 8), it could be concluded that there is still amplification occurring in the blank sample when using the *H. arabidopsidis* RLXR29 primer pair, having a Ct-value of 18.372. Additionally, no significant difference could be observed between the average Ct-values of the infected and uninfected samples. Concerning the average $2^{-\Delta\Delta C_T}$ -values, there was only a 0.5-fold higher amplification in the infected samples. This however is rather low compared to the use of the *H. arabidopsidis* actin primers, which had a 385-fold higher amplification compared to the uninfected samples.

4.2.1.3 Optimized qPCR setup

When inspecting the results of both tests that were conducted to find a suitable primer pair to use for the qPCR experiment, it can be concluded that the actin primers are the most suitable. However, a correction needs to be conducted since there is also minimal amplification of *A. thaliana* DNA considering the *H. arabidopsidis* actin primer. On account of this, uninfected samples are as well included in the qPCR experiment to form a coefficient, expressed as the mass of *A. thaliana* DNA (ng) amplified by *H. arabidopsidis* actin primer over the mass of *A. thaliana* DNA (ng) amplified by *A. thaliana* actin primer, to correct for misamplified DNA.

To summarize, the biomass of *H. arabidopsidis* will be determined relatively compared to *A. thaliana* by making use of qPCR. For the reaction itself, both actin primer pairs are used, with the *H. arabidopsidis* actin primer at a concentration of 20 $\mu\text{mol/ml}$, alongside the iTaq[™] Universal SYBR[®] Green SuperMix. The amplification reaction follows a course as described previously (Table 2). The sample DNA itself is derived from the same setup used in Figure 10 after a DNA extraction using a DNeasy Powersoil Pro Kit. All samples were ran in duplicates to serve as a technical control. Absolute quantification is performed by making use of a calibration curve derived from MySPEC measurements. Since the *H. arabidopsidis* actin primer pair is not fully specific, a correction needs to be performed by making use of a correction factor derived from uninfected *A. Thaliana* DNA samples. To confirm pathogen biomass results, a confirmation experiment is included following an identical setup except for the DNA extraction being conducted using phenol/chloroform extraction instead of the DNeasy Powersoil Pro Kit (Qiagen, n.d.).

4.2.2 Absolute quantification of *H. arabidopsidis* biomass

4.2.2.1 Calibration curve determination

To deduct an absolute quantification on qPCR results, calibration curves were constructed for each primer set. Also, separate calibration curves were made for both DNA extraction methods due to the high probability of differences in extract quality. These curves can be found in the appendix (Fig. 28; 29; 30; 31) (Table 18; 19; 20; 21)

Regarding the R^2 -values of the curves, representing the level of linearity, all values were above 0.98, being the general minimum from which a dataset can be considered linear (Bio-rad, 2013). The E-values of the curves of the kit extraction are 0.64 and 0.86, both being lower than 1. This indicates non-optimal amplification of target DNA, most probably due to the presence of interfering compounds (e.g. the high polyphenol content in *A. thaliana*) (Birtić & Kranner, 2006; Mattioli et al., 2019), the use of a non-optimal annealing temperature or loose 3' ends since these both primers do not contain a G or a C nucleotide for both primer pairs. However, this will lead to an underestimation of target-DNA quantity and will thus not influence conclusions drawn from qPCR data since differences in pathogenic biomass in between treatments would be even bigger in reality. E-values of the calibration curves of the phenol/chloroform extraction were 1.107 and 1.033 for the *A. thaliana* and *H. arabidopsidis* primers respectively, indicating optimal exponential growth.

4.2.2.2 Correction factor determination

In order to correct the DNA concentration found by the slightly aspecific *H. arabidopsidis* actin primer pair, a correction factor was determined. This was done by subjecting DNA coming from uninfected *A. thaliana* plants to a qPCR reaction using both the *A. thaliana* actin and *H. arabidopsidis* actin primer pairs. These reactions will provide an average DNA concentration using the Ct-values and calibration curves for both primer pairs. When the average DNA concentration for the *H. arabidopsidis* actin primer is divided by the average DNA concentration using the *A. thaliana* actin primer, a correction factor is obtained expressed in nanograms of *A. thaliana* DNA for the *H. arabidopsidis* primer over nanograms of *A. thaliana* actin DNA using the *A. thaliana* actin primer. This factor can be multiplied with the *A. thaliana* actin DNA concentrations for each sample and then be used to be subtracted from the *H. arabidopsidis* actin DNA concentration to compensate aspecific *A. thaliana* DNA amplification (Table 9).

Table 9: qPCR results correction factor construction.

Primer	Sample	Ct-AVG	DNA Conc. (ng/μl)	Average (ng/μl)	Correction factor (ng Arab. DNA Hpa primer / ng Arab. DNA Arab. primer)
Arab. Actin	Uninf. 1	16.904	18.356	19.915	0.00634
	Uninf. 2	16.060	28.072		
	Uninf. 3	17.568	13.318		
Hpa Actin	Uninf. 1	26.719	0.150	0.126	
	Uninf. 2	26.821	0.141		
	Uninf. 3	27.589	0.087		

The visual representation of the effect of the correction factor is given (Fig. 20). The correction factor represents the quantity of *A. thaliana* DNA that is wrongly amplified by the *H. arabidopsidis* actin primer per ng of *A. thaliana* DNA amplified by the *A. thaliana* actin primer.

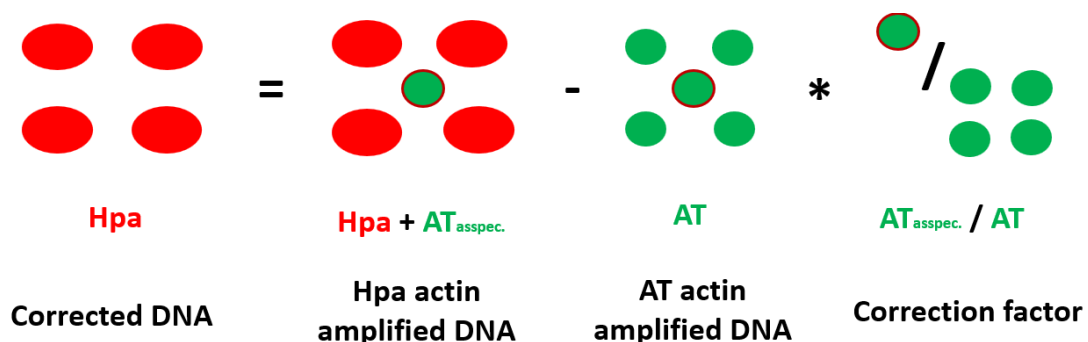


Figure 20: Visual representation of correction. To get *H. arabidopsidis* DNA solely, the correction factor is multiplied by the quantity of *A. thaliana* DNA amplified by the *A. thaliana* actin primer in a sample, the quantity of wrongfully amplified *A. thaliana* DNA is calculated for that sample. This quantity can then be used to be subtracted from the total DNA multiplied by the *H. arabidopsidis* actin primer to get the total amount of detected *H. arabidopsidis* DNA present in that sample.

4.2.2.3 *H. arabidopsidis* biomass analysis

The box and whisker plots (Fig. 21) of both the initial and confirmation experiments show similarities in terms of pathogenic biomass for all treatments, however, due to a different approach in DNA extraction, absolute numbers are of another magnitude and could therefore not be compared directly using pairwise comparison. Both plots show notable differences between the different groups.

The Shapiro-Wilk normality test revealed all datasets to be normally distributed and the Levene's test indicated equal variances (p-value = 0.256; 0.061). Therefore parametric tests could be used. The one-way ANOVA test yielded a p-value lower than 0.001, indicating that there were significant differences between treatments in terms of pathogenic biomass reducing effects. Based on a post hoc test ($\alpha = 0.05$), a visualising table (table 10) was set up for both the initial experiment as well as the confirmation experiment, containing p-values and shades of red, purple, and green that resemble different ranges of significance.

It was clear that the *E. maxima* seaweed extract treatment (Kelpak®) (SW2; 0.59 ± 0.23 ; 0.67 ± 0.32 Hpa cells / AT cells) performed the best in terms of pathogen biomass reducing effects, being comparable to the positive control (0.59 ± 0.15 ; 0.39 ± 0.11 Hpa cells / AT cells). Concerning the post hoc test, SW2 was found significantly different from the negative control in both experiments (Con.-; p-value = 0.026; 0.016) and not significantly different compared to the positive control (Con.+; p-value = 1.000; 0.951). Thus, it can be deduced that adding these compounds will have a positive pathogen-reducing effect compared to just adding water and a similar pathogen-reducing effect compared to adding a difenoconazole fungicide. This is confirmed by Gleń-Karolczyk & Boligłowa (2015), indicating that *E. maxima* seaweed extract treated plants (Kelpak®) showed a reduction in pathogen biomass dependant on biostimulant concentration for all 7 evaluated fungal plant pathogens. Additionally, none of the treatments were found significantly less performant as the negative control, leading to the conclusion that no biostimulant treatment promotes pathogenic growth.

The second best-performing biostimulant treatments would be the commercial soy extract (PH1; 0.69 ± 0.11 ; 1.20 ± 0.36 Hpa cells / AT cells) and malt extract (PH2; 0.78 ± 0.16 ; 1.05 ± 0.17 Hpa cells / AT cells), falling in the same range as the positive control with a slightly higher average relative pathogenic biomass content compared to the positive control. This contrasts with the spore count experiment where PH1 was the worst-performing biostimulant, containing the highest average relative spore load of all treatments. However, both treatments were not found to be significantly different from the negative control (PH1; p-value = 0.170; 0.707; PH2; p-value = 0.670; 0.304) and can thus not be concluded to have a significant pathogen biomass reduction.

Another remarkable result was that both humic substance (HA) treatments (HA1; 1.06 ± 0.17 ; 0.166 ± 0.54 Hpa cells / AT cells) (HA2; 1.00 ± 0.17 ; 1.62 ± 0.48 Hpa cells / AT cells) resulted in a proportional average *H. arabidopsidis* biomass content when compared to the negative control (0.96 ± 0.10 ; 0.169 ± 0.41 Hpa cells / AT cells), not being significantly different (HA1; p-value = 0.983; 1.000; HA2; p-value = 1.000; 1.000). This is notable since both HA1 and HA2 showed a promising reduction in sporulation in the spore count experiment. Differences in terms of biomass reduction and sporulation reduction can be due to the treatments' specific effect on the plant's defence mechanism. In the case of the humic substances, it might be the case that the treatments stimulate the plant's immune system to produce more spore-trapping structures such as callose deposition (Wang et al., 2021) or lignin barriers (Lee et al., 2019), resulting in lower sporulation and spread of disease but not lowering pathogenic growth.

However, this link between humic acid and lignin, callose or other spore-trapping structures could not be found in literature. In the case of PH1, the biostimulant may increase the production of defensive compounds that can inhibit the pathogen's growth. In this scenario, the pathogen may still produce a lot of spores, but it may not be able to establish a successful infection, resulting in a lower pathogenic biomass (Wang et al. 2021).

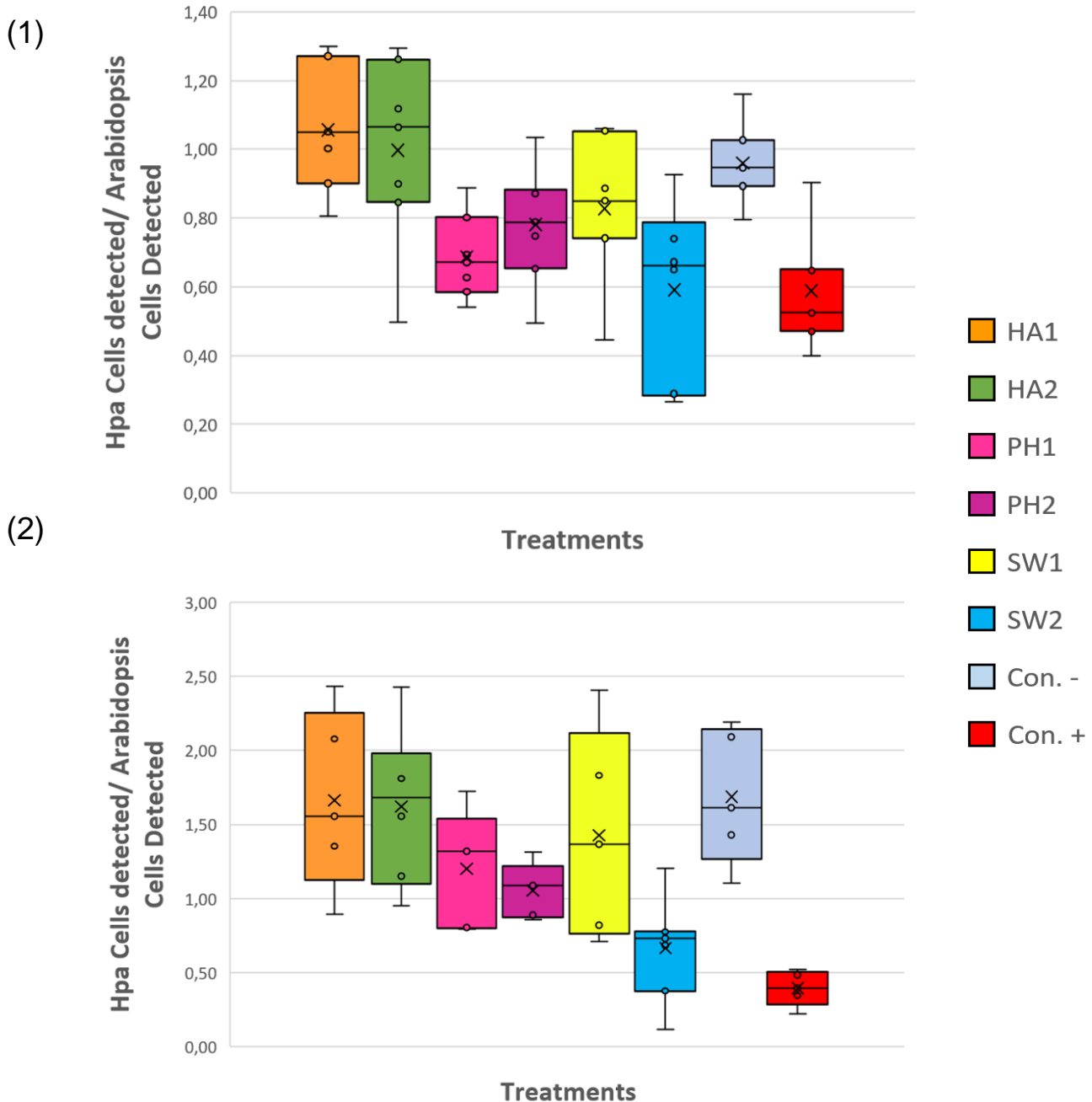


Figure 21: Box and whisker plot of the initial absolute pathogen biomass quantification experiment (1) and confirmation experiment (2), 7 days post-infection. On the y-axis, the number of *H. arabidopsis* cells per *A. thaliana* cell is depicted. On the x-axis, all treatments are given in their distinct colours (n=7). The plot is generated using Excel (Microsoft Corp. 2018).

Table 10: Post hoc test (Tukey HSD) p-values of the initial absolute pathogen biomass quantification experiment (1) and confirmation experiment (2), 7 days post-infection. Each section contains a p-value respective to the Tukey test result of the treatments in the same row and column. Significantly different results are indicated in green, results that are not significantly different are indicated in red/purple (n=7).

(1)

	HA1	HA2	PH1	PH2	SW1	SW2	CON -	
	0.001	0.006	0.979	0.588	0.316	1.000	0.017	Con +
		0.999	0.019	0.167	0.372	0.002	0.983	HA1
			0.078	0.443	0.728	0.010	1.000	HA2
				0.984	0.874	0.986	0.170	PH1
					1.000	0.649	0.670	PH2
						0.377	0.901	SW1
							0.026	SW2

p-value:

0.00 - 0.01	Lightest Green	Difference
0.01 - 0.03	Light Green	
0.03 - 0.05	Green	No difference
0.05 - 0.10	Light Red	
0.10 - 0.30	Red	
0.30 - 0.50	Dark Red	
0.50 - 0.80	Red	
0.80 - 0.95	Dark Red	
0.95 - 0.99	Purple	
0.99 - 1.00	Dark Purple	

(2)

	HA1	HA2	PH1	PH2	SW1	SW2	CON -	
	0.003	0.002	0.138	0.343	0.023	0.951	0.002	Con +
		1.000	0.757	0.444	0.989	0.020	1.000	HA1
			0.799	0.477	0.997	0.019	1.000	HA2
				1.000	0.993	0.574	0.707	PH1
					0.901	0.878	0.394	PH2
						0.151	0.985	SW1
							0.016	SW2

p-value:

0.00 - 0.01	Lightest Green	Difference
0.01 - 0.03	Light Green	
0.03 - 0.05	Green	No difference
0.05 - 0.10	Light Red	
0.10 - 0.30	Red	
0.30 - 0.50	Dark Red	
0.50 - 0.80	Red	
0.80 - 0.95	Dark Red	
0.95 - 0.99	Purple	
0.99 - 1.00	Dark Purple	

4.3 Assessing *A. thaliana* growth, productivity, and immune response to *H. arabidopsidis* by quantifying chlorophyll and carotenoid content

A pigment extraction was conducted on *Hyaloperonospora arabidopsidis*-infected *Arabidopsis thaliana* that was inoculated with all treatments. This to examine absolute chlorophyll content as a marker for plant growth, relative chlorophyll content as a marker for plant productivity, and finally relative carotenoid content as a marker for phytoalexin-mediated plant immune response.

4.3.1 Plant growth: absolute chlorophyll content

The Shapiro-Wilk normality test revealed all datasets to be normally distributed. However, the Levene's test indicated non-equal variances (p-value = 0.028), therefore non-parametric tests needed to be used. The Welch's ANOVA test yielded a p-value of 0.001, indicating that there were significant differences between treatments in terms of pathogenic biomass reducing effects. The results of a post hoc test ($\alpha = 0.05$), are summarized in Table 11, containing p-values and shades of red, purple, and green that resemble different ranges of significance.

The box and whisker plot (Fig. 22) showed that the highest absolute chlorophyll content can be coupled to the uninfected plant samples ($32.343 \pm 3.344 \mu\text{g}$ chlorophyll), which is an expected result since these plants did not undergo infection. The two treatments with the highest total chlorophyll and thus the highest growth were the malt extract (PH2; $29.833 \pm 5.233 \mu\text{g}$ chlorophyll) and the *E. maxima* extract (Kelpak®) (SW2; $29.630 \pm 3.104 \mu\text{g}$ chlorophyll) treatments. Both were found significantly different from the negative control (PH2; p-value = 0.013; SW2; p-value = 0.016), indicating that adding these treatments increased plant growth under pathogenic infection compared to adding water. These findings are similar to those claimed by Chatzissavvidis and Therios (2014), describing improved growth for wheat plant seedlings in terms of dry mass ratio after treatment with *E. maxima* extract (Kelpak®) and Colla et al. (2015) describing accelerated growth of tomato plant roots after a lime plant-derived PH treatment.

When comparing the treatment's absolute chlorophyll content to the uninfected plants, only the negative control (Con.-) was found to be significantly different, indicating that all other treatments induced plant growth that is not significantly different from the plants not being infected. Especially treatments PH2 (p-value = 0.996) and SW2 (p-value = 0.993) showed prominent levels of similarity.

Compared to the biostimulant treatments, the plants that were inoculated with the difenoconazole fungicide (Con. +) showed mediocre plant growth ($26.396 \pm 4.983 \mu\text{g}$ chlorophyll). This is confirmed by no treatment being labelled as significantly different, with all biostimulant treatments showing a high degree of similarity (p-value > 0.950). This possibly indicating that this compound did not only reduce pathogen biomass as seen in the qPCR experiment (Section 4.2.2.3), but also resulted in reduced plant growth, either through shifting resources to plant defence or by being directly phytotoxic. However, the positive control was also not found to be significantly different from the uninfected plants, indicating that the addition of difenoconazole fungicides does not alter plant growth significantly. When reviewing literature, difenoconazole is found to decrease plant growth significantly in wheat seedlings

(Liu et al. 2021) when used in high concentrations (50-200 mg/L), however this is a factor higher than the used concentration (16.7 mg/L) used in this thesis.

The lowest average plant growth was observed with the water treatment (18.252 ± 3.784 µg chlorophyll). However, the fulvic acid treatment (HA2) also showed replicates that had lower plant growth (23.204 ± 7.691 µg chlorophyll) compared to the negative control due to its large variation.

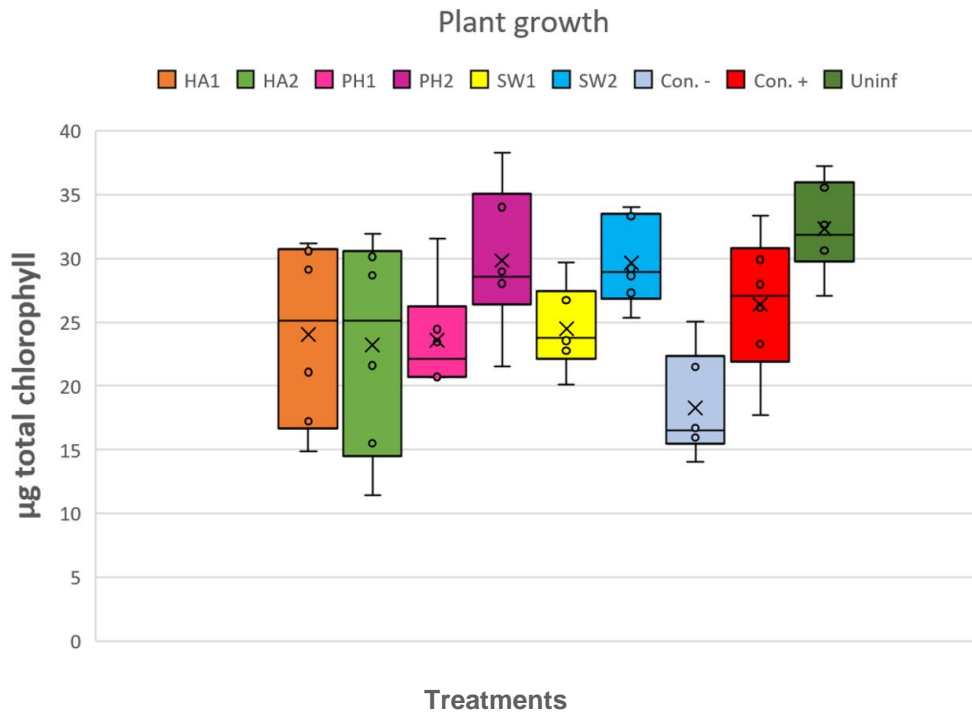


Figure 22: Box and whisker plot of the total absolute chlorophyll content indicating plant growth and biomass, 10 days post-infection. On the y-axis, the total amount of chlorophyll is depicted in micrograms. On the x-axis, all treatments are given in their distinct colours (n=7). The plot is generated using Excel (Microsoft Corp. 2018).

Table 11: Post hoc test (Dunnett's T3) p-values of the absolute chlorophyll content experiment 10 days post-infection. Each section contains a p-value respective to the Tukey test result of the treatments in the same row and column. Significantly different results are indicated in green, results that are not significantly different are indicated in red/purple (n=7).

	HA1	HA2	PH1	PH2	SW1	SW2	CON -	Uninf	
	0.997	0.980	0.992	0.969	0.999	0.978	0.198	0.597	CON +
		1.000	1.000	0.625	1.000	0.668	0.668	0.176	HA1
			1.000	0.453	1.000	0.496	0.796	0.100	HA2
				0.539	1.000	0.582	0.720	0.134	PH1
					0.722	1.000	0.013	0.996	PH2
						0.762	0.536	0.237	SW1
							0.016	0.993	SW2
								0.001	CON -

p-value:

- 0.00 - 0.01
- 0.01 - 0.03
- 0.03 - 0.05
- 0.05 - 0.10
- 0.10 - 0.30
- 0.30 - 0.50
- 0.50 - 0.80
- 0.80 - 0.95
- 0.95 - 0.99
- 0.99 - 1.00

Difference
No difference

4.3.2 Plant productivity: relative chlorophyll content

The Shapiro-Wilk normality test revealed all datasets to be normally distributed. However, the Levene's test indicated non-equal variances (p-value = 0.015), therefore non-parametric tests needed to be used. The Welch's ANOVA test yielded a p-value of 0.007, indicating that there are significant differences between treatments in terms of pathogenic biomass reducing effects. The results of a post hoc test ($\alpha = 0.05$), are summarized in Table 12, containing p-values and shades of red, purple, and green that resemble different ranges of significance.

The box and whisker plot (Fig. 23) shows that the highest relative chlorophyll content can be coupled to the uninfected plant samples ($0.165 \pm 0.047 \mu\text{g chlorophyll} / \text{mg plant material}$) as expected since infection did not occur in these plants. This is confirmed by the uninfected plants being significantly different from the negative control (Con.-; p-value = 0.008).

Among the treatments, the *Ecklonia maxima* extract (Kelpak®) treatment (SW2; $0.146 \pm 0.016 \mu\text{g chlorophyll} / \text{mg}$) and the malt extract (PH2) treatment ($0.159 \pm 0.032 \mu\text{g chlorophyll} / \text{mg}$) exhibited the highest relative chlorophyll content and consequently the highest level of productivity and photosynthetic capacity under pathogenic infection. Both were also found to be significantly different from the negative control treatments (SW2; p-value = 0.008; PH2; p-value = 0.017) and exhibited no significant difference compared to the uninfected plants (PH2; p-value = 1.000; SW2; p-value = 0.992). This is in line with literature, claiming that *E. maxima* seaweed extract improved plant productivity under stress (Shukla et al., 2021) and that a PH treatment in banana plants attributed to high chlorophyll content (Colla et al.)

Conversely, the plants treated with the difenoconazole fungicide (Con. +) displayed proportional plant productivity ($0.129 \pm 0.022 \mu\text{g chlorophyll} / \text{mg}$) compared to the biostimulant treatments, suggesting that the fungicide lowers plant productivity since it did show a reduction in pathogenic biomass (Section 4.2.2.3) and is thus expected to have high productivity. When comparing the positive control to the uninfected plants, no significant difference was found, indicating that the addition of difenoconazole fungicides did not significantly alter plant growth. According to the literature, high concentrations of difenoconazole (50-200 mg/L) have been found to significantly decrease photosynthetic capacity in wheat seedlings (Liu et al., 2021). However, the concentration used in this study (16.7 mg/L) is much lower and does not show to have a significant impact on relative chlorophyll levels.

When comparing the relative chlorophyll content of the treatments to the uninfected plants, only the negative control (Con.-) showed a significant difference. This suggests that all other treatments induced plant productivity that was not significantly different from the uninfected plants.

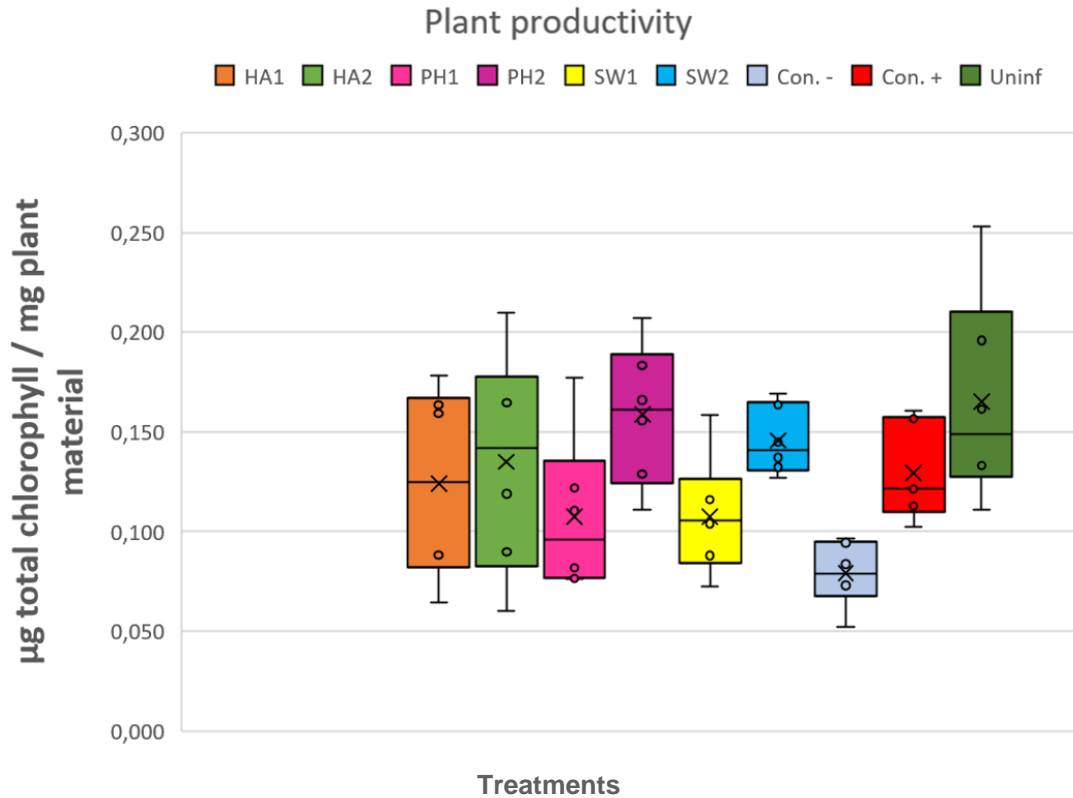


Figure 23: Box and whisker plot of the total relative chlorophyll content indicating plant health and photosynthetic capacity, 10 days post-infection. On the y-axis, the total relative amount of chlorophyll is depicted in micrograms per mg of plant material. On the x-axis, all treatments are given in their distinct colours (n=7). The plot is generated using Excel (Microsoft Corp. 2018).

Table 12: Post hoc test (Dunnett's T3) p-values of the total relative chlorophyll content experiment 10 days post-infection. Each section contains a p-value respective to the Tukey test result of the treatments in the same row and column. Significantly different results are indicated in green, results that are not significantly different are indicated in red/purple (n=7).

	HA1	HA2	PH1	PH2	SW1	SW2	CON -	Uninf	
	1.000	1.000	0.983	0.912	0.984	0.998	0.356	0.777	CON +
		1.000	0.997	0.806	0.998	0.985	0.506	0.627	HA1
			0.933	0.975	0.936	1.000	0.224	0.902	HA2
				0.335	1.000	0.714	0.925	0.196	PH1
					0.339	1.000	0.017	1.000	PH2
						0.719	0.922	0.199	SW1
							0.008	0.992	SW2
								0.008	CON -

p-value:	
0.00 - 0.01	
0.01 - 0.03	
0.03 - 0.05	
0.05 - 0.10	Difference
0.10 - 0.30	No difference
0.30 - 0.50	
0.50 - 0.80	
0.80 - 0.95	
0.95 - 0.99	
0.99 - 1.00	

4.3.3 Plant immune reaction: relative carotenoid content

The Shapiro-Wilk normality test revealed all datasets to be normally distributed and the Levene's test indicated equal variances (p-value = 0.053), therefore parametric tests could be used. The one-way ANOVA test yielded a p-value lower than 0.001, indicating that there are significant differences between treatments in terms of pathogenic biomass reducing effects. The results of a post hoc test ($\alpha = 0.05$), are summarized in Table 13, containing p-values and shades of red, purple, and green that resemble different ranges of significance.

The box and whisker plot (Fig. 24) shows high relative carotenoid content for both the malt extract (PH2; $0.067 \pm 0.006 \mu\text{g carotenoid} / \text{mg}$) and the *Ecklonia maxima* seaweed extract (SW2; $0.062 \pm 0.005 \mu\text{g carotenoid} / \text{mg plant material}$) treatments, indicating a notable increase in carotenoid-mediated immune response compared to the water treatment (Con.-; $0.036 \pm 0.008 \mu\text{g carotenoid} / \text{mg}$). Both treatments have been found to induce a significantly higher relative carotenoid content and thus an increased immune reaction compared to the water treatment (PH2; p-value = 0.003; SW2; p-value = 0.021). Even though no information is available on the use of malt extract as a biostimulant, protein hydrolysates (PH) have been proven to increase phytoalexin production (Lucini et al., 2022), which is mediated by carotenoids. In the study of Zodape et al., (2011) *E. maxima* (Kelpak®) sprayed carrot plants also showed fewer disease symptoms related to *Botrytis cinerea*, a fungal disease similar to oomycete *H. arabidopsidis*, due to an accumulation of phytoalexins.

The lowest immune reaction can be found in the uninfected plant samples ($0.023 \pm 0.007 \mu\text{g carotenoid} / \text{mg}$); which was expected since these were not infected and thus did not experience an *H. arabidopsidis* mediated immune system activation. However, the uninfected plant samples did not show a significantly lower carotenoid content compared to the negative control (p-value = 0.751). Carotenoid levels in these plants are not equal to zero since these compounds are also present in specialized plant tissues such as roots (Wang et al. 2013). Also, these low carotenoid levels could be the result of the abiotic stress caused by the plants being transferred to the slightly colder infection growth chamber (16 °C, 65% RH) which has been proven for *A. thaliana* by Havaux & Kloppstech (2001).

The positive control ($0.047 \pm 0.017 \mu\text{g carotenoid} / \text{mg}$) showed relatively higher immune responses than the negative control, and comparable to biostimulant treatments HA1 ($0.053 \pm 0.013 \mu\text{g carotenoid} / \text{mg}$), HA2 ($0.053 \pm 0.015 \mu\text{g carotenoid} / \text{mg}$) and SW1 ($0.045 \pm 0.017 \mu\text{g carotenoid} / \text{mg}$). This is a notable result since the claimed mode of action of the fungicide is through inhibiting pathogen enzymatic pathways, rather than inducing an immune response in the host crop. However, the difenoconazole itself, or the preservative 1,2-benzisothiazolin-3-one (BIT) that is also present in the fungicide may cause stress, leading to an increased immune response compared to the immune reaction it would undergo during ordinary *H. arabidopsidis* infection. However, when compared to the negative control, the fungicide (Con.+) did not show a significant difference (p-value = 0.838). Indicating that the difenoconazole or BIT did not cause a significant increase in immune response in the plant, compared to the plant only being infected with *H. arabidopsidis* after a water treatment. This is confirmed by experiments of Zheng et al. (2023), where carotenoid concentrations in difenoconazole-treated tomato plants (100 g / ha) were not significantly different from a negative control after a period of seven days. No applicable literature was found on the influence of BIT on plant carotenoid levels.

Finally, only biostimulant treatments PH1 (p-value = 0.575) and SW1 (p-value = 0.125) were found not to be significantly different when compared to the uninfected plants. Indicating that

only these did not show significantly higher levels of carotenoids compared to the uninfected samples. However, these showed high levels of similarity when compared to the negative control and can thus not be seen as lowering carotenoid-mediated immune response.

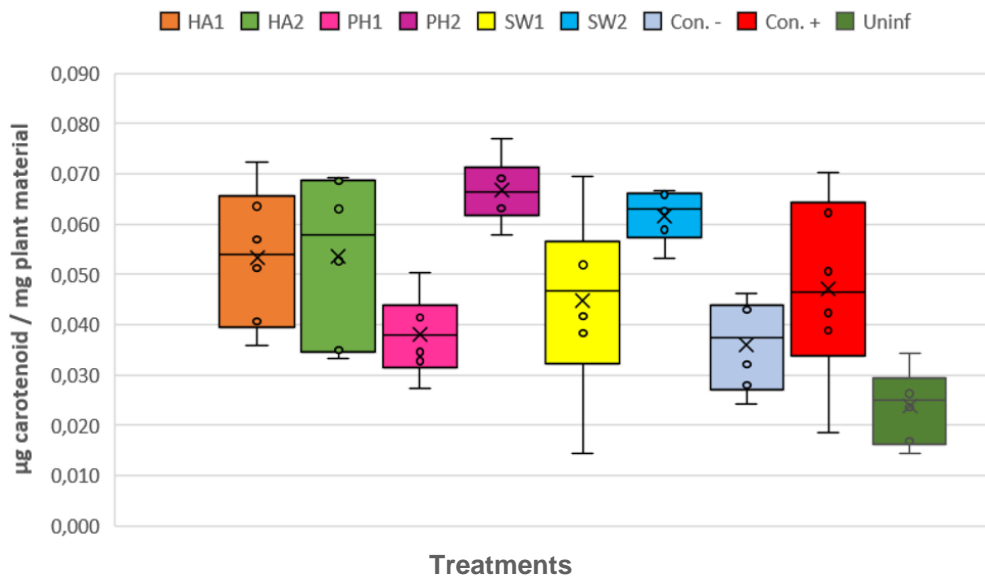


Figure 24: Box and whisker plot of the total relative carotenoid content indicating plant immune reaction, 10 days post-infection. On the y-axis, the total relative carotenoid content is depicted in micrograms per mg of plant material. On the x-axis, all treatments are given in their distinct colours (n=7). The plot is generated using Excel (Microsoft Corp. 2018).

Table 13: Post hoc test (Tukey HSD) p-values of the relative carotenoid content experiment 10 days post-infection. Each section contains a p-value respective to the Tukey test result of the treatments in the same row and column. Significantly different results are indicated in green, results that are not significantly different are indicated in red/purple (n=7).

	HA1	HA2	PH1	PH2	SW1	SW2	CON -	Uninf	
	0.992	0.990	0.941	0.167	1.000	0.514	0.838	0.047	CON +
		1.000	0.455	0.665	0.941	0.962	0.295	0.005	HA1
			0.440	0.680	0.934	0.966	0.283	0.004	HA2
				0.006	0.992	0.044	1.000	0.575	PH1
					0.078	0.999	0.003	0.001	PH2
						0.307	0.957	0.125	SW1
							0.021	0.001	SW2
								0.751	CON -

p-value:	
0.00 - 0.01	Green
0.01 - 0.03	Light Green
0.03 - 0.05	Dark Green
0.05 - 0.10	Red
0.10 - 0.30	Light Red
0.30 - 0.50	Dark Red
0.50 - 0.80	Red
0.80 - 0.95	Light Purple
0.95 - 0.99	Dark Purple
0.99 - 1.00	Light Purple

4.4 *H. arabidopsis* infection growth kinetics

Analysing the growth kinetics of *Hyaloperonospora arabidopsis* on *Arabidopsis thaliana* will give a direct view of the possible growth-reducing effects of the two overall best-performing biostimulant treatments, being the *Ecklonia maxima* extract (Kelpak®; SW2) and the malt extract (PH2). Kinetic parameters and growth curves are determined via a spore count to quantify pathogenic sporulation and via qPCR to quantify the total pathogenic biomass in the plants, using the same methods as described before. Values of pathogenic load such as the relative spore load and absolute pathogenic biomass can diverge from previous experiments since the infection itself was done by administering the spore solution via pipetting instead of spraying to ensure equal infection loads.

4.4.1 *H. arabidopsis* sporulation kinetics

On the *H. arabidopsis* sporulation growth curve (Fig. 25), differences between all treatments are visible, with spore loads following the results derived from the spore count experiment over the examined timeline. The fungicide treated plants (CON.+) showed the overall lowest sporulation of all treatments, followed by biostimulant treatments PH2 and SW2 respectively. The highest sporulation over the timeline could be seen with the water treatment (CON.-). The sporulation curves of both biostimulant treatments seemed to converge on days 8 and 10, which were confirmed not to be significantly different by t-tests yielding p-values of 0.375 and 0.512 for day 8 and day 10 respectively. The declining spore load was probably due to the spores being fully developed and released into the environment or due to germination itself.

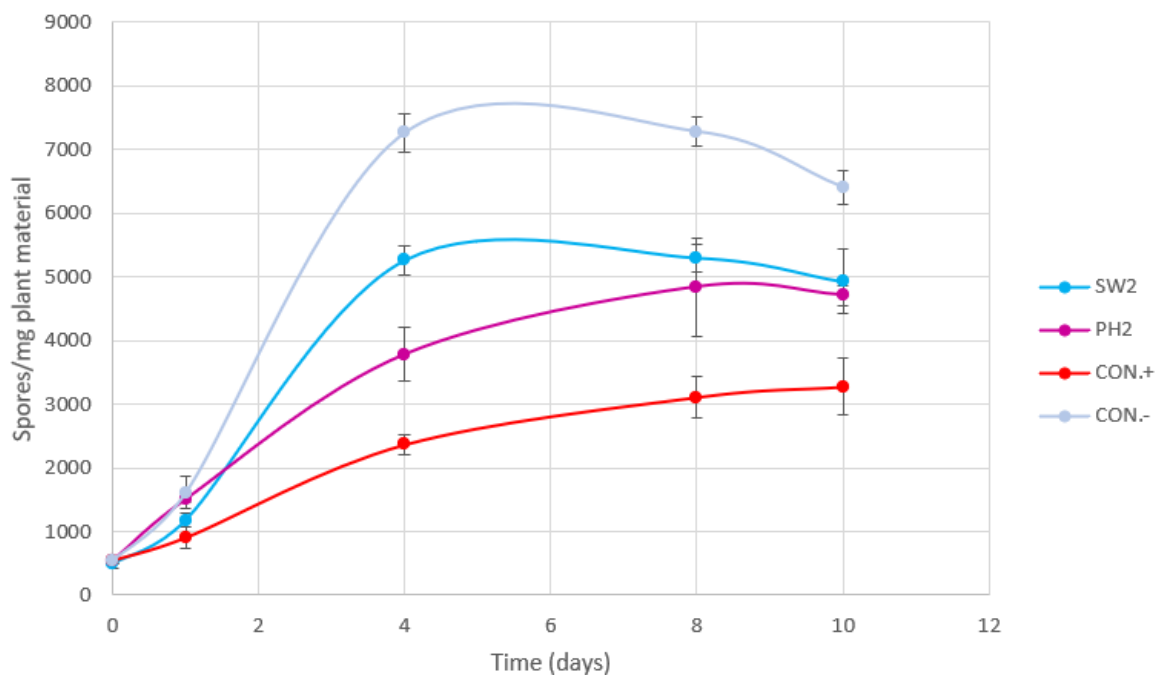


Figure 25: *H. arabidopsis* sporulation growth curves. On the y-axis, the spore load is given in spores per mg of plant material. On the x-axis, time is given in days. 4 different curves are plotted respective to the 4 different used treatments, being SW2, PH2, CON.+ and CON.- (n=4). Graph is generated using Excel (Microsoft Corp. 2018).

All models underwent a Type III analysis of variance test, including ANOVA (Omnibus test) to assess whether there were significant differences among the various treatments and cultivars and subsequently a post hoc pairwise comparison using the emmeans package to compare estimated marginal means. These showed all growth curves to be significantly different ($\alpha = 0.05$), apart from the two biostimulant treatments (p-value = 0.510) PH2 and SW2 based on a pairwise comparison of their estimated marginal means, indicating similar kinetic effects in terms of sporulation reduction. Thus, both biostimulant treatments can be seen as significantly different from the water treatment, meaning that adding one of these biostimulants would result in less sporulation over the analyzed time period. Concerning the PH2 treatment, no relevant literature was found on the influence of malt extract on plant pathogen sporulation. However, *Plasmopara viticola* (downy mildew causal organism in grapevines) spore content itself has been indicated to drop when host plants received a casein-containing protein hydrolysate treatment. For the SW2 treatment, this was also shown by Gleń-Karolczyk & Boligłowa (2015), where *E. maxima* seaweed extract (Kelpak®) treated horseradish plants showed a reduction in linear growth index for six out of seven evaluated fungal pathogens, which was determined via spore counts. However, since the difenoconazole fungicide is significantly different from both biostimulant treatments, it cannot be concluded that these have similar effects in reducing sporulation. Results from the Kenward-Roger degrees-of-freedom analysis indicated that pathogen sporulation is significantly influenced by treatment (p-value < 0.001), by timepoint (p-value < 0.001) and the interaction between both (p-value = 0.007).

When examining the kinetic parameters (Table 14), similar trends were observed, with the positive control performing the best on all parameters, followed by PH2 and SW2 respectively. It is notable that, due to adding a treatment the max load is lowered and the time of max load (TOML) is delayed, with the positive control not having reached a visible maximum over the examined timeline, possibly even surpassing the biostimulants over time. This leads to the conclusion that adding a biostimulant treatment triggers plant mechanisms that could delay and lower sporulation, overgrowing pathogen sporangia and trapping the attached spores thus lowering the spread of the pathogen (e.g. lignin barriers or callose deposition) (Bhatnagar & Dantu, 2015; Hardy & McComb, 2008) or via directly inhibiting the growth and spread of *H. arabidopsidis* hyphae (e.g. phytoalexins or ROS).

Table 14: Effect of treatment on *H. arabidopsidis* sporulation kinetic parameters. These being growth rate, specific growth rate (μ), doubling time (Td), maximal load and time of maximal load (TOML).

	Growth rate (spores/mg) /day	μ (day ⁻¹)	Td (days)	Max load (spores/mg)	TOML (days)
CON.-	1817.311	0.806	0.860	7750	5
SW2	1236.080 -31.98%	0.726 -9.92%	0.954 +11.01%	5900 -23.87%	6 +20.00%
PH2	886.815 -51.20%	0.581 -28.00%	1.194 +38.89%	4820 -37.81%	9 +80.00%
CON.+	473.206 -73.96%	0.435 -46.07%	1.594 +85.42%	3274 -57.75%	10 +100.00%

4.4.2 *H. arabidopsis* biomass growth kinetics

On the *H. arabidopsis* biomass growth curve, all treatments showed similar results in terms of absolute pathogen biomass until sampling day 4 (0.497 ± 0.190 Hpa cells / AT cells). From day 8 on, differences between treatments could be observed, with the fungicide (CON.+) still showing the lowest pathogenic biomass of all treatments, followed by biostimulant treatments PH2 and SW2 respectively. The biostimulant treatments stayed in the same range, not being significantly different on day 8 (p-value = 0.290) (PH2; 1.674 ± 0.021 Hpa cells / AT cells; SW2; 2.028 ± 0.6253 Hpa cells / AT cells), but diverged at day 10, being significantly different (p-value = 0.001), with the malt extract treatment (PH2) experiencing a sudden decline in pathogen biomass (Day 10 = 1.215 ± 0.233 Hpa cells / AT cells)

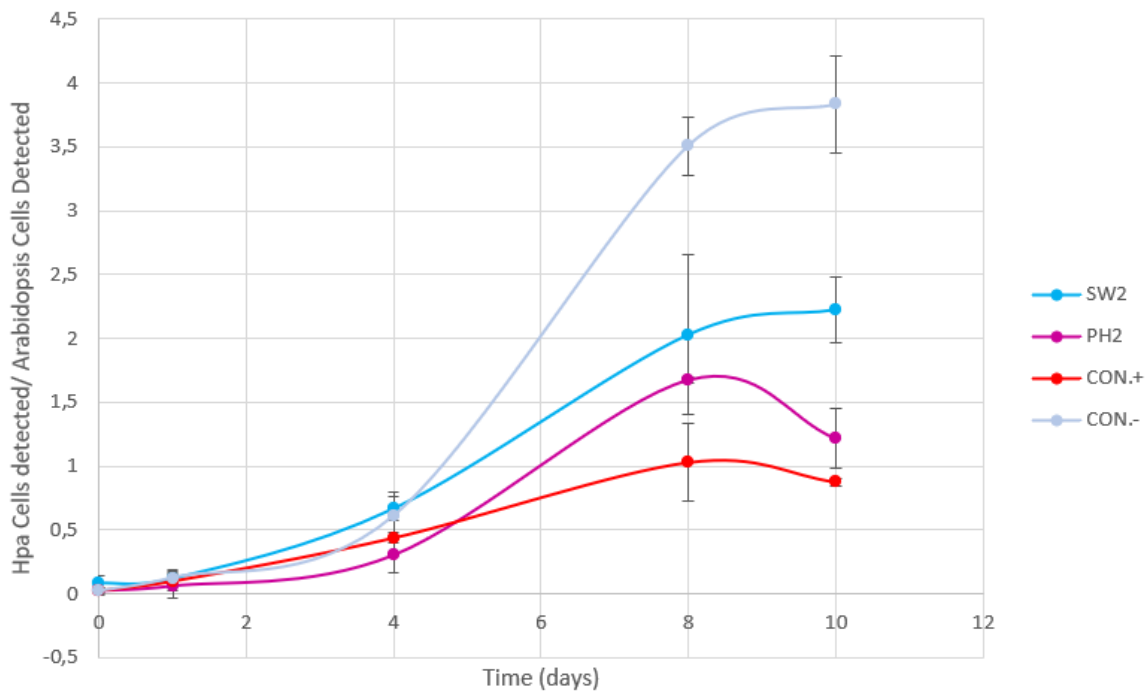


Figure 26: *H. arabidopsis* biomass growth curves. On the y-axis, the absolute pathogenic biomass is given in *H. arabidopsis* cells detected per *A. thaliana* cell detected. On the x-axis, time is given in days. 4 different curves are plotted respective to the 4 different used treatments, being SW2, PH2, CON.+ and CON.- (n=4). Graph is generated using Excel (Microsoft Corp. 2018).

All models underwent a Type III analysis of variance test, including ANOVA (Omnibus test) to assess whether there were significant differences among the various treatments and subsequently a post hoc pairwise comparison using the emmeans package to compare estimated marginal means, with the ANOVA indicating significant differences (p-value < 0.001). When comparing with the positive control in the post hoc test ($\alpha = 0.05$) (Table 15), significant differences can be observed with the negative control (Con.-; p-value < 0.001) and *Ecklonia maxima* seaweed extract (Kelpak®; SW2; p-value = 0.041) based on a pairwise comparison of their estimated marginal means. However, no significant difference (p-value = 0.984) was observed when comparing it to the malt extract treatment (PH2), suggesting that these show a similar reduction in *H. arabidopsis* biomass over the examined time period. However, while there isn't any relevant literature available on the growth rate-reducing effect of malt extract or other plant-derived protein hydrolysates on plant pathogens, reduced *Botrytis cinerea* growth has been demonstrated by Lachhab et al. (2016) on protein hydrolysate-treated wine grapes. When comparing the treatments to the negative control, significant differences appear with the positive control (p-value = 0.001) and PH2 (p-value = 0.001). However, the

SW2 treatment was not found to be significantly different (p-value = 0.089), thus not causing a significant reduction in pathogen biomass compared to the negative control over the examined time period. Results from the Kenward-Roger degrees-of-freedom analysis indicated that pathogen sporulation was significantly influenced by treatment (p-value < 0.001), by timepoint (p-value < 0.001) and the interaction between both (p-value < 0.001).

Table 15: Type III analysis p-values of the biomass kinetic curves. Each section contains a p-value respective to the treatments in the same row and column. Significantly different results are indicated in green, results that are not significantly different are indicated in red/purple (n=7).

PH2	SW2	Con.-	
0.984	0.041	0.001	Con.+
	0.086	0.001	PH2
		0.089	SW2

p-value:	
0.00 - 0.01	
0.01 - 0.03	
0.03 - 0.05	
0.05 - 0.10	
0.10 - 0.30	
0.30 - 0.50	
0.50 - 0.80	
0.80 - 0.95	
0.95 - 0.99	
0.99 - 1.00	

When examining the kinetic parameters (Table 16), it can be concluded that the fungicide (CON.+) showed the greatest pathogen biomass reduction of all treatments. Regarding the pathogenic biomass growth parameters, the *Ecklonia maxima* treatment (Kelpak®; SW2) outperformed the malt extract (PH2) treatment in specific growth rate (μ) and doubling time compared to the negative control. However, these results are nuanced by the fact that the PH2 curve entered the exponential phase on a later stage and experienced a lower maximal pathogenic load in comparison. Another notable result is that unlike in the sporulation kinetics experiment, pathogen-reducing treatments such as CON.+ and PH2 resulted in an accelerated time of max load (TOML). This could, in case of the PH2 treatment, indicate an increased production of phytoalexins or other antimicrobial compounds leading to an inhibition of pathogenic growth and eventually a reduction in absolute pathogenic biomass (Hammerschmidt, 2009).

Table 16: Effect of treatment on *H. arabidopsidis* biomass growth parameters. These being growth rate, specific growth rate (μ), doubling time (Td), maximal load and time of maximal load (TOML).

	Growth rate ((Hpa cells /AT cell) /day)	μ (day ⁻¹)	Td (days)	Max load (Hpa cells/AT cell)	TOML (days)
CON.-	0.2381	0.7429	0.9330	3.2830	10
SW2	0.1828 -23.23%	0.5125 -31.01%	1.3525 +44.96%	2.2230 -32.32%	10 0%
PH2	0.1624 -31.79%	0.6074 -18.24%	1.1412 +22.31%	1.6744 -49.09%	8 -20.00%
CON.+	0.1269 -46.69%	0.4775 -35.72%	1.4516 +55.58%	1.0279 -68.60%	8 -20.00%

5 CONCLUSION

Given the current dependence on synthetic pesticides for plant disease management and its implications for global food security, there is a significant need to explore and develop biological alternatives capable of replacing these hazardous substances. This demand arises from the growing recognition of the detrimental environmental and health impacts associated with the use of synthetic pesticides.

In conclusion, this thesis investigated the effectiveness of various organic plant biostimulants in suppressing *Hyaloperonospora arabidopsidis* on *Arabidopsis thaliana* plants as a model system for downy mildew infections. The biostimulants included humic acid (HA1), fulvic acid (HA2), a commercial soybean extract (PH1), malt extract (PH2), and commercial *Ecklonia maxima* seaweed extracts from two suppliers (SW1) and (SW2). These were compared to water (Con.-) as a negative control and difenoconazole fungicide (Con.+) as a positive control. Notably, the existing literature provided limited insights into the specific impact of these biostimulants on this particular plant pathogen. Therefore, this study aimed to quantify the potential reduction in pathogen severity when model plants were treated with these different biostimulant treatments.

The results revealed that out of the six examined biostimulants, two demonstrated a notable reduction in sporulation, pathogenic biomass, and growth parameters, these being the malt extract (PH2) and the *E. maxima* seaweed extract (SW2) biostimulant treatments. Both also showed increases in plant growth, photosynthetic capacity, and carotenoid-mediated immune response under infection conditions. These findings highlight the potential of these specific biostimulants as effective tools in managing the spread of *H. arabidopsidis*-like plant pathogens and mitigating their impact on economically relevant crops (e.g. *Plasmopara viticola* in grapevine and *Rhizoctonia solani* in tomato plants). However, it is important to acknowledge that the remaining four biostimulants did not exhibit significant disease-suppressive effects in all experiments conducted in this particular study.

These findings contribute to the understanding of the potential of biostimulants in plant disease management and provide valuable insights for future research and the development of targeted strategies in global agriculture to combat downy mildew infections. In this way, an increased food certainty would be developed that will ultimately reduce or even eliminate the extensive use of pesticides that is seen today.

Further investigation is warranted to explore the mechanisms underlying the disease-suppressive effects of the identified biostimulants and to optimize their application protocols for maximum efficacy, such as optimizing concentration and the method of administration.

Overall, this study serves as a foundation for future advancements in the utilization of biostimulants as sustainable and environmentally friendly alternatives to pesticides in plant disease control strategies.

Table 17: Overview of all experimental outcomes. In the first column, all experiments are given. In the second column, all experimental parameters are given. These are followed by the respective average results of all treatments for that parameter, of which the 3 best-performing treatments are depicted in shades of green, and the worst-performing treatments are depicted in shades red. The lighter the shade, the better the performance of the biostimulant for the respective parameter. Treatments with a significant difference compared the negative control (CON.-) are indicated with (*), treatments that are not significantly different from the positive control (CON.+) are indicated with (**), and treatments satisfying both criteria are indicated with (***)

Experiment	Parameter	HA1	HA2	PH1	PH2	SW1	SW2	CON. +	CON. -	Uninf.
Sporulation Quantification	Spore content (Spores/mg)	828 **	986 **	1610	442 ***	1411	1441 **	605	1423	
Biomass Quantification	Absolute biomass (Hpa cells/AT cells)	1.06	1.00	0.69 **	0.78 **	0.83 **	0.59 ***	0.59	0.96	
Pigment Extraction	Growth: Abs. chlorophyll content (μg)	24.02 **	23.20 **	23.61 **	29.83 ***	24.48 **	29.63 ***	26.40	18.25	32.34 ***
	Productivity: Rel. chlorophyll content ($\mu\text{g}/\text{mg}$)	0.124 **	0.135 **	0.107 **	0.159 ***	0.108 **	0.146 ***	0.129	0.079	0.165 ***
	Immune response: Rel. carotenoid content ($\mu\text{g}/\text{mg}$)	0.053 **	0.054 **	0.038 **	0.067 ***	0.045 **	0.062 ***	0.047	0.036	0.024
Sporulation Kinetics	Specific growth rate μ (Day^{-1})				0.581 *		0.7264 *	0.435	0.806	
	Max load (spores/mg)				4820 *		5900 *	3274	7750	
Pathogenic growth Kinetics	Specific growth rate μ (Day^{-1})				0.607 ***		0.513	0.478	0.743	
	Max load (Hpa cells/AT cells)				1.674 ***		2.223	1.028	3.283	

6 LIMITATIONS

The limitations of any research play a crucial role in shaping the understanding and interpretation of its findings. This section aims to provide a comprehensive exploration of the limitations encountered throughout the course of this thesis. By acknowledging these constraints, transparency is ensured, and a balanced perspective is established, thereby enhancing the validity and reliability of the study.

First of all, lab conditions can heavily influence experimental outcomes. An example of this is the lack of environmental realism, since fluctuations in environmental factors (e.g. temperature, humidity, light intensity, air movement) are not present in growth chambers. All these factors are optimized for plant growth or pathogenic development and therefore only reflect optimal conditions that are unlikely in nature. Also, the lack of diverse microbial communities from the environment might influence experiments since these often interact with the plant or pathogen in a beneficial or antagonistic way.

Secondly, artificial inoculation was used, leading to relatively high infection dosages. Thus, these methods may not accurately replicate natural modes of pathogen transmission through vectors such as air movement. However, the use of high dosages was justified since it assured that the pathogen will overcome host resistance and accelerate disease development to shorten the timeframe of experimental work.

Furthermore, the aim of this thesis was limited to identifying which of the used biostimulants induce an increased resistance to the pathogen responsible for downy mildew (*H. arabidopsidis*). Therefore, no optimal concentrations of these biostimulants were determined. Thus, it could be possible that, when used at a higher or lower concentration, low performing biostimulants could also show significant effects and high performing biostimulants could show the opposite (Vernieri et al., 2005).

Finally, this paper discussed the administration of biostimulants via leaf contact in laboratory conditions. These compounds are then taken up via foliar feeding. However, foliar uptake can be influenced by various factors that are not present in laboratory conditions and can reduce effectiveness and may need to be considered. For example, the intensity of sunlight and high temperature may cause the biostimulant solutions to evaporate, reducing the contact with the leaf's surface and lowering the uptake rate (Patil et al., 2018). Factors such as wind or rain may cause the solution sprayed onto the leaves to be diluted, washed away, or blown away. Low temperatures cause the cuticle layer on the leaves' surface to become thicker and have a lower elasticity (Edelmann et al., 2005), fostering a reduced foliar uptake. Finally, air humidity can also play a role in foliar feeding. A high humidity can help prolong contact between the solution and the leaf surface, a low humidity on the other hand will result in faster evaporation and thus a lower contact time. Ideal weather conditions for biostimulant spraying will thus be a dry, cloudy, windless day with a temperature between 10-30 °C and a high humidity.

References.

- A. C., Schürmann, P., & Buchanan, B. B. (1976). Effect of powdery mildew infection on photosynthesis by leaves and chloroplasts of sugar beets. *Plant Physiology*, 57(4), 486-489.
- Al-Huqail, A., El-Dakak, R. M., Sanad, M. N., Badr, R. H., Ibrahim, M. M., Soliman, D., & Khan, F. (2020). Effects of climate temperature and water stress on plant growth and accumulation of antioxidant compounds in sweet basil (*Ocimum basilicum* L.) leafy vegetable. *Scientifica*, 2020.
- Alabouvette, C., Olivain, C., & Steinberg, C. (2006). Biological control of plant diseases: the European situation. *European journal of plant pathology*, 114, 329-341.
- Alghamdi, B. A., Alshumrani, E. S., Saeed, M. S. B., Rawas, G. M., Alharthi, N. T., Baeshen, M. N., ... & Suhail, M. (2020). Analysis of sugar composition and pesticides using HPLC and GC-MS techniques in honey samples collected from Saudi Arabian markets. *Saudi Journal of Biological Sciences*, 27(12), 3720-3726.
- Ali, A., Shah, L., Rahman, S., Riaz, M. W., Yahya, M., Xu, Y. J., ... & Cheng, B. (2018). Plant defense mechanism and current understanding of salicylic acid and NPRs in activating SAR. *Physiological and molecular plant pathology*, 104, 15-22.
- Alshammari, G. M., Al-Daghri, N. M., & Yakout, S. M. (2021). Difenoconazole and human health: A systematic review of exposure levels, toxicity, and health effects. *Journal of Environmental Science and Health, Part C*, 39(1), 22-44.
- Anderson, R. G., & McDowell, J. M. (2015). A PCR assay for the quantification of growth of the oomycete pathogen *Hyaloperonospora arabidopsidis* in *Arabidopsis thaliana*. *Molecular Plant Pathology*, 16(8), 893-898.
- Arabidopsis Genome Initiative. (2000). Analysis of the genome sequence of the flowering plant *Arabidopsis thaliana*. *Nature*, 408(6814), 796-815.
- Arrus, K., Blank, G., Abramson, D., Clear, R., & Holley, R. A. (2005). Aflatoxin production by *Aspergillus flavus* in Brazil nuts. *Journal of Stored Products Research*, 41(5), 513-527.
- Atreya, K., Johnsen, F. H., & Sitaula, B. K. (2012). Health and environmental costs of pesticide use in vegetable farming in Nepal. *Environment, Development and Sustainability*, 14, 477-493.
- Ayala, G., Torres, R., & Canseco, M. (2021). Microbial growth curve. In *StatPearls* [Internet]. StatPearls Publishing.
- Bailey, K., Çevik, V., Holton, N., Byrne-Richardson, J., Sohn, K. H., Coates, M., ... & Tör, M. (2011). Molecular cloning of ATR5Emoy2 from *Hyaloperonospora arabidopsidis*, an avirulence determinant that triggers RPP5-mediated defense in *Arabidopsis*. *Molecular plant-microbe interactions*, 24(7), 827-838.
- Barrada, A., Delisle-Houde, M., Nguyen, T. T. A., Tweddell, R. J., & Dorais, M. (2022). Drench Application of Soy Protein Hydrolysates Increases Tomato Plant Fitness, Fruit Yield, and Resistance to a Hemibiotrophic Pathogen. *Agronomy*, 12(8), 1761.
- Behind The Bench Staff (2019, September 25). PCR Primer Design Tips. Behind the Bench.
- Beketov, M. A., Kefford, B. J., Schäfer, R. B., & Liess, M. (2013). Pesticides reduce regional biodiversity of stream invertebrates. *Proceedings of the National Academy of Sciences*, 110(27), 11039-11043.
- Benami, M., Isack, Y., Grotzky, D., Levy, D., & Kofman, Y. (2020). The economic potential of arbuscular mycorrhizal fungi in agriculture. *Grand challenges in fungal biotechnology*, 239-279.
- Bent, A.F., Innes, R.W., Ecker, J.R. and Staskawicz, B.J. (1992) Disease development in ethylene-insensitive *Arabidopsis thaliana* infected with virulent and avirulent *Pseudomonas* and *Xanthomonas*
- Bernoux, M., Cerri, C.E.P., (2005). GEOCHEMISTRY | Soil, Organic Components, Encyclopedia of Analytical Science (Second Edition), Pages 203-208, ISBN 9780123693976,
- Bevan, M., Mayer, K., White, O., Eisen, J. A., Preuss, D., Bureau, T., ... & Mewes, H. W. (2001). Sequence and analysis of the *Arabidopsis* genome. *Current opinion in plant biology*, 4(2), 105-110.
- Bhalerao, R. P., & Fischer, U. (2017). Environmental and hormonal control of cambial stem cell dynamics. *Journal of experimental botany*, 68(1), 79-87.
- Birtić, S., & Kranner, I. (2006). Isolation of high-quality RNA from polyphenol-, polysaccharide- and lipid-rich seeds. *Phytochemical Analysis: An International Journal of Plant Chemical and Biochemical Techniques*, 17(3), 144-148.
- Bliffeld, M., Mundy, J., Potrykus, I., & Fütterer, J. (1999). Genetic engineering of wheat for increased resistance to powdery mildew disease. *Theoretical and Applied Genetics*, 98, 1079-1086.
- Bocanegra, M. P., Lobartini, J. C., & Orioli, G. A. (2006). Plant uptake of iron chelated by humic acids of different molecular weights. *Communications in soil science and plant analysis*, 37(1-2), 239-248.
- Bock, C. H., Parker, P. E., & Cook, A. Z. (2017). Diseases caused by fungi. In *Plant disease epidemiology: Facing challenges of the 21st century* (pp. 41-71). Springer.
- Bozdoğan, A. M. (2014). Assessment of total risk on non-target organisms in fungicide application for agricultural sustainability. *Sustainability*, 6(2), 1046-1058.
- Brouwer, M., Lievens, B., Van Hemelrijck, W., Van den Ackerveken, G., Cammue, B. P., & Thomma, B. P. (2003). Quantification of disease progression of several microbial pathogens on *Arabidopsis thaliana* using real-time fluorescence PCR. *FEMS Microbiology Letters*, 228(2), 241-248.
- Burns, M. J., Nixon, G. J., Foy, C. A., & Harris, N. (2005). Standardisation of data from real-time quantitative PCR methods—evaluation of outliers and comparison of calibration curves. *BMC biotechnology*, 5(1), 1-13.
- Bustin, S. A. (2010). Why the need for qPCR publication guidelines? --The case for MIQE. *Methods*, 50(4), 217-226.
- Bustin, S. A., Benes, V., Garson, J. A., Hellems, J., Huggett, J., Kubista, M., ... & Wittwer, C. T. (2009). The MIQE guidelines: minimum information for publication of quantitative real-time PCR experiments. *Clinical chemistry*, 55(4), 611-622.
- Bustin, S.A., Benes, V., Garson, J.A., Hellems, J., Huggett, J., Kubista, M., Mueller, R., Nolan, T., Pfaffl, M.W., Shipley, G.L., et al. (2009). The MIQE guidelines: minimum information for publication of quantitative real-time PCR experiments. *Clin. Chem.* 55, 611–622.
- Cabral, A., Stassen, J. H., Seidl, M. F., Bautor, J., Parker, J. E., & Van den Ackerveken, G. (2011). Identification of *Hyaloperonospora arabidopsidis* transcript sequences expressed during infection reveals isolate-specific effectors. *PLoS One*, 6(5), e19328.
- Canellas, L. P., Olivares, F. L., Aguiar, N. O., Jones, D. L., Nebbioso, A., Mazzei, P., & Piccolo, A. (2015). Humic and fulvic acids as biostimulants in horticulture. *Scientia Horticulturae*, 196, 15–27.
- Cao, H., & Shockey, J. M. (2012). Comparison of TaqMan and SYBR Green qPCR methods for quantitative gene expression in tung tree tissues. *Journal of agricultural and food chemistry*, 60(50), 12296-12303.
- Cerdán, M., Sánchez-Sánchez, A., Jordá, D.J., Juárez, M., Andreu, J.S., 2013. Effect of commercial amino acids on iron nutrition of tomato plants grown under lime-induced iron deficiency. *J. Plant Nutr. Soil Sci.* 176, 1–8.

- Chambers, J. E., Greim, H., Kendall, R. J., Segner, H., Sharpe, R. M., & Van Der Kraak, G. (2014). Human and ecological risk assessment of a crop protection chemical: a case study with the azole fungicide epoxiconazole. *Critical reviews in toxicology*, 44(2), 176-210.
- Chatzissavvidis, C., & Therios, I. (2014). Role of algae in agriculture. *Seaweeds* (Ed. Pomin VH), 1-37.
- Chen, J., Feng, L., Ma, W., Jiang, J., Jiang, X., Yang, Y., ... & Liu, X. (2019). Sybr Green-based qPCR for quantitative detection of the membrane transporter gene *LmrS* in *Lactococcus lactis*. *Journal of microbiological methods*, 166, 105734.
- Cheng, Z., Wang, J., Hu, X., Zhou, Y., Zhang, W., & Yang, X. (2020). A novel and efficient approach to synthesize 1,2-benzisothiazolin-3-one. *Chemical Engineering Journal*, 382, 122909.
- Chet I and Baker R (1981) Isolation and biocontrol potential of *Trichoderma harzianum* from soil naturally suppressive to *Rhizoctonia solani*. *Phytopathology* 71: 286–290
- Chew, A. L., & Maibach, H. I. (1997). 1, 2-benzisothiazolin-3-one (Proxel®): irritant or allergen? A clinical study and literature review. *Contact dermatitis*, 36(3), 131-136.
- Chojnacka, K., Saeid, A., Witkowska, Z., & Tuhy, L. (2012). Biologically active compounds in seaweed extracts-the prospects for the application. In *The open conference proceedings journal* (Vol. 3, No. 1, pp. 20-28). Bentham Science Publishers Ltd.
- Coates, M. E., & Beynon, J. L. (2010). *Hyaloperonospora arabidopsidis* as a pathogen model. *Annual review of phytopathology*, 48, 329-345.
- Colla, G., Nardi, S., Cardarelli, M., Ertani, A., Lucini, L., Canaguier, R., & Roupael, Y. (2015). Protein hydrolysates as biostimulants in horticulture. *Scientia Horticulturae*, 196, 28-38.
- Crandall, S. G., Rahman, A., Quesada-Ocampo, L. M., Martin, F. N., Bilodeau, G. J., & Miles, T. D. (2018). Advances in diagnostics of downy mildews: Lessons learned from other oomycetes and future challenges. *Plant disease*, 102(2), 265-275.
- Crowell, D. N., Packard, C. E., Pierson, C. A., Giner, J. L., Downes, B. P., & Chary, S. N. (2003). Identification of an allele of *CLA1* associated with variegation in *Arabidopsis thaliana*. *Physiologia Plantarum*, 118(1), 29-37.
- De Melo, B. A. G., Motta, F. L., & Santana, M. H. A. (2016). Humic acids: Structural properties and multiple functionalities for novel technological developments. *Materials Science and Engineering: C*, 62, 967-974.
- Demmig-Adams, B., Gilmore, A. M., & Iii, W. W. A. (1996). In vivo functions of carotenoids in higher plants. *The FASEB Journal*, 10(4), 403-412.
- Desjardins, P. R., Zentmyer, G. A., & Reynolds, D. A. (1969). Electron microscopic observations of the flagellar hairs of *Phytophthora palmivora* zoospores. *Canadian Journal of Botany*, 47(7), 1077-1079.
- Dieffenbach, C. W., & Dveksler, G. S. (2009). PCR primer design. *Cold Spring Harbor protocols*, 2009(6), pdb-prot5179.
- DNeasy PowerSoil Pro Kits. (n.d.). Qiagen.com.
- Douglas, P. E., & Flannigan, B. (1988). A microbiological evaluation of barley malt production. *Journal of the Institute of Brewing*, 94(2), 85-88.
- Du Jardin, P. (2015). Plant biostimulants: Definition, concept, main categories and regulation. *Scientia horticulturae*, 196, 3-14.
- Edelmann, H. G., Neinhuis, C., & Bargel, H. (2005). Influence of hydration and temperature on the rheological properties of plant cuticles and their impact on plant organ integrity. *Journal of Plant Growth Regulation*, 24, 116-126.
- El-Ghamry, A. M., Abd El-Hai, K. M., & Ghoneem, K. M. (2009). Amino and humic acids promote growth, yield and disease resistance of faba bean cultivated in clayey soil. *Aust. J. Basic Appl. Sci*, 3(2), 731-739.
- Ertani, A., Cavani, L., Pizzeghello, D., Brandellero, E., Altissimo, A., Ciavatta, C., Nardi, S., 2009. Biostimulant activities of two protein hydrolysates on the growth and nitrogen metabolism in maize seedlings. *J. Plant. Nutr. Soil. Sci.* 172 – 237.
- Ertani, A., Schiavon, M., & Nardi, S. (2017). Transcriptome-wide identification of differentially expressed genes in *Solanum lycopersicon* L. in response to an alfalfa-protein hydrolysate using microarrays. *Frontiers in Plant Science*, 8, 1159.
- Evans, M. L., & Cleland, R. E. (1985). The action of auxin on plant cell elongation. *Critical Reviews in Plant Sciences*, 2(4), 317-365.
- Fantozzi, E. (2016). Investigating PAMP-triggered immunity in the *Arabidopsis thaliana/Hyaloperonospora arabidopsidis* interaction (Doctoral dissertation, University of Worcester).
- Farrar, J. S., Wittwer, C. T., & Extreme PCR Methods Workshop, M. (2015). Extreme PCR: efficient and specific DNA amplification in the presence of inhibitors. In *Extreme PCR* (pp. 3-15). Springer.
- Fetch Jr, T. G., & Steffenson, B. J. (1999). Rating scales for assessing infection responses of barley infected with *Cochliobolus sativus*. *Plant disease*, 83(3), 213-217.
- Fiedor, J., & Burda, K. (2014). Potential role of carotenoids as antioxidants in human health and disease. *Nutrients*, 6(2), 466-488.
- Fones, H. N., Bebbler, D. P., Chaloner, T. M., Kay, W. T., Steinberg, G., & Gurr, S. J. (2020). Threats to global food security from emerging fungal and oomycete crop pathogens. *Nature Food*, 1(6), 332-342.
- Form Mixture, P. Pel| C SH Harrison Road, Airfield Busines5 Park. Signal, 3, 3.
- Fuller, S. J., Denyer, S. P., Hugo, W. B., Pemberton, D., Woodcock, P. M., & Buckley, A. J. (1985). The mode of action of 1, 2-benzisothiazolin-3-one on *Staphylococcus aureus*. *Letters in applied microbiology*, 1(1), 13-15.
- Furumura, M. T., Delforno, T. P., Cabral, E., & de Oliveira, L. M. (2018). Sublethal concentrations of biocides increase antibiotic resistance in swine *Escherichia coli* isolates. *Microbial Pathogenesis*, 114, 291-296.
- Gadjev, I., Vanderauwera, S., Gechev, T. S., Laloi, C., Minkov, I. N., Shulaeva, V., ... & Van Breusegem, F. (2006). Transcriptomic footprints disclose specificity of reactive oxygen species signaling in *Arabidopsis*. *Plant physiology*, 141(2), 436-445.
- García-Angulo, V. A. (2017). Overcoming the barriers of plant immunity by *Salmonella*. *Virulence*, 8(7), 1350-1354.
- García-Sánchez, F., García-Sánchez, R., Mounzer, O., & Noguera, V. (2018). Effect of autoclaving on the activity of a commercial biostimulant based on seaweed extracts. *Journal of Plant Nutrition and Soil Science*, 181(1), 147-154.
- Gessler, C., Pertot, I., and Perazzolli, M. 2011. *Plasmopara viticola*: a review of knowledge on downy mildew of grapevine and effective disease management. *Phytopathol. Mediterr.* 50:3-44.
- Gisi, U. (2002). Chemical control of downy mildews. *Advances in downy mildew research*, 119-159.
- GMO legislation. (n.d.). Food Safety.
- González-Rodríguez, R. M., Rial-Otero, R., Cancho-Grande, B., & Simal-Gándara, J. (2008). Occurrence of fungicide and insecticide residues in trade samples of leafy vegetables. *Food Chemistry*, 107(3), 1342-1347.
- Graham, J. H., & Madden, L. V. (2014). Interpretation of disease severity values. *Phytopathology*, 104(1), 3-6.
- Gruvberger, B., Isaksson, M., & Julander, A. (2018). Allergic contact dermatitis caused by 1,2-benzisothiazolin-3-one in a washing machine cleaner. *Contact Dermatitis*, 78(4), 262-263.

- Guillemaut C (2003) Identification et étude de l'écologie de *Rhizoctonia solani*, responsable de la maladie de pourriture brune de la betterave sucrière. PhD Thesis Université Claude Bernard Lyon. 90 p.
- Gupt, S. K., Chand, R., Mishra, V. K., Ahirwar, R. N., Bhatta, M., & Joshi, A. K. (2021). Spot blotch disease of wheat as influenced by foliar trichome and stomata density. *Journal of Agriculture and Food research*, 6, 100227.
- Hammerschmidt, R. (2009). Systemic acquired resistance. *Advances in botanical research*, 51, 173-222.
- Hardy, G., & McComb (2008), J. Project Period and Period Covered by this Report.
- Havaux, M., & Kloppstech, K. (2001). The protective functions of carotenoid and flavonoid pigments against excess visible radiation at chilling temperature investigated in *Arabidopsis npq* and *tt* mutants. *Planta*, 213, 953-966.
- Hoffman, T., Schmidt, J.S., Zheng, X. and Bent, A.F. (1999) Isolation of ethylene-insensitive soybean mutants that are altered in pathogen susceptibility and gene-for-gene disease resistance. *Plant Physiol.* 119, 935-950
- Horsfall, J. G., & Barratt, R. W. (1945). An improved grading system for measuring plant diseases. *Phytopathology*, 35(8), 655-665.
- Hua, M., Liu, X., Ma, Y., Zhang, Z., Wang, Z., Sun, X., ... & Wu, J. (2020). Distribution and fate of difenoconazole in greenhouse vegetable soil-water system. *Environmental Pollution*, 258, 113722.
- Huibers, R.P., de Jong, M., Dekter, R.W. and Van den Ackerveken, G. (2009) Disease-specific expression of host genes during downy mildew infection of *Arabidopsis*. *Mol. Plant-Microbe Interact.* 22, 1104-1115.
- IBM Corp. (2020). IBM SPSS Statistics for Windows (Version 27.0). Armonk, NY: IBM Corp.
- Ioio, R. D., Linhares, F. S., Scacchi, E., Casamitjana-Martinez, E., Heidstra, R., Costantino, P., & Sabatini, S. (2007). Cytokinins determine *Arabidopsis* root-meristem size by controlling cell differentiation. *Current biology*, 17(8), 678-682.
- Isenring, R. (2010). Pesticides and the loss of biodiversity. *Pesticide Action Network Europe*, London, 26.
- iTaq Universal SYBR Green SuperMix. (n.d.). Bio-Rad Laboratories.
- Kamran, S., Sinniah, A., Abdulghani, M. A., & Alshawh, M. A. (2022). Therapeutic potential of certain terpenoids as anticancer agents: a scoping review. *Cancers*, 14(5), 1100.
- Kaur, M., Bhari, R., & Singh, R. S. (2021). Chicken feather waste-derived protein hydrolysate as a potential biostimulant for cultivation of mung beans. *Biologia*, 76, 1807-1815.
- Kim, H. J., Yoo, D. H., Kim, D. H., & Lee, C. H. (2014). Interaction of 1,2-benzisothiazolin-3-one with metal ions and its effect on metalloenzymes. *Journal of Enzyme Inhibition and Medicinal Chemistry*, 29(5), 617-623.
- Kim, T. K. (2015). T test as a parametric statistic. *Korean journal of anesthesiology*, 68(6), 540-546.
- Knapp, J. S., & Bromley-Challoner, K. C. A. (2003). Recalcitrant organic compounds. *Handbook of water and wastewater microbiology*, 559-595.
- Koch, E., & Slusarenko, A. (1990). *Arabidopsis* is susceptible to infection by a downy mildew fungus. *The Plant Cell*, 2(5), 437-445.
- Koornneef, M., & Meinke, D. (2010). The development of *Arabidopsis* as a model plant. *The Plant Journal*, 61(6), 909-921.
- Kudela, V. (2009). Potential impact of climate change on geographic distribution of plant pathogenic bacteria in Central Europe. *Plant Protection Science*, 45(Special Issue).
- Küpers, J. J., Oskam, L., & Pierik, R. (2020). Photoreceptors regulate plant developmental plasticity through auxin. *Plants*, 9(8), 940.
- Lachhab, N., Sanzani, S. M., Bahouaoui, M. A., Boselli, M., & Ippolito, A. (2016). Effect of some protein hydrolysates against gray mould of table and wine grapes. *European Journal of Plant Pathology*, 144, 821-830.
- Lahlali, R., Ezrari, S., Radouane, N., Kenfaoui, J., Esmaeel, Q., El Hamss, H., ... & Barka, E. A. (2022). Biological control of plant pathogens: A global perspective. *Microorganisms*, 10(3), 596.
- Lamberth, C., Rendine, S., & Sulzer-Mosse, S. (2021). Agrochemical disease control: The story so far. In *Recent Highlights in the Discovery and Optimization of Crop Protection Products* (pp. 65-85). Academic Press
- Lapertot, M., Pulgarín, C., Fernández-Ibáñez, P., Maldonado, M. I., Pérez-Estrada, L., Oller, I., ... & Malato, S. (2006). Enhancing biodegradability of priority substances (pesticides) by solar photo-Fenton. *Water research*, 40(5), 1086-1094.
- Lebeda, A., & Cohen, Y. (2011). Cucurbit downy mildew (*Pseudoperonospora cubensis*)—biology, ecology, epidemiology, host-pathogen interaction and control. *European journal of plant pathology*, 129, 157-192.
- Leboldus, J. M., & Isabel, N. (2018). Quantitative polymerase chain reaction (qPCR) detection and quantification of foliar fungal pathogens of poplar. In *Poplar and Willow Culture* (pp. 221-234). Springer.
- Lee, M. H., Jeon, H. S., Kim, S. H., Chung, J. H., Roppolo, D., Lee, H. J., ... & Park, O. K. (2019). Lignin-based barrier restricts pathogens to the infection site and confers resistance in plants. *The EMBO journal*, 38(23), e101948.
- Lhermie, G., Sauvage, P., Tauer, L. W., Chiu, L. V., Kanyiamattam, K., Ferchiou, A., ... & Grohn, Y. T. (2020). Economic effects of policy options restricting antimicrobial use for high risk cattle placed in US feedlots. *PLoS One*, 15(9), e0239135.
- Lin, Y., Wang, X., Zhang, X., Song, Y., & Xie, X. (2021). Prenatal exposure to difenoconazole disturbs placental amino acid transport and causes fetal growth retardation in mice. *Environmental Pollution*, 273, 116450.
- Livak, K. J., & Schmittgen, T. D. (2001). Analysis of relative gene expression data using real-time quantitative PCR and the 2⁻ΔΔCT method. *methods*, 25(4), 402-408.
- Lu, L., Guo, Y., & Wang, X. (2021). Understanding bacterial growth curve and applications in microbiology. *Frontiers in Microbiology*, 12, 652069.
- Lucini, L., Miras-Moreno, B., Roupael, Y., Cardarelli, M., & Colla, G. (2020). Combining molecular weight fractionation and metabolomics to elucidate the bioactivity of vegetal protein hydrolysates in tomato plants. *Frontiers in Plant Science*, 11, 976.
- Madden, L. V., Hughes, G., & van den Bosch, F. (2007). The study of plant disease epidemics. *American Phytopathological Society*. Magyarosy,
- Mahmood, I., Imadi, S. R., Shazadi, K., Gul, A., & Hakeem, K. R. (2016). Effects of pesticides on environment. *Plant, soil and microbes: volume 1: implications in crop science*, 253-269.
- Mandal, K., Saravanan, R., Maiti, S., & Kothari, I. L. (2009). Effect of downy mildew disease on photosynthesis and chlorophyll fluorescence in *Plantago ovata* Forsk. *Journal of Plant Diseases and Protection*, 116(4), 164.
- Mattioli, R., Francioso, A., d'Erme, M., Trovato, M., Mancini, P., Piacentini, L., ... & Mosca, L. (2019). Anti-inflammatory activity of a polyphenolic extract from *Arabidopsis thaliana* in *in vitro* and *in vivo* models of Alzheimer's disease. *International journal of molecular sciences*, 20(3), 708.
- McDowell, J. M., Hoff, T., Anderson, R. G., & Deegan, D. (2011). Propagation, storage, and assays with *Hyaloperonospora arabidopsidis*: a model oomycete pathogen of *Arabidopsis*. *Plant Immunity: Methods and Protocols*, 137-151.

- Meinke, D. W., Cherry, J. M., Dean, C., Rounsley, S. D., & Koornneef, M. (1998). *Arabidopsis thaliana*: a model plant for genome analysis. *Science*, 282(5389), 662-682.
- Meléndrez, M. M. (2020). Humic acid: The science of humus and how it benefits soil. *Eco Farming Daily*
- Microvolume spectrophotometer, mySPEC. (n.d.). VWR.
- Miedes, E., Vanholme, R., Boerjan, W., & Molina, A. (2014). The role of the secondary cell wall in plant resistance to pathogens. *Frontiers in plant science*, 5, 358.
- Mok, M. C. (2019). Cytokinins and plant development—an overview. *Cytokinins*, 155-166.
- Mondino, P., Casanova, L., Celio, A., Bentancur, O., Leoni, C., & Alaniz, S. (2015). Sensitivity of *Venturia inaequalis* to trifloxystrobin and difenoconazole in Uruguay. *Journal of Phytopathology*, 163(1), 1-10.
- Mrid, R. B., Benmrid, B., Hafsa, J., Boukcim, H., Sobeh, M., & Yasri, A. (2021). Secondary metabolites as biostimulant and bioprotectant agents: A review. *Science of The Total Environment*, 777, 146204.
- Mu, X., Pang, S., Sun, X., Gao, J., Chen, J., Chen, X., ... & Wang, C. (2013). Evaluation of acute and developmental effects of difenoconazole via multiple stage zebrafish assays. *Environmental Pollution*, 175, 147-157.
- Mészáros, É. (2022, May 11). qPCR: How SYBR® Green and TaqMan® real-time PCR assays work. INTEGRA.
- Niemeier, R. T., Sivasubramani, S. K., Reponen, T., & Grinshpun, S. A. (2006). Assessment of fungal contamination in moldy homes: comparison of different methods. *Journal of occupational and environmental hygiene*, 3(5), 262-273.
- NISHI, A., & KUROSAKI, F. (2012). of Carotenoids and Phytoalexins. *Medicinal and Aromatic Plants V*, 24, 178.
- Oshchepkov, M. S., Kalistratova, A. V., Savelieva, E. M., Romanov, G. A., Bystrova, N. A., & Kochetkov, K. A. (2020). Natural and synthetic cytokinins and their applications in biotechnology, agrochemistry and medicine. *Russian Chemical Reviews*, 89(8), 787.
- Palta, J. P. (1990). Leaf chlorophyll content. *Remote sensing reviews*, 5(1), 207-213.
- Palumbo, G., Schiavon, M., Nardi, S., Ertani, A., Celano, G., & Colombo, C. M. (2018). Biostimulant potential of humic acids extracted from an amendment obtained via combination of olive mill wastewaters (OMW) and a pre-treated organic material derived from municipal solid waste (MSW). *Frontiers in Plant Science*, 9, 1028.
- Pandey, A. K., Pandey, S. D., & Misra, V. (2000). Stability constants of metal–humic acid complexes and its role in environmental detoxification. *Ecotoxicology and environmental safety*, 47(2), 195-200.
- Patil, B., & Chetan, H. T. (2018). Foliar fertilization of nutrients. *Marumegh*, 3(1), 49-53.
- Paul, K., Sorrentino, M., Lucini, L., Roupheal, Y., Cardarelli, M., Bonini, P., Reynaud, H., Canaguier, R., Trtílek, M., Panzarová, K., & Colla, G. (2019). Understanding the Biostimulant Action of Vegetal-Derived Protein Hydrolysates by High-Throughput Plant Phenotyping and Metabolomics: A Case Study on Tomato. *Frontiers in Plant Science*, 10.
- Pel, M. J., Wintermans, P. C., Cabral, A., Robroek, B. J., Seidl, M. F., Bautor, J., ... & Pieterse, C. M. (2014). Functional analysis of *Hyaloperonospora arabidopsidis* RXLR effectors. *PLoS one*, 9(11), e110624.
- Pfeufer, E., & Harrison, L. (2022). High incidence of *Hyaloperonospora cardamines-laciniatae* on *Cardamine concatenata* in Maryland, USA. *New Disease Reports*, 46(2).
- Pimentel, D., Acquay, H., Biltonen, M., Rice, P., Silva, M., Nelson, J., ... & D'amore, M. (1992). Environmental and economic costs of pesticide use. *BioScience*, 42(10), 750-760.
- Piubelli, G. C., Hoffmann-Campo, C. B., Moscardi, F., Miyakubo, S. H., & Neves De Oliveira, M. C. (2005). Are chemical compounds important for soybean resistance to *Anticarsia gemmatilis*? *Journal of Chemical ecology*, 31, 1509-1525.
- Prilutskaya, N., Popova, L., Korelskaya, T., Nikitina, M., & Gerasimova, L. (2019). The estimation of the humus acids structural and composition in the soils of the euro-arctic zone and their ecoprotective role to trace metals. *International Multidisciplinary Scientific GeoConference: SGEM*, 19(3.2), 467-474.
- Prince, A., Roy, S., & McDonald, D. (2022). Exploration of the antimicrobial synergy between selected natural substances on *Streptococcus mutans* to identify candidates for the control of dental caries. *Microbiology Spectrum*, 10(3), e02357-21.
- Quan, H., Li, H., Zhang, X., Huang, K., & Li, P. (2021). Growth curve and cell cycle analysis of *Streptococcus suis*. *BMC Microbiology*, 21(1), 44.
- R Core Team (2013). *R: A language and environment for statistical computing*. R Foundation for Statistical Computing, Vienna, Austria. ISBN 3-900051-07-0
- Rausher, M. D. (2001). Co-evolution and plant resistance to natural enemies. *Nature*, 411(6839), 857-864.
- Ried, M. K., Banhara, A., Hwu, F. Y., Binder, A., Gust, A. A., Höfle, C., ... & Parniske, M. (2019). A set of *Arabidopsis* genes involved in the accommodation of the downy mildew pathogen *Hyaloperonospora arabidopsidis*. *PLoS pathogens*, 15(7), e1007747.
- Roberts, C. A. (1995). Microbiology of stored forages. Post-harvest physiology and preservation of forages, 22, 21-38.
- Rossi, V., Caffi, T., Giosuè, S., & Bugiani, R. (2008). A mechanistic model simulating primary infections of downy mildew in grapevine. *Ecological modelling*, 212(3-4), 480-491.
- Rouabhi, R. (2010). Introduction and toxicology of fungicides. INTECH Open Access Publisher.
- Roupheal, Y., Cardarelli, M., Bonini, P., & Colla, G. (2017). Synergistic action of a microbial-based biostimulant and a plant-derived protein hydrolysate enhances lettuce tolerance to alkalinity and salinity. *Frontiers in Plant Science*, 8, 131.
- Rychlik, W. (2007). Selection of primers for polymerase chain reaction. In *PCR primer design* (pp. 31-40). Humana Press.
- Santos, M. S., Nogueira, M. A., & Hungria, M. (2019). Microbial inoculants: reviewing the past, discussing the present and previewing an outstanding future for the use of beneficial bacteria in agriculture. *Amb Express*, 9, 1-22.
- Saunders, H., & Watkins, F. (2001). Allergic contact dermatitis due to thiuram exposure from a fungicide. *Australasian journal of dermatology*, 42(3), 217-218.
- Savary, S., Willocquet, L., Elazegui, F. A., Castilla, N. P., & Teng, P. S. (2012). Rice pest constraints in tropical Asia: quantification of yield losses due to rice pests in a range of production situations. *Plant Disease*, 96(5), 596-604.
- Schena, L., Nigro, F., & Ippolito, A. (2013). Rapid detection methods for plant pathogens: principles, applications, and prospects. In *Rapid Detection of Infectious Agents* (pp. 267-295). Springer.
- Schikora, A., Carreri, A., Charpentier, E., & Hirt, H. (2008). The dark side of the salad: *Salmonella typhimurium* overcomes the innate immune response of *Arabidopsis thaliana* and shows an endopathogenic lifestyle. *PLoS One*, 3(5), e2279.
- Schoina, C., & Govers, F. (2015). The oomycete *Phytophthora infestans*, the Irish potato famine pathogen. *Principles of Plant-Microbe Interactions: Microbes for Sustainable Agriculture*, 371-378.
- Shimizu-Sato, S., Tanaka, M., & Mori, H. (2009). Auxin–cytokinin interactions in the control of shoot branching. *Plant molecular biology*, 69, 429-435.

- Shukla, P. S., Borza, T., Critchley, A. T., & Prithviraj, B. (2021). Seaweed-based compounds and products for sustainable protection against plant pathogens. *Marine drugs*, 19(2), 59.
- Sible, C. N., Seebauer, J. R., & Below, F. E. (2021). Plant biostimulants: A categorical review, their implications for row crop production, and relation to soil health indicators. *Agronomy*, 11(7), 1297.
- Singer, V. L., Lawlor, T. E., & Yue, S. (1999). Comparison of SYBR® Green I nucleic acid gel stain mutagenicity and ethidium bromide mutagenicity in the Salmonella/mammalian microsome reverse mutation assay (Ames test). *Mutation Research/Genetic Toxicology and Environmental Mutagenesis*, 439(1), 37-47.
- Smilkova, M., Smilek, J., Kalina, M., Klucakova, M., Pekar, M., & Sedlacek, P. (2019). A simple technique for assessing the cuticular diffusion of humic acid biostimulants. *Plant methods*, 15, 1-11.
- Steelink, C. (1963). What is humic acid?.
- Stevenson, F.J., 1994. *Humus Chemistry: Genesis, Composition, Reaction* (Second ed.), Wiley, New York.
- Stirk, W. A., & Van Staden, J. (1996). Comparison of cytokinin-and auxin-like activity in some commercially used seaweed extracts. *Journal of Applied Phycology*, 8, 503-508.
- Stoytcheva, M. (Ed.). (2011). *Pesticides in the modern world: trends in pesticides analysis*. BoD–Books on Demand.
- Telli, O., Jimenez-Quiros, C., McDowell, J. M., & Tör, M. (2020). Effect of light and dark on the growth and development of downy mildew pathogen *Hyaloperonospora arabidopsidis*. *Plant Pathology*, 69(7), 1291-1300.
- Thakur, R. P., & Mathur, K. (2002). Downy mildews of India. *Crop Protection*, 21(4), 333-345.
- Thines, M. (2018). Oomycetes. *Current Biology*, 28(15), R812-R813.
- Tomé, D. F., Steinbrenner, J., & Beynon, J. L. (2014). A growth quantification assay for *Hyaloperonospora arabidopsidis* isolates in *Arabidopsis thaliana*. *Plant-Pathogen Interactions: Methods and Protocols*, 145-158.
- Travadon, R., Rolshausen, P. E., Gubler, W. D., Cadle-Davidson, L., & Baumgartner, K. (2013). Susceptibility of cultivated and wild *Vitis* spp. to wood infection by fungal trunk pathogens. *Plant Disease*, 97(12), 1529-1536.
- Tremblay, A., Seabolt, S., Zeng, H., Zhang, C., Böckler, S., Tate, D. N., ... & Lu, H. (2016). A role of the Fuzzy Onions Like gene in regulating cell death and defense in *Arabidopsis*. *Scientific Reports*, 6(1), 37797.
- Tsuchiya, H., Ohta, T., & Masuda, S. (2015). Optimization of qPCR primer design using in silico PCR software and its application for detecting SNPs in a gene involved in iron metabolism. *BMC research notes*, 8(1), 1-7.
- USDA. 2015. United States Department of Agriculture, National Agricultural Statistics Service, *Crop Production 2014 Summary, Vegetables 2014 Summary, and Quick Stats*.
- Van Den Bosch, F., Paveley, N., Shaw, M., Hobbelen, P., & Oliver, R. (2011). The dose rate debate: does the risk of fungicide resistance increase or decrease with dose?. *Plant Pathology*, 60(4), 597-606.
- Vega, K., & Kalkum, M. (2012). Chitin, chitinase responses, and invasive fungal infections. *International journal of microbiology*, 2012.
- Venbrux, M., Crauwels, S., & Rediers, H. (2023). Current and emerging trends in techniques for plant pathogen detection. *Frontiers in Plant Science*, 8, 1186.
- Vernieri, P., Borghesi, E., Ferrante, A., & Magnani, G. (2005). Application of biostimulants in floating system for improving rocket quality. *Journal of Food Agriculture and Environment*, 3(3/4), 86.
- Voiculescu, D. I., Roman, D. L., Ostafe, V., & Isvoran, A. (2022). A cheminformatics study regarding the human health risks assessment of the stereoisomers of difenoconazole. *Molecules*, 27(15), 4682.
- Walters, D. R., & McRoberts, N. (2006). Plants and biotrophs: a pivotal role for cytokinins?. *Trends in plant science*, 11(12), 581-586.
- Wang, R. K., Wang, C. E., Fei, Y. Y., Gai, J. Y., & Zhao, T. J. (2013). Genome-wide identification and transcription analysis of soybean carotenoid oxygenase genes during abiotic stress treatments. *Molecular biology reports*, 40, 4737-4745.
- Wang, Y., Li, X., Fan, B., Zhu, C., & Chen, Z. (2021). Regulation and function of defense-related callose deposition in plants. *International Journal of Molecular Sciences*, 22(5), 2393.
- Wang, Y., Liu, Z., Zhang, Y., & Guo, H. (2019). Effects of 1,2-benzisothiazolin-3-one on glutathione peroxidase activity and oxidative stress in human neuroblastoma cells. *Environmental Toxicology and Pharmacology*, 67, 60-65.
- Wang, Y., Pruitt, R. N., Nürnberger, T., & Wang, Y. (2022). Evasion of plant immunity by microbial pathogens. *Nature Reviews Microbiology*, 20(8), 449-464.
- Wang, Z., Hong, X., Hu, K., Wang, Y., Wang, X., Du, S., ... & Li, Y. (2017). Impaired magnesium protoporphyrin IX methyltransferase (ChIM) impedes chlorophyll synthesis and plant growth in rice. *Frontiers in plant science*, 8, 1694.
- Weller DM and Thomashow LS (1993) Microbial metabolites with biological activity. In: Lumsden D and Vaughn JL (eds.) *Pest Management: Biologically Based Technologies* (pp. 173–180) American Chemical Society, Washington, USA
- Whisson, S. C., Boevink, P. C., Moleleki, L., Avrova, A. O., Morales, J. G., Gilroy, E. M., ... & Birch, P. R. (2007). A translocation signal for delivery of oomycete effector proteins into host plant cells. *Nature*, 450(7166), 115-118.
- Worthington, P. (2012). Sterol biosynthesis inhibiting triazole fungicides. *Bioactive heterocyclic compound classes*, 129.
- Ye, J., Coulouris, G., Zaretskaya, I., Cutcutache, I., Rozen, S., & Madden, T. L. (2012). Primer-BLAST: a tool to design target-specific primers for polymerase chain reaction. *BMC bioinformatics*, 13(1), 1-11.
- Zacchino, S. A., Butassi, E., Di Liberto, M., Raimondi, M., Postigo, A., & Sortino, M. (2017). Plant phenolics and terpenoids as adjuvants of antibacterial and antifungal drugs. *Phytomedicine*, 37, 27-48.
- Zhang, Y. J., Xie, Z. K., Wang, Y. J., Su, P. X., An, L. P., & Gao, H. (2011). Effect of water stress on leaf photosynthesis, chlorophyll content, and growth of oriental lily. *Russian Journal of Plant Physiology*, 58, 844-850.
- Zodape, S. T., Gupta, A., Bhandari, S. C., Rawat, U. S., Chaudhary, D. R., Eswaran, K., & Chikara, J. (2011). Foliar application of seaweed sap as biostimulant for enhancement of yield and quality of tomato (*Lycopersicon esculentum* Mill.).

Appendix

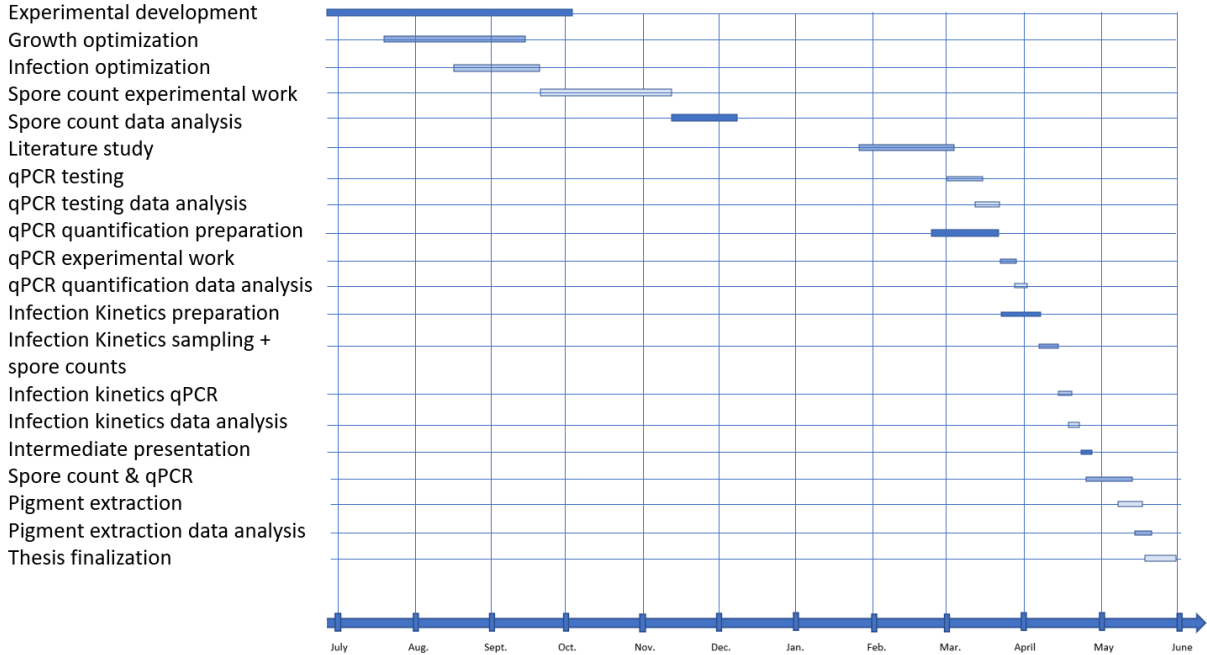


Figure 27: Flow diagram of all individual tasks over time. On the y-axis, all tasks can be seen, and, on the x-axis, time is depicted. The length and placement of each bar represents the time and period a task is conducted.

Calibration curve information: *A. thaliana* actin primers, DNeasy Powersoil Pro Kit DNA extraction

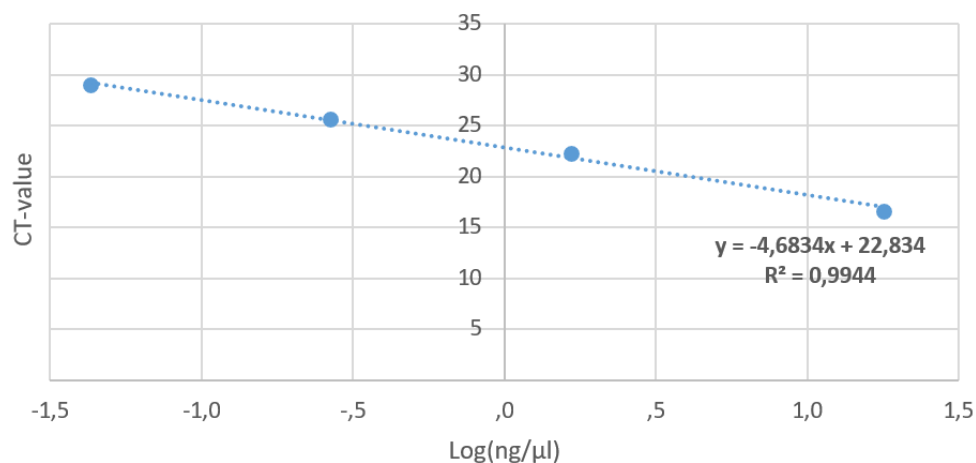


Figure 28: Calibration curve *A. thaliana* actin primers of DNA extracted using the DNeasy Powersoil Pro Kit (Qiagen, n.d.). On the x-axis, Ct values are given. On the y-axis, the natural logarithm of the MySPEC DNA concentration is given. Together forming a calibration curve as well as a R²-value.

Table 18: Calibration curve values *A. thaliana* actin primers of DNA extracted using the DNeasy Powersoil Pro Kit (Qiagen, n.d.).

	CT1	CT2	AVG CT	Ng DNA/μl	LOG (ng/μl)
1X	15.737	15.523	15.630	17.869	1.252
10X	22.277	22.357	22.317	1.062	0.026
100X	25.811	25.438	25.624	0.765	-0.116
1000X	28.473	29.461	28.967	0.143	-0.845
10000X	30.607	30.171	30.389	0.000	/

Calibration curve information: *H. arabidopsidis* actin primers, DNeasy Powersoil Pro Kit DNA extraction

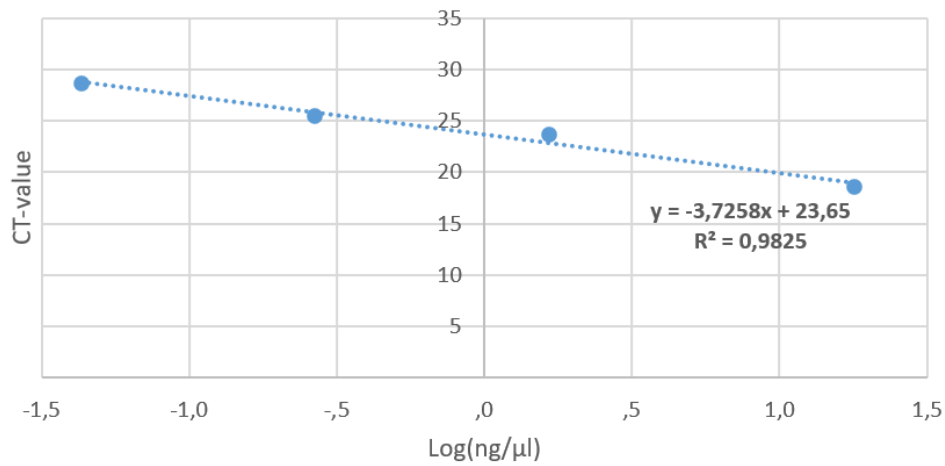


Figure 29: Calibration curve *H. arabidopsidis* actin primers of DNA extracted using the DNeasy Powersoil Pro Kit (Qiagen, n.d.). On the x-axis, Ct values are given. On the y-axis, the natural logarithm of the MySPEC DNA concentration is given. Together forming a calibration curve as well as a R²-value.

Table 19: Calibration curve values *H. arabidopsidis* actin primers of DNA extracted using the DNeasy Powersoil Pro Kit (Qiagen, n.d.).

	CT1	CT2	AVG CT	Ng DNA/μl	LOG (ng/μl)
1X	18.683	18.528	18.605	17.869	1.252
10X	24.190	23.878	24.034	1.062	-0.017
100X	25.240	25.625	25.433	0.765	-0.177
1000X	28.601	28.754	28.677	0.143	-1.367
10000X	Undefined	Undefined	Undefined	0.000	/

Calibration curve information: *A. thaliana* actin primers, phenol/chloroform DNA extraction

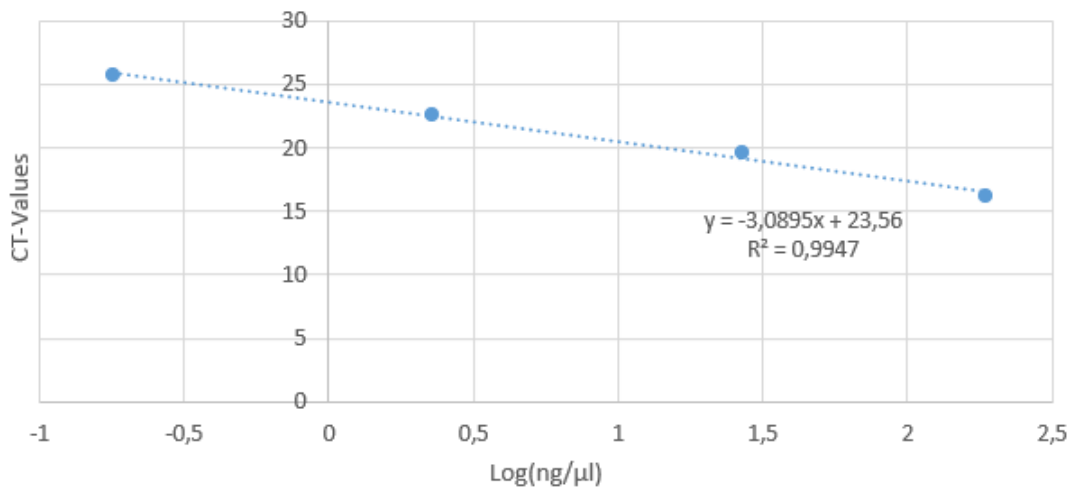


Figure 30: Calibration curve *A. thaliana* actin primers of DNA extracted using phenol/chloroform extraction. On the x-axis, Ct values are given. On the y-axis, the natural logarithm of the MySPEC DNA concentration is given. Together forming a calibration curve as well as a R²-value.

Table 20: Calibration curve values *A. thaliana* actin primers of DNA extracted using phenol/chloroform extraction.

	CT1	CT2	AVG CT	Ng DNA/μl	LOG (ng/μl)
1X	16.241	16.235	16.238	187.500	2.273
10X	19.496	19.553	19.524	27.090	1.433
100X	22.630	22.383	22.507	2.271	0.356
1000X	25.757	25.701	25.729	0.179	-0.747
10000X	27.967	27.970	27.969	0.000	/

Calibration curve information: *H. arabidopsis* actin primers, phenol/chloroform DNA extraction

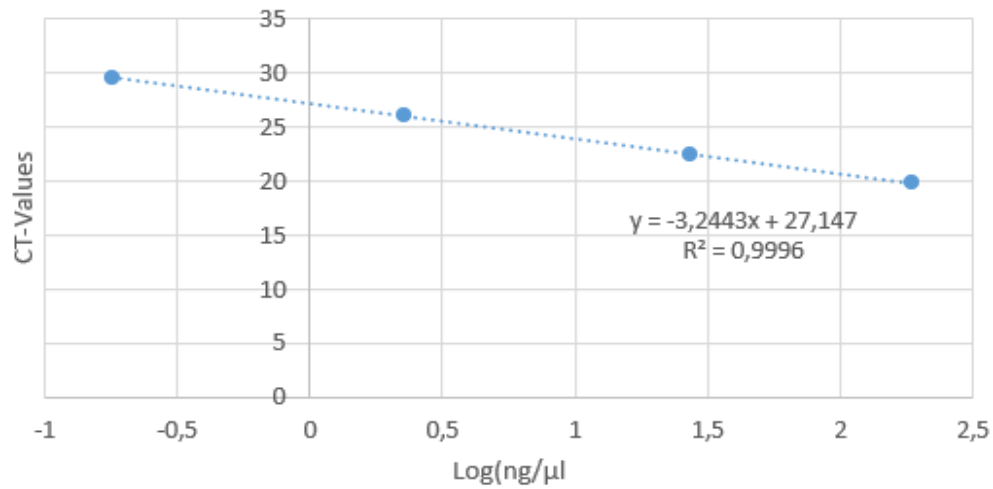


Figure 31: Calibration curve *H. arabidopsis* actin primers of DNA extracted using phenol/chloroform extraction. On the x-axis, Ct values are given. On the y-axis, the natural logarithm of the MySPEC DNA concentration is given. Together forming a calibration curve as well as a R²-value.

Table 21: Calibration curve values *H. arabidopsis* actin primers of DNA extracted using phenol/chloroform extraction.

	CT1	CT2	AVG CT	Ng DNA/μl	LOG (ng/μl)
1X	19.806	19.783	19.795	187.500	2.273
10X	22.492	22.337	22.415	27.090	1.433
100X	26.310	25.881	26.095	2.271	0.356
1000X	29.553	29.502	29.528	0.179	-0.747
10000X	Undefined	Undefined	Undefined	0.000	/

FACULTEIT INDUSTRIËLE INGENIEURSWETENSCHAPPEN
CAMPUS GROEPT LEUVEN
Andreas Vesaliusstraat 13
3000 LEUVEN, België
tel. + 32 16 30 10 30
iiw.groept@kuleuven.be
www.iw.kuleuven.be

